Meereswissenschaftliche Berichte

Marine Science Reports

No 119 2021

Hydrographic-hydrochemical assessment of the Baltic Sea 2020

Michael Naumann, Ulf Gräwe, Volker Mohrholz, Joachim Kuss, Marion Kanwischer, Helena Osterholz, Susanne Feistel, Ines Hand, Joanna J. Waniek. Detlef E. Schulz-Bull

"Meereswissenschaftliche Berichte" veröffentlichen Monographien und Ergebnisberichte von Mitarbeitern des Leibniz-Instituts für Ostseeforschung Warnemünde und ihren Kooperationspartnern. Die Hefte erscheinen in unregelmäßiger Folge und in fortlaufender Nummerierung. Für den Inhalt sind allein die Autoren verantwortlich.

"Marine Science Reports" publishes monographs and data reports written by scientists of the Leibniz-Institute for Baltic Sea Research Warnemünde and their co-workers. Volumes are published at irregular intervals and numbered consecutively. The content is entirely in the responsibility of the authors.

Schriftleitung / Editorship: Dr. Sandra Kube (sandra.kube@io-warnemuende.de)

Die elektronische Version ist verfügbar unter / The electronic version is available on: http://www.io-warnemuende.de/meereswissenschaftliche-berichte.html

ISSN 2195-657X

Dieser Artikel wird zitiert als /This paper should be cited as:

Michael Naumann[1], Ulf Gräwe[1], Volker Mohrholz[1], Joachim Kuss[1], Marion Kanwischer[1], Helena Osterholz[1], Susanne Feistel[1], Ines Hand[1], Joanna J. Waniek[1], Detlef E. Schulz-Bull[1]: Hydrographic-hydrochemical assessment of the Baltic Sea 2020. Meereswiss. Ber., Warnemünde, 119 (2021), doi:10.12754/msr-2021-0119.

Adressen der Autoren:
[1] Leibniz Institute for Baltic Sea Research (IOW), Seestraße 15, D-18119 Rostock-Warnemünde, Germany

Corresponding author: michael.naumann@io-warnemuende.de

Table of content

Kurz- /Zusammenfassung

Die Arbeit beschreibt die hydrographisch-hydrochemischen Bedingungen in der westlichen und zentralen Ostsee im Jahr 2020. Basierend auf den meteorologischen Verhältnissen werden die horizontalen und vertikalen Verteilungsmuster von Temperatur, Salzgehalt, Sauerstoff/ Schwefelwasserstoff und Nährstoffen mit saisonaler Auflösung dargestellt.

Für den südlichen Ostseeraum ergab sich im Winter 2019/2020 an der Station Warnemünde für die Lufttemperatur eine Kältesumme von 0 Kd. Im Langzeitvergleich setzt er damit einen neuen Rekord als wärmster Winter seit Beginn der Aufzeichnungen im Jahr 1948 und wird als extrem mild klassifiziert. Der Sommer 2020 nimmt mit einer Wärmesumme von 234,3 Kd den 14. Platz in der 72jährigen Datenreihe ein und liegt weit unter dem Rekordwert von 2018 (394,5 Kd). Das Langzeitmittel liegt bei 159,7 +/- 75,1 Kd.

Die Situation in den Tiefenbecken der Ostsee war weiterhin geprägt durch stagnierende Bedingungen mit ausgedehnten Sauerstoffmangelgebieten. Kleinere Einstromereignisse ereigneten sich im November 2019 sowie Januar und Februar 2020 in der westlichen Ostsee und prägten das Tiefenwasser im Arkona Becken und Bornholm Becken. Ein weiterer schwacher Einstrom folgte Mitte bis Ende Oktober. Anhand der Temperatur und Salinitätsverhältnisse an den Schlüsselstationen Bornholm Tief und Stolper Rinne hat keines dieser Ereignisse die Stolper Schwelle gequert. Das Bodenwasser in der Stolper Rinne blieb mit 9,1 - 9,5 °C im Jahresverlauf deutlich wärmer im Vergleich zur Temperaturentwicklung im Bornholm Becken, das durch die Wintereinströme geprägt war (Jahresmittel 8,4 °C). Das Tiefenwasser im östlichen Gotland Becken war immer noch geprägt von den warmen Einströmen in den Vorjahren und mit Bodenwerten von 7,2 °C deutlich erhöht.

Aufgrund der Daten von 9 Referenzstationen wurde ermittelt, dass die Winterkonzentrationen der Nährstoffe Nitrat und Phosphat im Oberflächenwasser der westlichen und zentralen Ostsee 2020 etwas niedriger als im Jahr 2019 lagen. Eine Ausnahme bildete die Mecklenburger Bucht, die eine höhere Nitratkonzentration als in 2019 aufwies. Ein klarer Trend über die letzten Jahre zeichnete sich aber nicht ab. Auffällig war noch das Verhältnis des gelösten anorganischen Stickstoffs und Phosphors im Oberflächenwasser im Winter, das in der Mecklenburger Bucht über 11 und in der westlichen Gotlandsee bei immerhin 8 lag, deutlich höher als in den vergangenen Jahren. Dies könnte die Bedeutung der Cyanobakterien in den Seegebieten etwas zurückgedrängt haben.

Die euxinischen Bedingungen im Tiefenwasser der zentralen Ostsee verschärften sich im Jahr 2020 weiter. Dies bestimmte auch die Nährstoffsituation in den Baltischen Tiefs entlang des Talwegs. Im Bornholmtief nahmen die Phosphat und Ammonium Konzentrationen noch leicht ab. Im Gotlandtief, Landsorttief und Karlsötief akkumulierten diese Nährstoffe weiter, sogar bis auf über 5 µmol/l Phosphat und etwa 20 µmol/l Ammonium im Gotlandtief in 2020. Eine leichte Erholung zeigte das Fårötief, das in 2020 einen Schub sauerstoffhaltiges Wasser erhielt. Dadurch nahmen die Schwefelwasserstoffkonzentration und die Nährstoffkonzentrationen leicht ab. Unter den herrschenden euxinischen Bedingungen wurde im Tiefenwasser kein Nitrat mehr vorgefunden. Eine Ausnahme bildete das Bornholmtief, das im Jahresmittel noch 0,9 ml/l Sauerstoff und damit auch eine hohe Nitratkonzentration von etwa 8 µmol/l aufwies. So konnte

hier noch kein Ammonium nachgewiesen werden und die Phosphatkonzentration lag mit etwa 3 µmol/l in einem normalen Bereich für oxisches Tiefenwasser.

In diesem Bericht sind die während des Ostsee-Umweltmonitorings im Januar/Februar 2020 ermittelten Oberflächenwasserkonzentrationen und -sedimentgehalte für chlorierte Kohlenwasserstoffe (CHC) und polyzyklische aromatische Kohlenwasserstoffe (U.S. EPA PAH), sowie Oberflächensedimentgehalte für Organozinnsubstanzen (OT) zusammengefasst.

Für alle im Oberflächenwasser untersuchten Schadstoffe zeigt sich ein Konzentrationsgradient von der westlichen Ostsee im Bereich der Kieler Bucht/Fehmarnbelt (ΣDDTsum: 5,72 pg/L, ΣPCBICES,SUM: 7,20 pg/L, HCBSUM: 4,90 pg/L, ΣPAKSUM: 4660 pg/L) bis zur östlichen Gotlandsee (ΣDDTsum: 1,96 pg/L, ΣPCBICES,SUM: 1,22 pg/L, HCBSUM: 3,43 pg/L, ΣPAKSUM: 1344 pg/L) mit zudem auffälligen Konzentrationen im Bereich der Pommerschen Bucht (ΣDDTsum: 13,06 pg/L, ΣPCBICES,SUM: 5,15 pg/L, HCBSUM: 9,30 pg/L, ΣPAKSUM: 5626 pg/L). Die Daten lassen darauf schließen, dass die Oder eine Quelle für Schadstoffe in der Ostsee ist, besonders für partikulär gebundene. Die höchsten CHC- und PAH-Gehalte im Oberflächensediment wurden für das Arkonabecken nachgewiesen (ΣDDT: 90,7 ng/g TOC, ΣPCBICES: 91,3 ng/g TOC, HCB: 5,0 ng/g TOC, ΣPAH: rd. 37000 ng/g TOC), während höchste Organozinngehalte in der Mecklenburger Bucht detektiert wurden (ΣOT: 275 ng/g TOC).

Die Bewertung der Daten auf Grundlage der UQN der Wasserrahmenrichtlinie zeigt, dass eine schädliche Wirkung auf marine Organismen durch die Konzentrationen des hochmolekularen PAK Benzo(b)fluoranthen für die Bereiche Kieler Bucht/Fehmarnbelt, östliche und westliche Gotlandsee zu erwarten sind. Die Gehalte für Anthracen im Oberflächensediment überstiegen den Grenzwert des HELCOM-Indikators PAH an der Station N1 im Fehmarnbelt. Die Oberflächensedimentgehalte von Tributylzinn überstiegen an allen untersuchten Stationen den Grenzwert des HELCOM-TestindikatorsTBT and imposex.

Die Zeitreihenanalysen der Oberflächenwasserdaten zurückliegend zum Teil bis zum Jahr 2001 zeigen abnehmende Trends der Konzentrationen für PCBICES sowie DDT und seine Metabolite; die der Oberflächensedimentdaten zeigen keine Trends im betrachteten Zeitraum.

Abstract /Summary

The article summarizes the hydrographic-hydrochemical conditions in the western and central Baltic Sea in 2020. Based on the meteorological conditions, the horizontal and vertical distribution of temperature, salinity, oxygen/hydrogen sulphide and nutrients are described on a seasonal scale.

For the southern Baltic Sea area, the Warnemünde station recorded in the winter 2019/2020 a "cold sum" of the air temperature of 0 Kd leading to a classification of an extreme mild winter season, setting a new record as warmest winter since the beginning of the time-series in 1948. The summer "heat sum" of 234.3 Kd ranks on the 14th position over the past 72 years and is far below the record of 394.5 Kd during 2018. The long-term average is 159.7 +/- 75.1 Kd.

The situation in the deep basins of the Baltic Sea was mainly characterized by stagnation and widespread hypoxic to euxinic areas. In wintertime 2019/2020 three weak inflow phases occurred in November, January and February which dominated the situation in the deep water of Arkona Basin and Bornholm Basin. A next weak inflow pulse occurred from mid to end of October. Comparing of temperature and salinity measurements at the key stations Bornholm Deep and Slupsk Channel, none of these events crossed the Slupsk Sill. The deep water temperature in the Slupsk Sill stayed warm between 9.1 to 9.5 °C whereas an annual mean of 8.4 °C was found the Bornholm Deep, which was influenced by colder water of the winterly inflow pulses. The deep water at the eastern Gotland Basin was still influenced by the warm inflows of previous years and with bottom temperatures of 7.2 °C above average.

The winter nutrient concentrations of nitrate and phosphate in surface water in the western and central Baltic Sea were slightly lower in 2020 compared to 2019 according to 9 reference stations. An exception was the Mecklenburg Bight that showed an elevated nitrate concentration in 2020. However, a clear trend over the last years could not be registered. It may be emphasized that the dissolved inorganic nitrogen/phosphorus ratio in winter in surface water was above 11 in the Mecklenburg Bight and almost 8 in the western Gotland Sea, significantly higher compared to recent years. This might have reduced the cyanobacteria abundance in 2020 in these areas.

The euxinic conditions in the deep water of the Baltic proper continued to intensify in the year 2020. This determined the nutrient situation in the Baltic Deeps along the Thalweg. In the Bornholm Deep phosphate and nitrate concentrations still slightly declined. The Gotland, Landsort and Karlsö Deeps showed ongoing accumulation, with a maximum in the Gotland Deep of about 5 µmol/l phosphate and 20 µmol/l ammonium in 2020. A slight improvement was documented for the Fårö Deep that received some oxygenated water. So hydrogen sulphide concentration and nutrient accumulation were reduced there. Under the prevailing euxinic conditions nitrate was depleted in deep waters. An exception was the Bornholm Deep, that showed an annual average of 0.9 ml/l oxygen and consequently a high annual average nitrate concentration of 8 µmol/l. So, no ammonium could be detected and the phosphate concentration was determined at 3 µmol/l, a quite normal value for oxic deep water.

This report summarizes surface water concentrations and sediment contents for chlorinated hydrocarbons (CHC) and polycyclic aromatic hydrocarbons (U.S. EPA PAH), as well as surface

sediment contents for organotin substances (OT) which were determined during the Baltic Sea monitoring in January/February 2020.

Seawater concentration gradients for the analysed contaminants ranging from the western Baltic Sea in the area of the Kiel Bight/Fehmarn Belt (ΣDDTsum: 5.72 pg/L, ΣPCBICES,SUM: 7.20 pg/L, HCBSUM: 4.90 pg/L, ΣPAKSUM: 4660 pg/L) to the eastern Gotland Sea (ΣDDTsum: 1.96 pg/L, ΣPCBICES,SUM: 1.22 pg/L, HCBSUM: 3.43 pg/L, ΣPAKSUM: 1344 pg/L) with noticeable concentrations in the Pomeranian Bight (ΣDDTsum: 13.06 pg/L, ΣPCBICES,SUM: 5.15 pg/L, HCBSUM: 9.30 pg/L, ΣPAKSUM: 5626 pg/L). The data suggest that the Odra River is a source of pollution in the Baltic Sea, especially for particulate contaminants. The highest CHC and PAH levels in the surface sediment were detected for the Arkona Basin (ΣDDT: 90.7 ng/g TOC, ΣPCBICES: 91.3 ng/g TOC, HCB: 5.0 ng/g TOC, ΣPAH: about 37000 ng/g TOC); while highest organotin levels were detected in the Mecklenburg Bight (ΣOT: 275 ng/g TOC).

The assessment of the data based on the EQS of the Water Framework Directive shows that a harmful effect on marine organisms must be expected from concentrations of the high molecular weight PAH benzo(b)fluoranthene for the Kiel Bight/Fehmarn Belt, eastern and western Gotland Sea areas. Contents for anthracene in surface sediment exceeded the threshold value of the HELCOM indicator PAH at station N1 in the Fehmarn Belt. Surface sediment contents of tributyltin exceeded the threshold value of the HELCOM test indicator TBT and imposex at all sites studied.

Time series data for surface water back to year 2001 show decreasing trends for concentrations of PCBICES and DDT and its metabolites. No trends can be observed for surface sediment time series data within the studied time period.

1 Introduction

This assessment of hydrographic and hydrochemical conditions in the Baltic Sea in 2020 has partially been produced on the basis of the Baltic Sea Monitoring Programme that the Leibniz Institute for Baltic Sea Research Warnemünde (IOW) undertakes on behalf of the Federal Maritime and Hydrographic Agency, Hamburg and Rostock (BSH). Within the scope of an administrative agreement, the German contribution to the Helsinki Commission's (HELCOM) monitoring programme (COMBINE) for the protection of the marine environment of the Baltic Sea has been devolved to IOW. It basically covers Germany's Exclusive Economic Zone. Beyond these borders, the IOW is running an observation programme on its own account in order to obtain and maintain long-term data series and to enable analyses of the conditions in the Baltic Sea's central basins, which play a decisive role in the overall health of the sea.

The combination of both programmes leads to a yearly description of the water exchange between the North Sea and the Baltic Sea, the hydrographic and hydrochemical conditions in the study area, their temporal and spatial variations, as well as the investigation and identification of long-term trends.

Five routine monitoring cruises are undertaken each year covering all four seasons. The data obtained during these cruises, as well as results from other research activities by IOW, form the basis of this assessment. Selected data from other research institutions, especially the Swedish Meteorological and Hydrological Institute (SMHI) and the Maritime Office of the Polish Institute of Meteorology and Water Management (IMGW), are also included in the assessment.

HELCOM guidelines for monitoring in the Baltic Sea form the basis of the routine hydrographical and hydrochemical monitoring programme within its COMBINE Programme (HELCOM 2000). The five monitoring cruises in January/February, May, July, September and November were performed by RV Elisabeth Mann Borgese. Details about water sampling, investigated parameters, sampling techniques and their accuracy are given in NEHRING et al. (1993, 1995).

Ship-based investigations were supplemented by measurements at three autonomous stations within the German MARNET environmental monitoring network, the ARKONA BASIN (AB), the DARSS SILL (DS) station and the ODER BANK (OB) station. The latter was in operation from beginning-July (later than usual due to pandemic circumstances) to mid-November 2020 and taken out of service over the winter of 2020/2021. A second system of a new buoy construction more resistant against damages caused by ice was operated in parallel at the Oder Bank position.

Besides meteorological parameters at these stations, water temperature and salinity as well as oxygen concentrations were measured at different depths:

AB:	8 horizons T + S	+	2 horizons O2
DS:	6 horizons T + S	+	2 horizons O2
OB:	2 horizons T + S	+	2 horizons O2

All data measured at the MARNET stations are transmitted via METEOSAT to the BSH database as hourly means of six measurements (KRÜGER et al. 1998, KRÜGER 2000). An acoustic doppler current profiler (ADCP) records current speeds and directions at AB and DS. The ADCP arrays are

located on the seabed in some two hundred metres distance from the main stations and protected by a trawl-resistant bottom mount mooring. They are operated in real time: via an hourly acoustic data link, they send their readings to the main station for storage and satellite transmission. For quality assurance and service purposes, data stored by the devices itself are read retrospectively during maintenance measures at the station once or twice a year.

As a general overview of the state of the Baltic Sea Fig. 1 shows the recent hypoxic to euxinic conditions. Oxygen deficiency is one of the major factors influencing the Baltic Sea ecosystem. An overlay of the conditions in winter and summer are shown in this map, visualising the development during the year 2020. A large extend of bottom water in the deep basins is influenced by hypoxia (black dotted areas) and the situation is more or less stagnant. In July, measurements at the northern station 283 failed due to bad weather. Thus, the northern extend of the hydrogen sulphide areas is locally interrupted in the map by that time (see missing vertical red lines in Fig. 1), but certainly spreading all over the northern deep water.

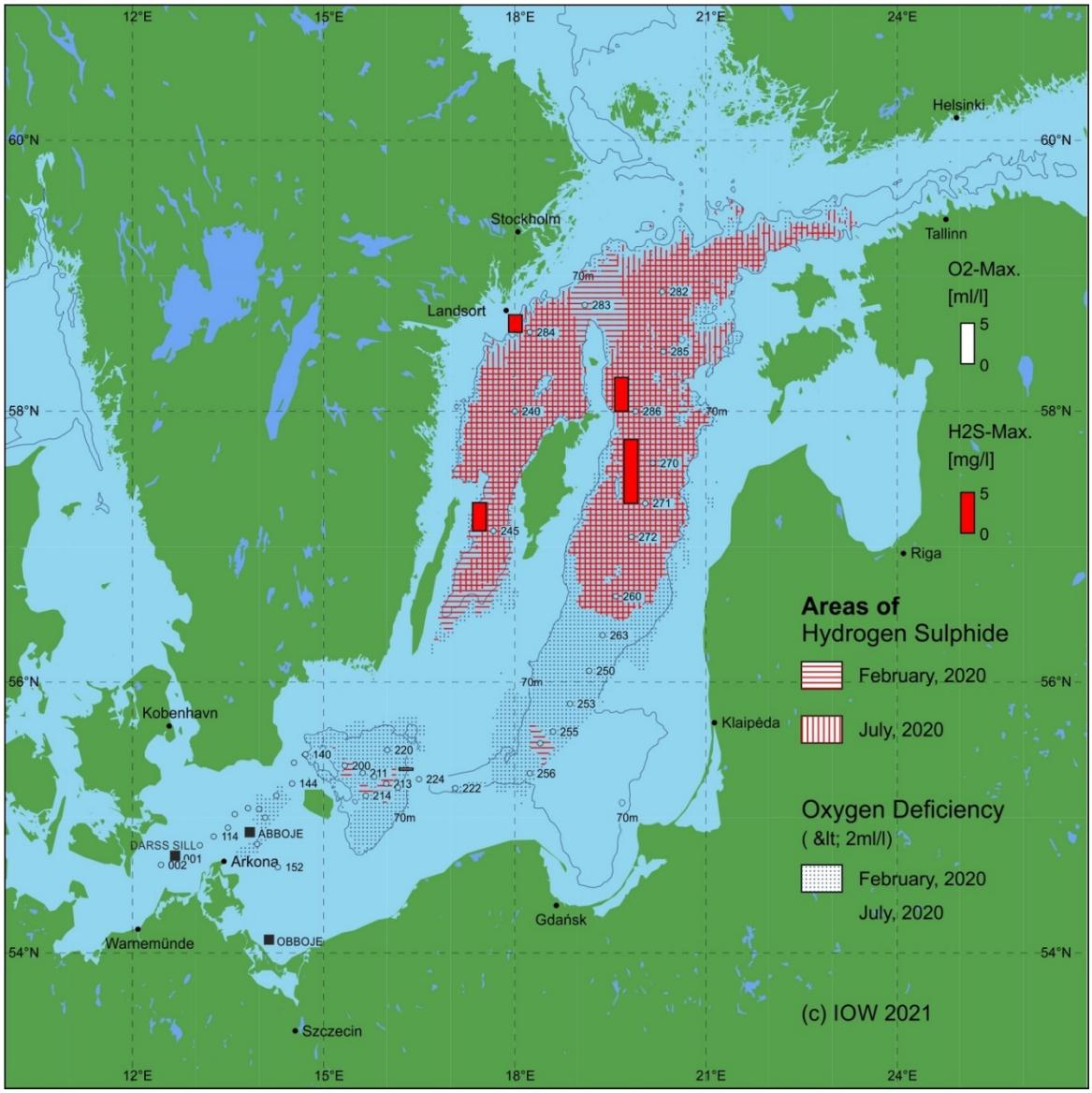

Fig. 1: Location of stations (■ MARNET- stations) and areas of oxygen deficiency and hydrogen sulphide in the near bottom layer of the Baltic Sea. Bars show the maximum oxygen and hydrogen sulphide concentrations of this layer in 2020; the figure additionally contains the 70 m -depth line.

2 General meteorological conditions

The following description of weather conditions in the southern Baltic Sea area is based on an evaluation of data from the Germany's National Meteorological Service (DWD), the Federal Maritime and Hydrographic Agency (BSH), the Swedish Meteorological and Hydrological Institute (SMHI), the Institute of Meteorology and Water Management (IMGW), Freie Universität Berlin (FU) as well as IOW itself. Table 1 gives a general outline of the year's weather with monthly mean temperature, sunshine duration, precipitation as well as the number of days of frost and ice at Arkona weather station. Solar radiation at Gdynia weather station is given in addition. The warm and cold sums at Warnemünde weather station, and in comparison with Arkona, are listed in Table 2 and Table 3.

According to the analysis of DWD (DWD 2020), 2020 like previous years was too warm, too dry and of a longer sunshine duration than usual. With 10.4 °C, Germany's annual mean temperature was 2.2 K warmer than those of the reference period 1961-1990 and 1.5 K warmer compared to reference period 1981-2010. After 2018 with 10.5 °C it was the second warmest year since 1881, the beginning of continuous measurements. 2014 with 10.3 °C and 2019 with 10.2 °C are following in the hit list of warm years and 9 years out of the top ten occurred in the 21st century, the four warmest in the last decade 2011-2020. Across Germany, 11 months showed temperatures above average and January, February, April as well as August showed extreme levels of over 3 K above average. Only May stayed below average. Focussing at the Baltic Sea, the meteorological data reflect the same situation (cf. Table 1). Almost all monthly mean temperature values were above average. Only the July values lied below.

The mean amount of precipitation in Germany in 2020 was 730 l/m² covering 90 % of the long-term mean value (789 l/m²). Together with that were nine years to dry during the decade 2011-2020. Only in 2017 precipitation was above average. The highest daily rainfall of 154 l/m² was registered in Aschau-Innerkoy (southeastern Germany) at August 3rd and the maximum annual value of up to 2000 l/m² in the Schwarzwald and Alpes mountains. The lowest precipitation with values below 500 l/m² was observed in most areas of northern Germany. In the coastal states along Germany's Baltic Sea coast precipitation ranged from 733 l/m² (avg. 788 l/m²) in Schleswig-Holstein to 551 l/m² (avg. 595 l/m²) in Mecklenburg-Vorpommern.

In Germany, the average annual sum of 1,901 hours of sunshine was the 4th sunniest in the record and well above the average of 1,544 hours (+20 %). The record-breaking value of 2,020 hours of sunshine was observed in the year 2018. Schleswig-Holstein registered 1,855 hours in 2020 (long-term mean: 1,567 hours) and Mecklenburg-Vorpommern recorded 1,893 hours (long-term mean: 1,648 hours), far below its value from 2018, when it reached the nation-wide highest value of 2,085 hours.

At Gdynia station (Gdansk Bight), an annual sum of 388,547 J/cm² of solar radiation was recorded. Within a data series covering 65 years back in time (first compiled by FEISTEL et al. 2008, continued to date), this value takes the 19th rank. It is much lower than the long-term maximum in 1959 with 457,751 J/cm², but slightly above the mean value of 374,979 J/cm². The sunniest month in 2020 by far was April (Table 1). With 50,760 J/m², it takes the fourth place in the long-term comparison of monthly mean values, but still falls well short of the peak value of 80,389 J/m² in July 1994, which represents the absolute maximum of the entire series since 1956.

Another top-ranked month of the year is February on 3rd position. The year's lowest value was 3,827 J/cm² in December, lying in 45th place in the time series and below the long-term average of 4,345 J/cm² for this month. All other months showed solar radiation monthly mean values compared to those of the last 65 years as follows: January rank 35, March rank 15, May rank 39, June rank 32, July rank 39, August rank 15; September rank 19; October rank 56; November rank 47.

Table 1: Monthly averaged weather data at Arkona station (Rügen Island, 42 m MSL) from DWD (2020). t: air temperature, Δt: air temperature anomaly, s: sunshine duration, r: precipitation, Frost: days with minimum temperature below 0 °C, Ice: days with maximum temperature below 0 °C. Solar: Solar Radiation in J/cm² at Gdynia station, 54°31' N, 18°33' O, 22 m MSL from IMGW (2021). Percentages are given with respect to the long-term mean. Maxima and minima are shown in bold.

Month	*t*/°C	Δ*t*/K	*s*/%	*r*/%	Frost	Ice	Solar
January	4.8	3.6	84	159	1	**-**	5706
February	5.0	**3.9**	125	189	-	-	13906
March	4.8	1.9	146	82	2	-	29313
April	8	2.0	**152**	13	-	-	50760
May	10.7	0.3	109	35	-	-	57104
June	15.9	1.7	117	78	-	-	**61048**
July	16.4	-0.7	93	113	-	-	57599
August	**19.1**	1.8	121	**221**	-	-	53557
September	15.6	1.6	129	75	-	-	34246
October	11.5	1.5	74	75	-	-	15064
November	8	2.5	89	48	-	-	6417
December	3.8	1.5	61	88	**4**	-	3827

Table 2: Sums of daily mean air temperatures at the weather station Warnemünde (data: DWD 2020). The 'cold sum' (CS) is the time integral of air temperatures below the line t = 0 °C, in Kd, the 'heat sum' (HS) is the corresponding integral above the line t = 16 °C. For comparison, the corresponding mean values 1948–2019 are given.

Month	CS 2019/20	Mean	Month	HS 2020	Mean
November	0	2.4 ± 6.0	April	0	1.0 ± 2.4
December	0	20.2 ± 27.6	May	0.2	6.1 ± 7.5
January	0	37.5 ± 39.0	June	42.4	25.0 ± 17.1
February	0	29.7 ± 37.1	July	45.5	58.5 ± 36.3
March	0	8.2 ± 12.0	August	124.6	55.2 ± 34.0
April	0	0 ± 0.2	September	21.6	12.5 ± 13.2
			October	0	0.5 ± 1.5
Σ 2019/2020	0	97.8 ± 84.5	Σ 2020	234.3	159.7 ± 75.1

Table 3: Sums of daily mean air temperatures at the weather station Arkona (data: DWD 2020). The 'cold sum' (CS) is the time integral of air temperatures below the line t = 0 °C, in Kd, the 'heat sum' (HS) is the corresponding integral above the line t = 16 °C.

Month	CS 2019/20	Month	HS 2020
November	0	April	0
December	0	May	0
January	0	June	22,2
February	0	July	26,2
March	0	August	95,1
April	0	September	16
		October	0
∑ 2019/2020	**0**	∑ 2020	**159,5**

2.1 Ice winter 2019/20

For the southern Baltic Sea area, the Warnemünde station shows a **cold sum of 0 Kd** referring to the air temperature of the winter 2019/2020. In comparative data from 1948 to date, it is the warmest winter recorded in this time-series. It continues the series of warm winters during the latest years showing low cold sums: 2018/2019 (18.3 kd), 2017/18 (67.7 Kd), 2016/17 (31.7 Kd) and 2015/2016 (63.5 Kd). Since the year 2012 all values plot below the long-term average of 97.8 Kd. In comparison, the cold sum at Arkona station is as well 0 Kd (Table 3), much lower than 2018/2019 with 14.6 Kd. Like in Warnemünde, it represents a very warm winter even warmer than other recent winter seasons 2017/18 (53.8 Kd), 2016/17 (27.2 Kd), 2015/2016 (36.1 Kd) and 2014/2015 (8.1 Kd). Given the exposed location of the Arkona station at a headland surrounded by water masses at the northernmost coast of Rügen Island, the local air temperature development is under an even stronger influence by the water temperature of the Baltic Sea than at Warnemünde. Thus, winter values at Arkona are frequently higher, while summer values are lower.

The winter season recorded only **6 days of frost and no ice days** (daily mean below 0 °C), but typical "cold spells" were missing (Table 1). All winter months from November 2019 to April 2020 showed positive temperature anomalies between 1.3 K in November 2019 and 3.9 K in February at station Arkona in the western Baltic Sea (cf. NAUMANN et al. 2020: 1.3 K in November 2019, 2.2 K in December 2019). Water temperatures stayed in this region well above the freezing point in all german offshore areas. The **local ice conditions at the German Baltic Sea** coast were classified as very weak, with absence of any icing at the coastal waters and sheltered lagoons HOLFORT (2020). Another measure for the strength of an ice winter is the **accumulated areal ice volume**. Besides various other indices, this index is used to describe the extent of icing, and was introduced in 1989 to allow assessment of ice conditions in German coastal waters (KOSLOWSKI 1989, BSH 2009). The duration of icing, the extent of ice cover, and ice thickness are considered, so as to take better account of the frequent interruptions to icing during individual winters. The daily values from the 13 ice climatological stations along Germany's Baltic Sea coast are summed. The season 2019/20 showed **a very low accumulated areal ice volume** of below 0.01 m (HOLFORT 2020). Compared to long-term data, winter seasons of this low value (nearly free of ice) occurred at the German Baltic Sea coast ten times since the year 1879 (in 1882, 1884, 1898, 1944,

1988, 1989, 1990, 1992, 2000 and 2007). In contrast, the highest values recorded in this data series are as follows: 26.83 m in 1942; 26.71 m in 1940; 25.26 m in 1947; and 23.07 m in 1963. In all other winters, values were well below 20 m (KOSLOWSKI 1989).

For the whole Baltic Sea area a **maximum ice coverage** of 36 000 km² was observed at March 4th (Fig. 3). This maximum extent of ice corresponds to some 9 % of the Baltic Sea's area (415 266 km²), and was largely centred in the Bothnian Bay as well as a small part in the eastern part of the Gulf of Finland. All other region stayed free of icing. The observed maximum ice extent is classified as extremely mild and sets a **new minimum** in a time series of 300 years (Fig. 2).

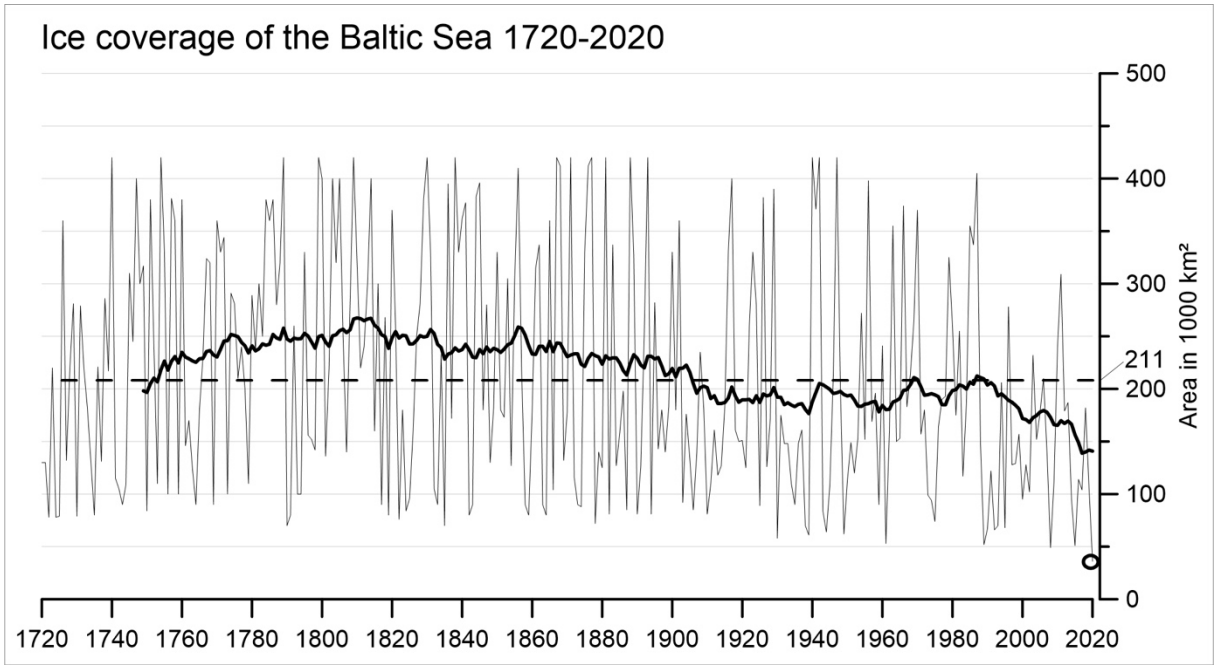

Fig. 2: Maximum ice covered area in 1.000 km² of the Baltic Sea in the years 1720 to 2020 (from data of SCHMELZER et al. 2008, HOLFORT 2020). The long-term average of 211 000 km² is shown as dashed line. The bold line is a running mean value over the past 30 years. The ice coverage in the winter 2019/2020 with 36 000 km² is encircled and the lowest value in the time series.

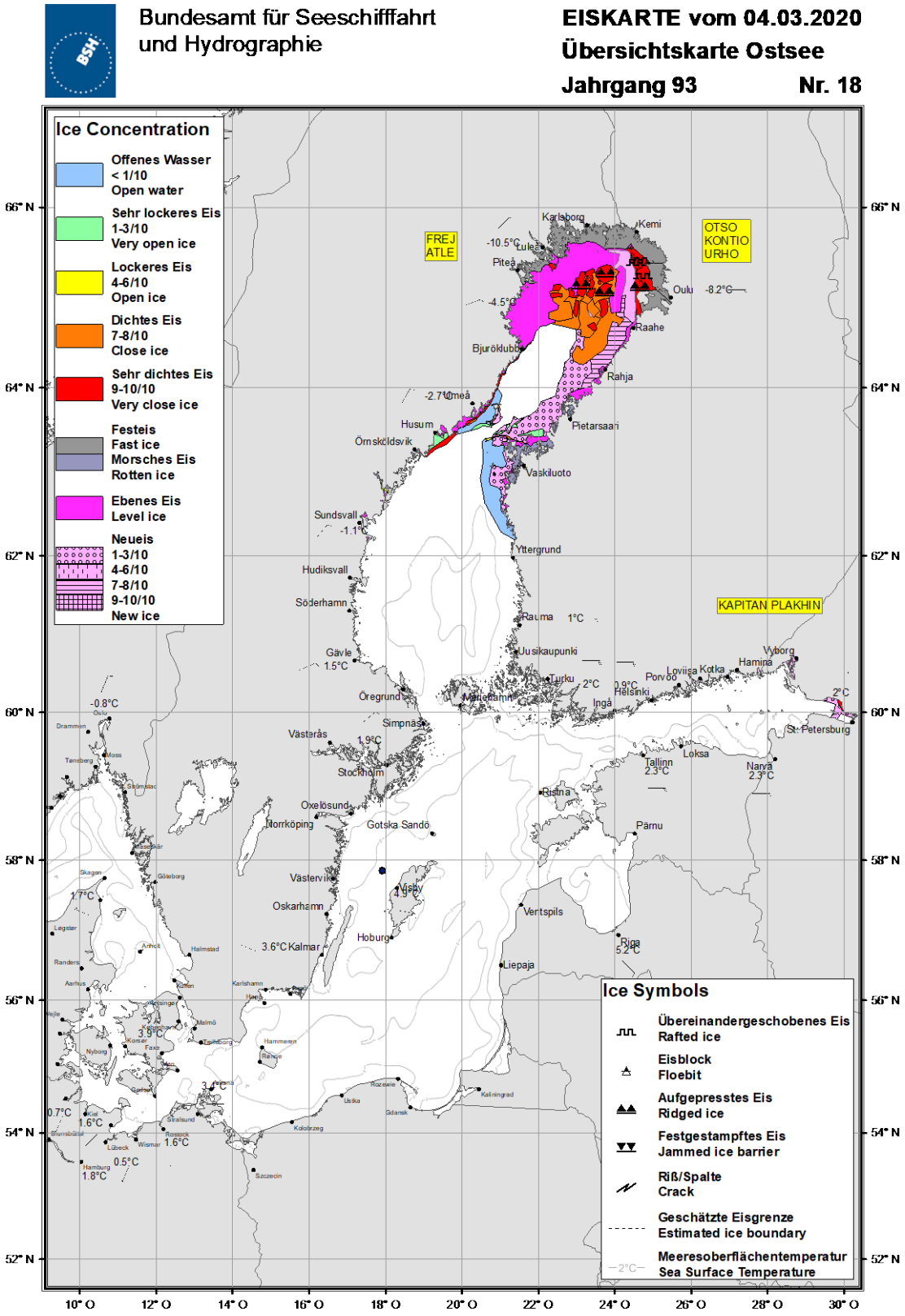

Fig. 3: Maximum ice coverage in the winter 2019/2020 on March 4th – ice concentration in colour code and ice type in symbols (HOLFORT 2020).

2.2 Wind conditions

During the year 2020, pressure systems and air currents changed not so often as in other years and westerly to south-westerly wind directions dominated the situation, comparable to the climatic mean for this region. North-western to south-western directed winds account for about 61 % of the annual sum and easterly to north-easterly to another 25 % (Fig. 5). The annual mean wind speed of 6.89 m/s (Fig. 4a) is below long-term average of 7.37 m/s.

Fig. 4 to Fig. 5 illustrate the **wind conditions at Arkona** throughout 2020. The **trend towards prevailing south-west winds** that began in 1981 (HAGEN & FEISTEL 2008) and continues today is evident over the year. Comparing the east component of the wind (positive westwards) with an average of 3 m/s (Fig. 4b) with the climatic mean of 1.7 m/s (HAGEN & FEISTEL 2008), westerly winds were in 2020 much more dominant than the mean.

According to the wind-rose diagram (Fig. 5), north-western to south-western directed winds account for about 61 % of the annual sum, which is on the same level compared to 2019 (62 %). This last years were much higher than previous ones, 50 % in hot and windless year 2018 and 75 % in 2017. Easterly to north-easterly winds account for another 24 % in 2020 (22 % in 2019). The **annual mean wind speed** of 6.89 m/s (Fig. 4a) is below the average and root mean square of 7.37 +/- 0.47 m/s of the last 41 years. The maximum wind speed in that period was reached with 8.41 m/s in 1990. The minimum value occurred in 2018 with 6.5 m/s (based on DWD data, 2021b). Only three high-wind days of over 15 m/s daily mean are registered at February 12th (15.6 m/s), February 22nd (15.6 m/s) of north-western and western direction and October 14th (15.2 m/s) of north-eastern direction. In addition to the daily means, a view at high values of hourly means and maximum gusts enables to detect short, but intensive wind events of violent character. Some storms are regionally restricted to some hours only with no significant impact on the daily mean value. However, they can lead to major damages. At March 12th, the maximum gust of the year occurred (31 m/s) and the maximum hourly means of 22.7 m/s was reached at the same day (often not usual). All these 2020 maximum values are below previous peak values, for example an hourly mean of 30 m/s in 2000, 26.6 m/s in 2005; and 25.9 m/s (hurricane “Xaver”) in December 2013. This is clearly illustrated by the wind-rose diagram (Fig. 6), in which orange and red colour signatures indicate values greater than 20 m/s. They did only slightly occur in 2020 (5 times an hourly mean ›20 m/s four times at March 12th (western direction) and once March 29th (eastern direction).

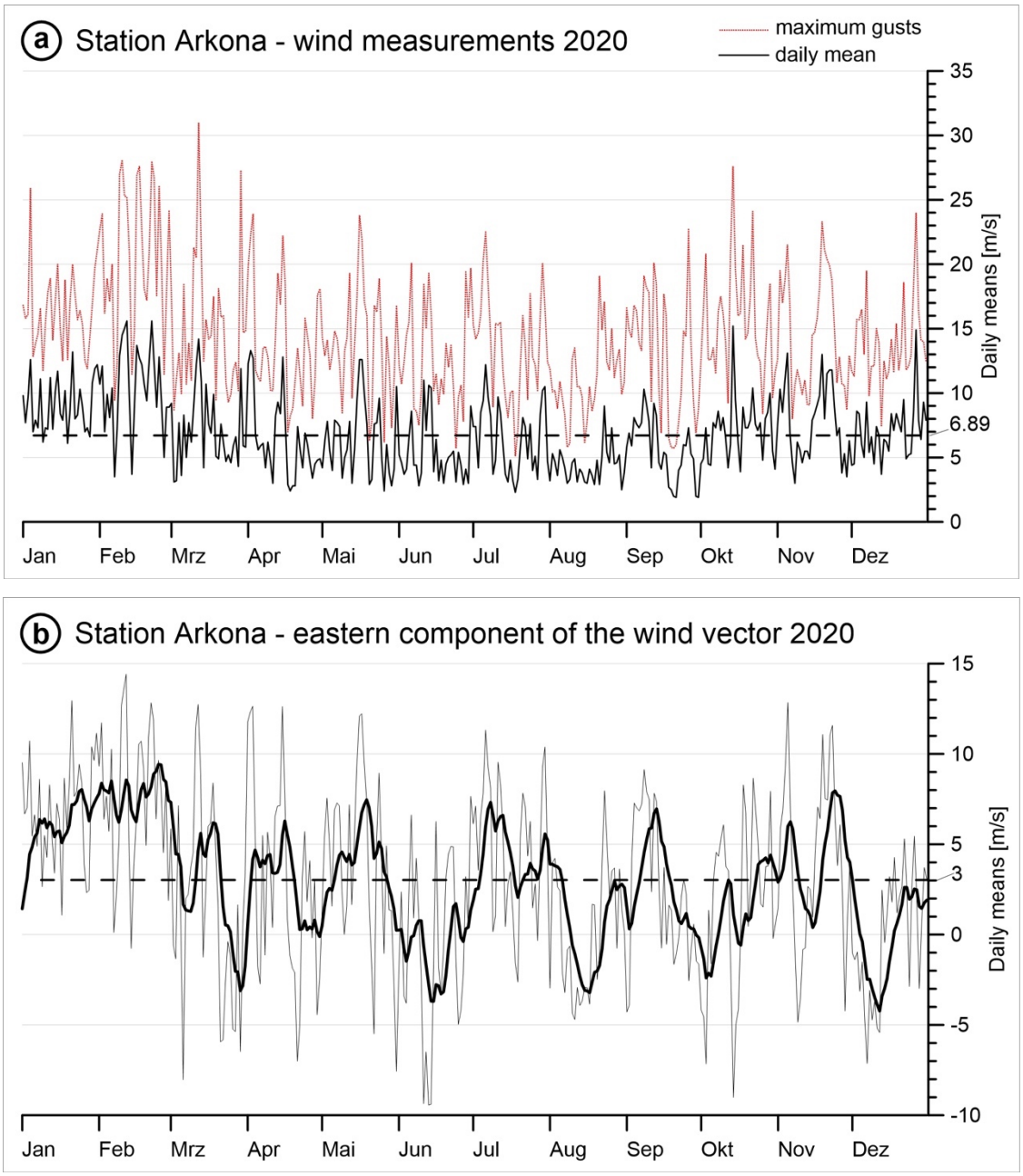

Fig. 4: Wind measurements at the weather station Arkona (from data of DWD, 2021a). a) Daily means and maximum gusts of wind speed, in m/s, the dashed black line depicts the annual average of 6.89 m/s. b) Daily means of the eastern component (westerly wind positive), the dashed line depicts the annual average of 2.95 m/s. The line in bold is filtered with a 10-days exponential memory.

Remarkable hydrographic events caused by wind drift are two storm surges of weak and medium intensity in beginning of February and mid-October 2020 which occurred regional at the south-western Baltic Sea coast. Fig. 6 shows the tide-gauge measurements /predictions for Warnemünde and other selected stations (BSH, 2020). At February 4th, low pressure "Ottilia II" (995 hPa) located across Skagerrak and high pressure "Frank" (1030 hPa) moved quickly from Great Britian to central Europe. The wind turned from westerly to northern direction with maximum gusts up to 18.9 m/s. Highest water levels were reached in the nighttime to February 5th, but decreased quickly to normal water levels at the end of the day (Fig. 6a). At Warnemünde

a maximum sea level of +0.99 m MSL was reached. Wismar (+1.21 m MSL) and Lübeck (+1,20 m MSL) showed slightly higher levels and this event was generally classified as weak storm surge (PERLET-MARKUS 2020a). A second one occurred at October 14th. Low pressure "Gisela" (994 hPa) moved from Hungary via Poland northeastwards on a classic track of so called Vb weather situations. High pressure "Otmar" (1035 hPa) moved from Island via the Faroer islands to mid Sweden. This air-pressure constellation induced strong to stormy northeaster winds at the Baltic Sea. Arkona station registered a daily mean of 15.2 m/s and maximum gusts up to 27.6 m/s. Highest water levels were reached at southern Baltic Sea coast during the afternoon of October 14th (Fig. 6b). Warnemünde tide gauge station registered +1.19 m MSL, highest levels at the German Baltic Sea coast again in Lübeck (1.43 m MSL) and Wismar (1.42 m MSL). This event was classified as weak to medium sized storm surge by PERLET-MARKUS (2020b). Damages were on a lower level and much less compared to storm surge "Zeetje" in the beginning of January 2019.

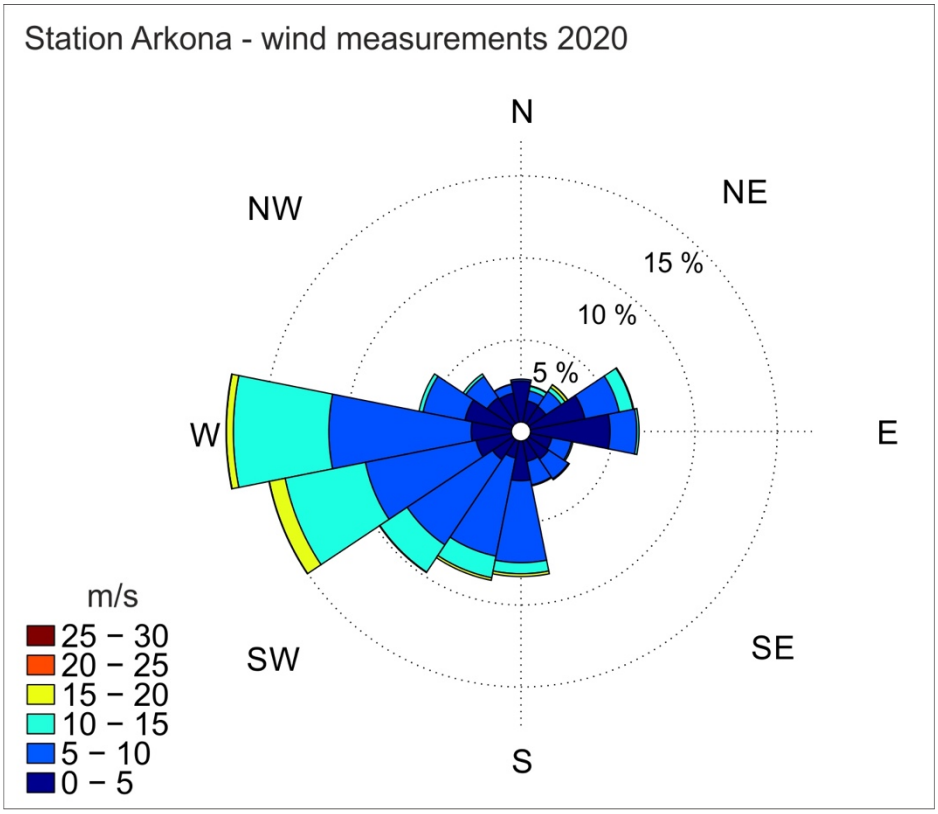

Fig. 5: Wind measurements at the weather station Arkona (from data of DWD 2021a) as windrose plot. Distribution of wind direction and strength based on hourly means of the year 2020.

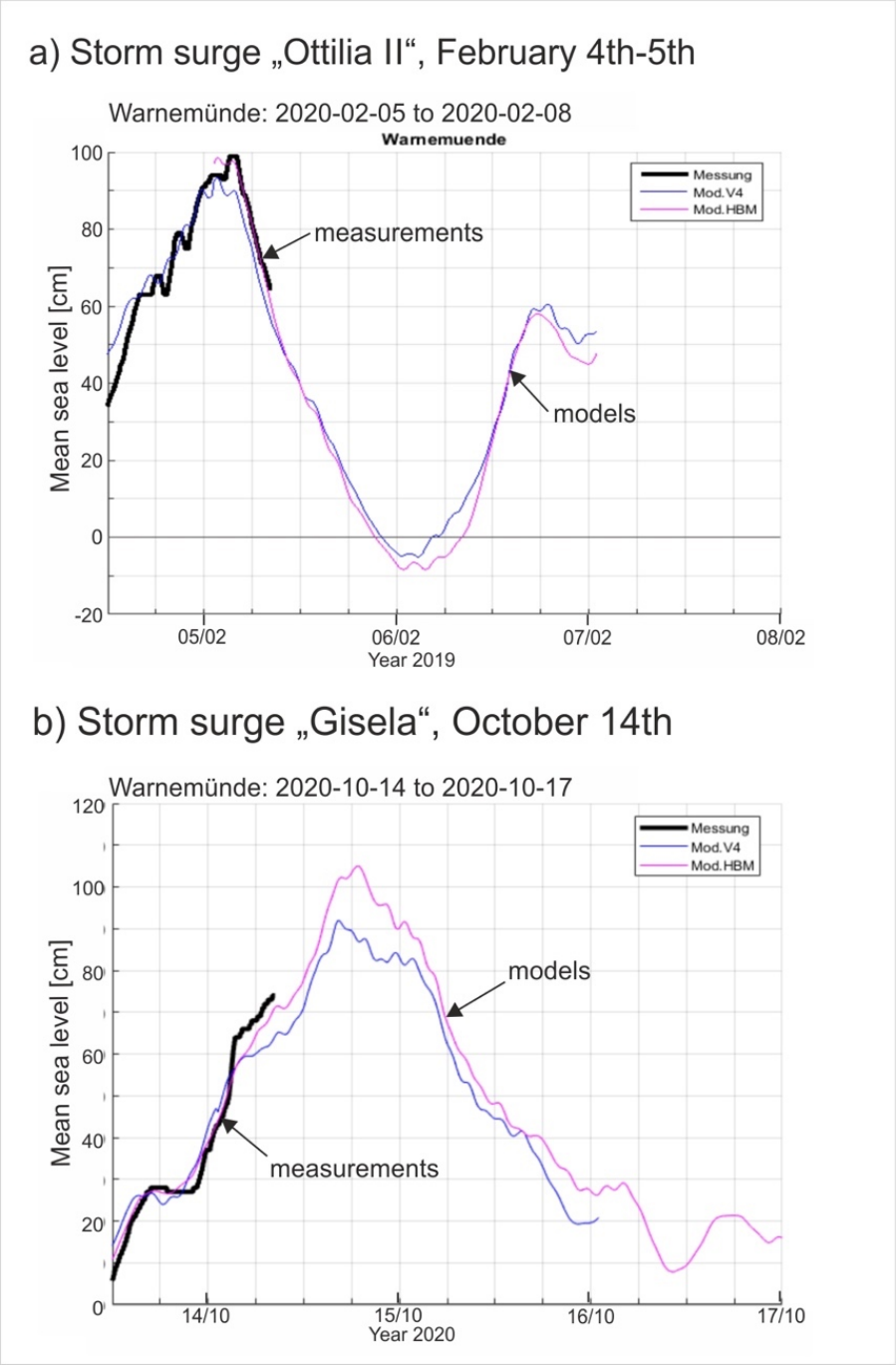

Fig. 6: Sturm surges in October 2020 - a) Storm surge b) Storm surge low pressure Gisela (from data of BSH 2020).

3 Water exchange through the straits

3.1 Water level at Landsort

The Swedish tide gauge station at Landsort Norra, south of Stockholm, provides a good description of the mean water level in the Baltic Sea (Fig. 7a), as it is more or less unaffected by windshift and located in the centre of the large scale seiche of the Baltic Basin (LISITZIN 1974, JACOBSEN 1980, FEISTEL et al. 2008). In the course of 2020, the Baltic Sea experienced no strong inflow activity. Only three minor inflow pulses occurred in January, February and November which ventilated the Arcona Basin, but no "classic" situations of continuous and rapid sea level changes of more than 50 cm could be observed, which indicate major events. Rapid rises of the sea level are usually only caused by an inflow of North Sea water through the Sound and Belts. They are of special interest for the ecological conditions of the deep-water in the Baltic Sea. Such events are produced by storms from westerly to north-westerly directions, as the clear correlation between the sea level at Landsort Norra and the filtered wind curves illustrates (Fig. 7b). No signs of longer intensified phases of a positive southeastern wind component (northwesterly wind) occurred during 2020.

Filtering is performed according to the following formula,

$$\bar{v}(t) = \int_0^\infty \mathrm{d}\tau \, v(t-\tau) \exp(-\tau / 10\,\mathrm{d})$$

in which the decay time of 10 days describes the low-pass effect of the Sound and Belts (well-documented both theoretically and through observations) in relation to fluctuations of the sea level at Landsort Norra in comparison with those in the Kattegat (LASS & MATTHÄUS 2008, FEISTEL et al. 2008).

Sea level fluctuations in the course of the year 2020. At the beginning of the year 2020, the gauge at Landsort Norra recorded a slow increase from 12 cm MSL (January 1st) to +50 cm MSL (February 4th). Calculation methods after MOHRHOLZ (2018), taking hydrographic data of the western Baltic Sea into account - MARNET autonomous stations and tide gauge stations of the Belt Sea and Landsort in the central Baltic Sea-, show a salt import of 0.8 Gt and a total volume of 77 km³. Usually total volumes 150-200 km³ and above indicate moderate to stronger inflow activity.

A general overview about the total import of volume can be calculated with the Landsort tide gauge data and the empirical approximation formula:

$\Delta V/km^3 = 3.8 \times \Delta L/cm - 1.3 \times \Delta t/d$ (NAUSCH et al. 2002, FEISTEL et al. 2008).

It is possible using the values of the difference in gauge level ΔL in cm and the inflow duration Δt in days to estimate the inflow volume ΔV.

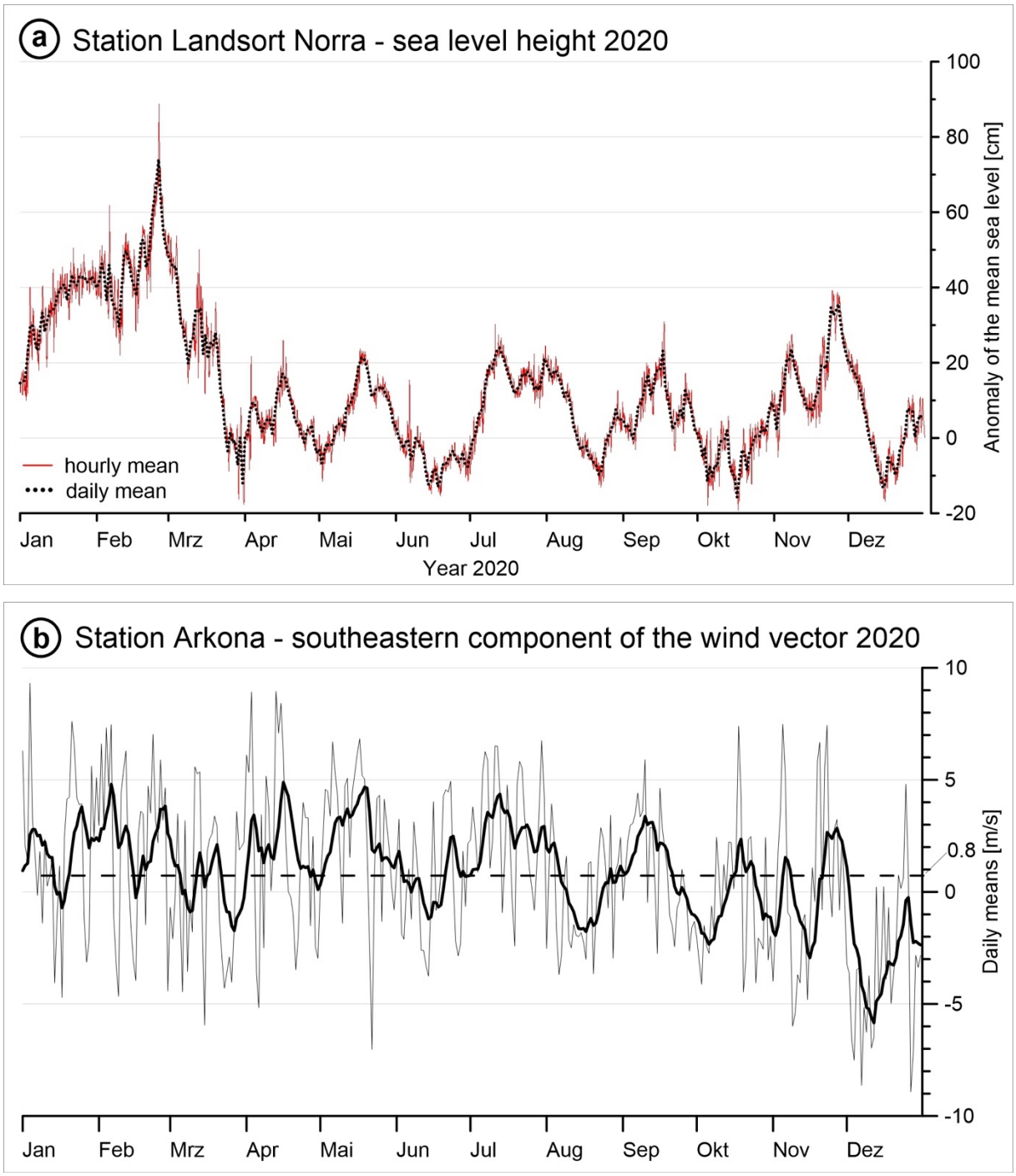

Fig. 7: above (a): Sea level at Landsort as a measure of the Baltic Sea fill factor (from data of SMHI 2021a). below (b): Strength of the southeastern component of the wind vector (northwesterly wind positive) at the weather station Arkona (from data of DWD 2021a). The bold curve appeared by filtering with an exponential 10-days memory and the dashed line depicts the annual average of 0.84 m/s.

A short interruption to moderate easterly winds (Fig. 7b) caused a slight sea level drop to 29 cm (February 10th). Afterwards, a stepwise sea level rise to +74 cm MSL (February 26th) occurred due to prevailing moderate-strong westerly winds. In total, a volume of 150 km³ and 1.4 Gt salt was imported. This was the highest level of the year. Up to end of March a longer and stepwise outflow period occurred (March 31st, -12 cm MSL). During spring, summer and early autumn the

sea level fluctuated only slightly between -10 cm MSL to +20 cm MSL. At October 17th the lowstand of the year of -16 cm MSL was reached. A short phase of stronger westerly winds caused a rapid rise from +7 cm to +35 cm MSL between October 16th-24th, which comprise a total volume of 96 km³ and 0.5 Gt of salt. Afterwards longer outflow occurred up to December 15th (-13 cm MSL). To the end of 2020 the sea level increased slightly up to +5 cm MSL.

Compared to previous years of very low inflow activity (2017) the year 2020 is characterized as a usual inflow year. This is visualized in Fig. 8 by the accumulated inflow volume through the Öresund (SMHI 2021b), where the inflow curve of 2020 runs around the long-term values since the year 1977 like the previous year 2019. In comparison the curve of 2014 is shown, the year in which in December the latest very strong Major Baltic Inflow occurred (MOHRHOLZ et al. 2015).

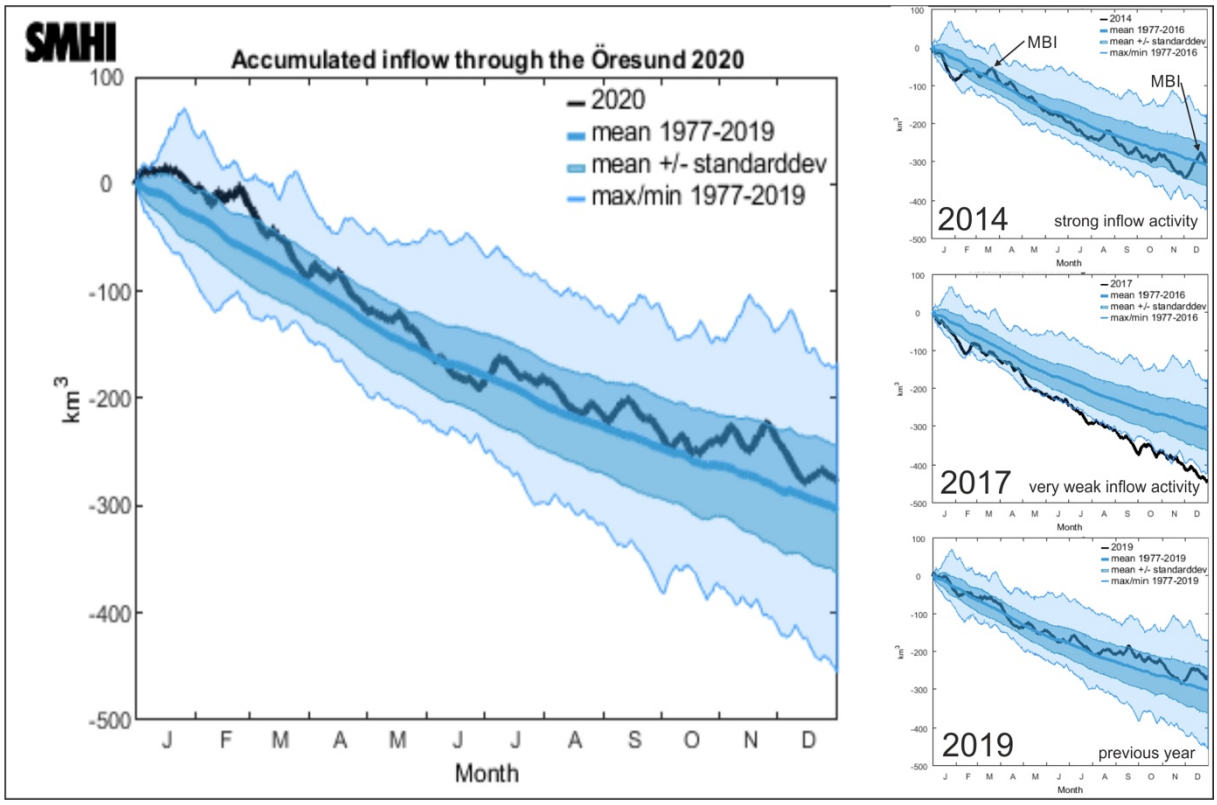

Fig. 8: Accumulated inflow (volume transport) through the Öresund during 2020 in comparison to the previous year and year 2017 of very weak inflow activity and 2014, characterized by the very strong Major Baltic Inflow in December (SMHI 2021b).

3.2 Observations at the MARNET monitoring platform "Darss Sill"

The monitoring station at the Darss Sill supplied complete records during the year 2020. Only the oxygen sensors data for the last two weeks of December are missing. The ADCP provided nearly complete data records throughout the observation period. However, due to some synchronisation issues between the instantaneous online data and the analogue stored data, a data gap in the database for the beginning of November exists. However, the raw data are recorded and will be soon fed into the database.

As usual, in addition to the automatic oxygen readings taken at the observation mast, discrete comparative measurements of oxygen concentrations were taken at the depths of the station's sensors using the Winkler method (cf. GRASSHOFF et al., 1983) during the regular maintenance cruises. Oxygen readings were corrected accordingly.

3.2.1 Statistical Evaluation

The bulk parameters determining the water mass properties at Darss Sill were determined from a statistical analysis based on the temperature and salinity time series at different depths. Short data gaps in salinity time series did not bias the annual statistics.

To expand first on the larger picture, Europe had its warmest year on record at 2.16 K above average, surpassing the previous record set in 2018 by 0.28 K. This was also the first year where Europe's annual temperature departure was over +2.0 K. The years 2014 through 2020 all rank among Europe's seven warmest years on record. The year 2020 marked the 24th consecutive year with above-average temperature departures.

Similar to the large scale **temperature** trend, the temperature recordings of 2020 in the surface waters of Darss Sill were also well above the record-setting year 2014 and 2018. The yearly mean temperatures (Table 4) for the year 2020 were with 10.75 °C higher than in 2014 (10.58 °C) and 2018 (10.54 °C). Annual mean surface-layer temperatures for 2020 are ranked first in the entire record since 1992 (i.e. in the upper quartile). The standard deviation of the surface layer temperatures shows lower than average values. The lowest temperature recorded was 4.74 °C (Table 6), 2 K warmer than usual.

This can also be seen in Fig. 9. Here, we show the anomaly of the near-surface temperature. The climatology was based on the data set of REYNOLDS et al., 2007 and covered the period 1982-2011. This period can be regarded as close to the national reference period (1981-2010). In spring and autumn, the water was up to 3 K warmer than the long-term mean. From June till late September, the surface waters were close to normal, only interrupted by a cold anomaly mid August at Darss Sill (caused by an upwelling event, see Sec. 3.3). From October on, water temperatures were again up to 3 K above the long-term mean. The temperatures in 17 m and 19 m also mark 2020 as the warmest year since 1992.

The mean **salinities** and their standard deviations at the station Darss Sill are given in Table 4. The values of the lowermost two sensors reflect the near-bottom variability in salinity and are therefore a sensitive measure for the overall inflow activity. Unlike the year 2016, and the year 2014, both characterised by strong inflow activity, the year 2020 shows below-average mean salinity and weak near-bottom salinity fluctuations. The variability at the 19m sensors can be ranked as below average. In combination with the low variability, the low mean salinity already indicated a weak inflow activity in 2020.

The amplitude and phase shift of the annual cycle were determined from a Fourier analysis of the temperature time series at 7 m depth (surface layer) and at the two lowermost sensors (17 m and 19 m depth). This method finds the optimal fit of a single Fourier mode (a sinusoidal function) to the data. The amplitude and phase can easily be inferred as the characteristic parameters of the annual cycle. The results are compiled inTable 5.

Table 4: Annual mean values and standard deviations of temperature (T) and salinity (S) at the Darss Sill. Maxima in boldface.

	7 m Depth		17 m Depth		19 m Depth	
	T	S	T	S	T	S
Year	°C	g/kg	°C	g/kg	°C	g/kg
1992	9.41 ± 5.46	9.58 ± 1.52	9.01 ± 5.04	11.01 ± 2.27	8.90 ± 4.91	11.77 ± 2.63
1993	8.05 ± 4.66	9.58 ± 2.32	7.70 ± 4.32	11.88 ± 3.14	7.71 ± 4.27	13.36 ± 3.08
1994	8.95 ± 5.76	9.55 ± 2.01	7.94 ± 4.79	13.05 ± 3.48	7.87 ± 4.64	14.16 ± 3.36
1995	9.01 ± 5.57	9.21 ± 1.15	8.50 ± 4.78	10.71 ± 2.27	–	–
1996	7.44 ± 5.44	8.93 ± 1.85	6.86 ± 5.06	13.00 ± 3.28	6.90 ± 5.01	14.50 ± 3.14
1997	9.39 ± 6.23	9.05 ± 1.78	–	12.90 ± 2.96	8.20 ± 4.73	13.87 ± 3.26
1998	8.61 ± 4.63	9.14 ± 1.93	7.99 ± 4.07	11.90 ± 3.01	8.10 ± 3.83	12.80 ± 3.22
1999	8.83 ± 5.28	8.50 ± 1.52	7.96 ± 4.39	12.08 ± 3.97	7.72 ± 4.22	13.64 ± 4.39
2000	9.21 ± 4.27	9.40 ± 1.33	8.49 ± 3.82	11.87 ± 2.56	8.44 ± 3.81	13.16 ± 2.58
2001	9.06 ± 5.16	8.62 ± 1.29	8.27 ± 4.06	12.14 ± 3.10	8.22 ± 3.86	13.46 ± 3.06
2002	9.72 ± 5.69	8.93 ± 1.44	9.06 ± 5.08	11.76 ± 3.12	8.89 ± 5.04	13.11 ± 3.05
2003	9.27 ± 5.84	9.21 ± 2.00	7.46 ± 4.96	14.71 ± 3.80	8.72 ± 5.20	15.74 ± 3.27
2004	8.95 ± 5.05	9.17 ± 1.50	8.36 ± 4.52	12.13 ± 2.92	8.37 ± 4.44	12.90 ± 2.97
2005	9.13 ± 5.01	9.20 ± 1.59	8.60 ± 4.49	12.06 ± 3.06	8.65 ± 4.50	13.21± 3.31
2006	9.47 ± 6.34	8.99 ± 1.54	8.40 ± 5.06	14.26 ± 3.92	9.42 ± 4.71	16.05 ± 3.75
2007	9.99 ± 4.39	9.30 ± 1.28	9.66 ± 4.10	10.94 ± 1.97	9.63 ± 4.08	11.39 ± 2.00
2008	9.85 ± 5.00	9.53 ± 1.74	9.30 ± 4.60	-	9.19 ± 4.48	-
2009	9.65 ±5.43	9.39 ±1.67	9.38 ±5.09	11.82 ±2.47	9.35 ±5.04	12.77 ±2.52
2010	8.16 ± 5.98	8.61 ± 1.58	7.14 ± 4.82	11.48 ± 3.21	6.92 ± 4.56	13.20 ± 3.31
2011	8.46 ± 5.62	-	7.76 ± 5.18	-	7.69 ± 5.17	-
2012	-	-	-	-	-	-
2013	-	-	-	-	-	-
2014	10.58 ± 5.58	9.71 ± 2.27	10.01 ± 4.96	13.75 ± 3.53	9.99 ± 4.90	14.91 ± 3.40
2015	-	-	-	-	-	-
2016	10.23 ± 5.63	9.69 ± 1.98	9.27 ± 4.59	14.07 ± 3.53	9.11 ± 4.43	15.56 ± 3.45
2017	9.67 ± 5.05	9.40 ± 1.58	9.23 ± 4.54	11.65 ± 2.50	9.20 ± 4.45	12.39 ± 2.61
2018	10.54 ±6.62	8.76 ± 1.16	9.24 ± 5.41	11.58 ±3.23	9.16 ± 5.27	12.56 ± 3.56
2019	10.34 ±5.25	9.57 ± 1.89	9.83 ± 4.65	12.50 ±2.95	9.83 ± 4.50	13.41 ± 3.07
2020	10.75 ±4.56	9.68 ± 1.59	10.39 ± 4.25	11.75 ±2.95	10.28 ± 4.11	12.44 ± 2.59

Table 5: Amplitude (K) and phase (converted into months) of the yearly cycle of temperature measured at the Darss Sill in different depths. Phase corresponds to the time lag between temperature maximum in summer and the end of the year. Maxima in boldface.

	7 m Depth		17 m Depth		19 m Depth	
	Amplitude	Phase	Amplitude	Phase	Amplitude	Phase
Year	K	Month	K	Month	K	Month
1992	7.43	4.65	6.84	4.44	6.66	4.37
1993	6.48	4.79	5.88	**4.54**	5.84	**4.41**
1994	7.87	4.42	6.55	4.06	6.32	4.00
1995	7.46	4.36	6.36	4.12	–	–
1996	7.54	4.17	6.97	3.89	6.96	3.85
1997	8.60	**4.83**	–	–	6.42	3.95
1998	6.39	4.79	5.52	4.46	–	–
1999	7.19	4.52	5.93	4.00	5.70	3.83
2000	5.72	4.50	5.02	4.11	5.09	4.01
2001	6.96	4.46	5.35	4.01	5.11	3.94
2002	7.87	4.53	6.91	4.32	6.80	4.27
2003	8.09	4.56	7.06	4.30	**7.24**	4.19
2004	7.11	4.48	6.01	4.21	5.90	4.18
2005	6.94	4.40	6.23	4.03	6.21	3.93
2006	**8.92**	4.32	7.02	3.80	6.75	3.72
2007	6.01	4.69	5.53	4.40	5.51	4.36
2008	6.84	4.60	6.23	4.31	6.08	4.24
2009	7.55	4.57	7.09	4.37	7.03	4.32
2010	8.20	4.52	6.54	4.20	6.19	4.08
2011	7.70	4.64	6.98	4.21	7.04	4.14
2012	–	–	–	–	–	–
2013	–	–	–	–	–	–
2014	7.72	4.43	6.86	4.17	6.77	4.13
2015	–	–	–	–	–	–
2016	7.79	4.65	6.33	4.33	6.11	4.23
2017	7.00	4.56	6.20	4.31	6.15	4.28
2018	8.82	4.53	**7.31**	4.08	7.18	4.01
2019	7.29	4.47	6.42	4.21	6.22	4.18
2020	6.29	4.36	5.85	4.17	5.66	4.07

Similar to the elevated mean temperatures and lower than average variability in 2020, discussed above, Table 5 shows that also the amplitudes of the annual cycle at different depths are below the long-term average. Thus, 2020 was characterised by a high mean temperature but a weak

yearly cycle. Compared to the pronounced phase lag of approximately 0.5 months between the surface and near-bottom temperatures in 2018, the near-bottom water temperature closely follows the onset of surface warming. The near-bottom temperature at 19 m depth also shows a weak annual cycle.

Table 6: Listing of the minimum and maximum temperature measured at 7m water depth at Darss Sill. Time indicates the date of occurrence. The column Range provides the difference between the minimum and maximum temperature. Minima and maxima are highlighted in boldface. For the event of the annual maximum, we indicated in boldface the first-ever recording.

	Minimum		Maximum		
	Temperature	Time	Temperature	Time	Range
Year	°C		°C		°C
1995	0.98	30.12	20.54	05.08	19.56
1996	0.37	27.01	17.65	09.08	17.28
1997	0.16	21.01	22.50	19.08	22.34
1998	2.59	16.12	16.61	10.08	14.02
1999	1.55	18.02	19.84	31.07	18.29
2000	2.65	25.01	17.87	14.08	15.22
2001	2.33	28.03	20.65	29.07	18.32
2002	2.03	13.01	20.24	30.08	18.21
2003	0.09	11.01	21.92	13.08	21.83
2004	1.45	28.02	19.11	20.08	17.66
2005	1.50	13.03	19.79	13.07	18.29
2006	0.40	30.01	22.80	21.07	**22.40**
2007	3.36	25.02	18.70	14.08	15.34
2008	3.12	17.02	19.67	29.07	16.55
2009	1.65	25.02	19.62	10.08	17.97
2010	**-0.44**	05.02	20.33	21.07	20.77
2011	-0.12	05.01	17.94	12.07	18.06
2012	–	–	–	–	-
2013	–	–	–	–	
2014	1.54	09.02	21.61	09.08	20.07
2015	2.95	04.02	18.14	13.08	15.19
2016	1.81	23.01	20.42	28.07	18.61
2017	2.09	19.02	18.61	30.08	16.52
2018	1.11	18.03	**23.10**	04.08	21.99
2019	2.82	26.01	20.91	01.09	18.09
2020	4.74	07.01	19.51	22.08	14.77

To provide a final statistical measure, we evaluated the minimum and maximum temperatures recorded at 7m water depth at Darss Sill. Table 6 indicates that we recorded in 2020 the warmest winter since 1995. The winter minimum temperature was 4.74 °C. As already shown in Fig. 9, the entire winter was nearly 3K to warm. The maximum value, recorded at the end of August, was with 19.51 °C close to the longer-term mean. Additionally, due to the warm winter and autumn, the temperature range in 2020 was below the long-term mean.

3.2.2 Temporal development at Darss Sill

Fig. 9 shows the development of water temperature and salinity in 2020 in the surface layer (7 m depth) and the near-bottom region (19 m depth). As in the previous years, the currents observed by the bottom-mounted ADCP in the surface and bottom layers were integrated in time, respectively, to emphasise the low-frequency baroclinic (depth-variable) component, plotted in Fig. 11 as a 'progressive vector diagram' (pseudo-trajectory). This integrated view of the velocity data filters short-term fluctuations and allows long-term phenomena such as inflow and outflow events to be identified more clearly. According to this definition, the average current velocity corresponds to the slope of the curves shown in Fig. 11, using the convention that positive slopes reflect inflow events.

The year 2020 started with the aftermath of a weak inflow event, which began mid December. Stratification in temperature and salinity was low, as indicated by the salinity stratification index G (MATTHÄUS & FRANK, 1992), as shown in the lower panel of Fig. 9. However, salinity values peaked at 17 g/kg. The weak inflow activity is also supported by the ADCP data, showing consistent inflow activity over the entire water column (Fig. 11). In February, the flow direction changed, and the regular outflow condition was re-established. This dynamics can also be seen in the sea level data at Landsort Norra, which showed a filling of the Baltic Sea until mid February, caused by westerly winds.

The anomalous high water temperatures of 5 °C lasted until mid April, until the spring stratification kicked in. The lowest temperature of 4.74 °C at Darss Sill was recorded at 07.01 (Table 6).

For the entire spring until the beginning of summer, salinity stratification was low, accompanied by low salinity. This outflow situation is also supported by the ADCP measurements (Fig. 9), showing negative values and a strong descent. In the second half of May, easterly winds of up to 13 m/s shortly reversed the outflow. However, the elevated wind speeds homogenised the water column at Darss Sill and removed any stratification in temperature and salinity (Fig. 9). The stratification measure (Fig. 9, lower panel), was close to zero, indicating the lack of stratification.

From June on until mid of August, a thermal stratification could build up with a maximum temperature difference between surface and bottom of 4 K. The two-layer flow lead to a decoupling of well oxygenised surface waters from the stagnant bottom waters. In August, the near bottom oxygen saturation dropped to 55% (Fig. 12).

In the second week of August, the wind turned to easterly directions but stayed calm. During the following two weeks, the surface temperature at Darss Sill dropped by 4 K. At the same time, the oxygen saturation fell below 20%. The change in water mass property was caused by an

upwelling event (Fig. 13), bringing colder, low oxygen waters from the western Arkona Basin to Darss Sill. A more detailed discussion about the upwelling is given in Sec 3.3.

After the wind turned again to westerly directions and increased to 10 m/s, the water level at Landsort Norra increased by 30 cm, leading to weak inflow activity. Although stratification at Darss Sill was still present, the bottom salinity increased to 17-18 g/kg. With the onset of the inflow, the oxygen saturation recovered to nearly 90%.

Three weeks later, a further period with easterly winds occupied the Baltic Sea. The average wind speed peaked at 15 m/s. However, gustiness reached values of up to 25 m/s. During this outflow activity, low oxygen water masses passed Darss Sill, showing saturation values of 35%. Simultaneously, the temperature of the near-bottom waters increased by 2 K. Likely, the origin of the water masses was again the western Arkona Basin. The newly arrived water masses also lead to a temperature inversion at Darss Sill, showing 2 K higher temperatures near the bottom than at the surface.

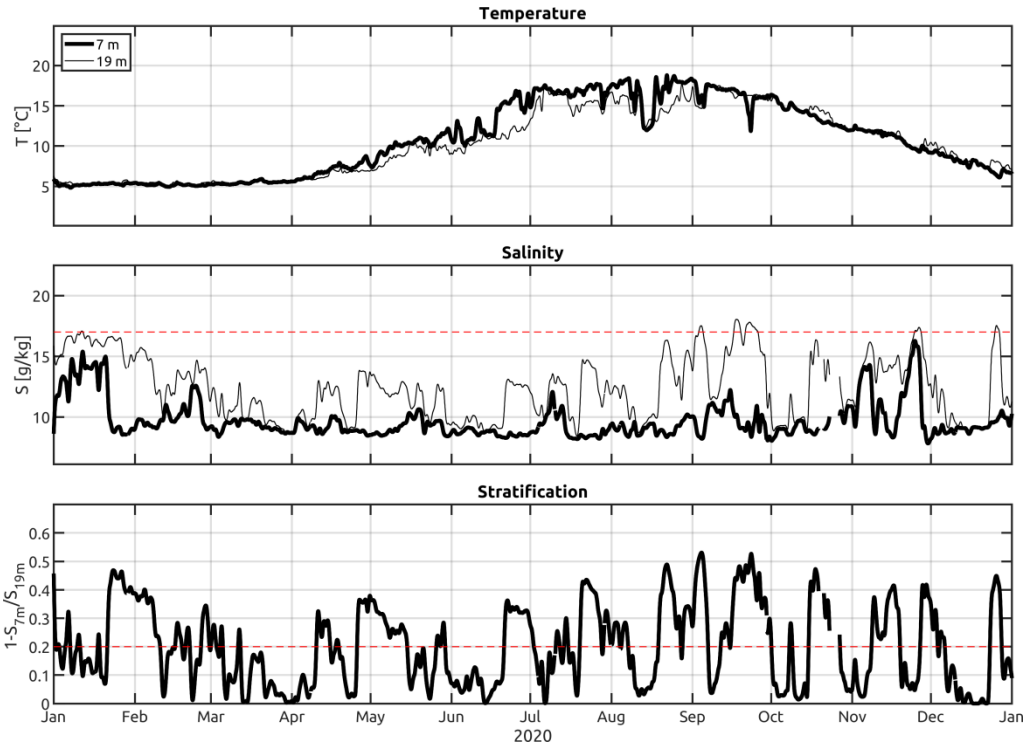

Fig. 9: Water temperature (upper panel) and salinity (middle panel) measured in the surface layer and the near-bottom layer at Darss Sill in 2020. The red dashed line indicates the salinity threshold of 17 g/kg.). In the lower panel, we show a stratification measure G according to MATTHÄUS & FRANK (1992). Here the red dashed line marks the stratification threshold of 0.2.

Like the first three months of the year, the last three months of the year showed a warm surface temperature anomaly of 2.5-3 K above normal (Fig. 10). The week westerly winds did not promote significant inflow activity. However, the bottom salinity steadily increased to reach at the end of November maximum values of 17 g/kg. End of November, the wind calmed down, leading to a relaxation of the water levels at Landsort Norra. Within some days, the Baltic Sea filling state

dropped by 50 cm, causing outflow at Darss Sill, and water masses with low salinity occupied the entire water column. The ADCP measurements also show a consistent outflow pattern over the water column as a whole.

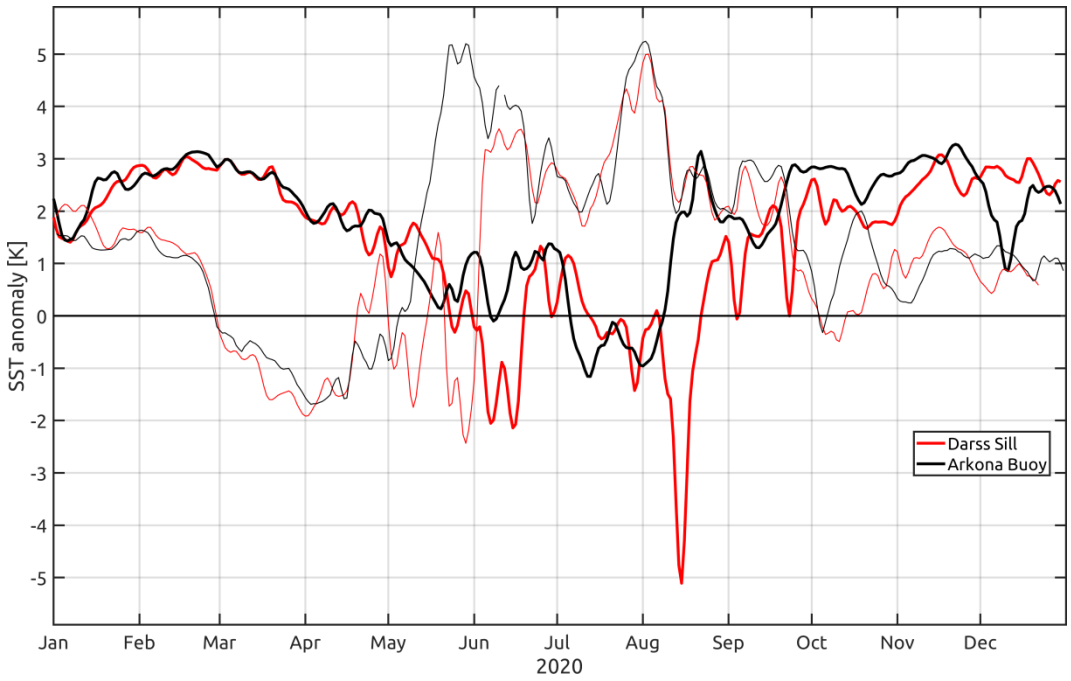

Fig. 10: Deviation of near-surface temperature from the climatology at Darss Sill and Arkona Buoy in 2020. The climatology was built for the national reference period 1981-2010 and is based on REYNOLDS et al., 2007. The thin lines show the anomaly from 2018.

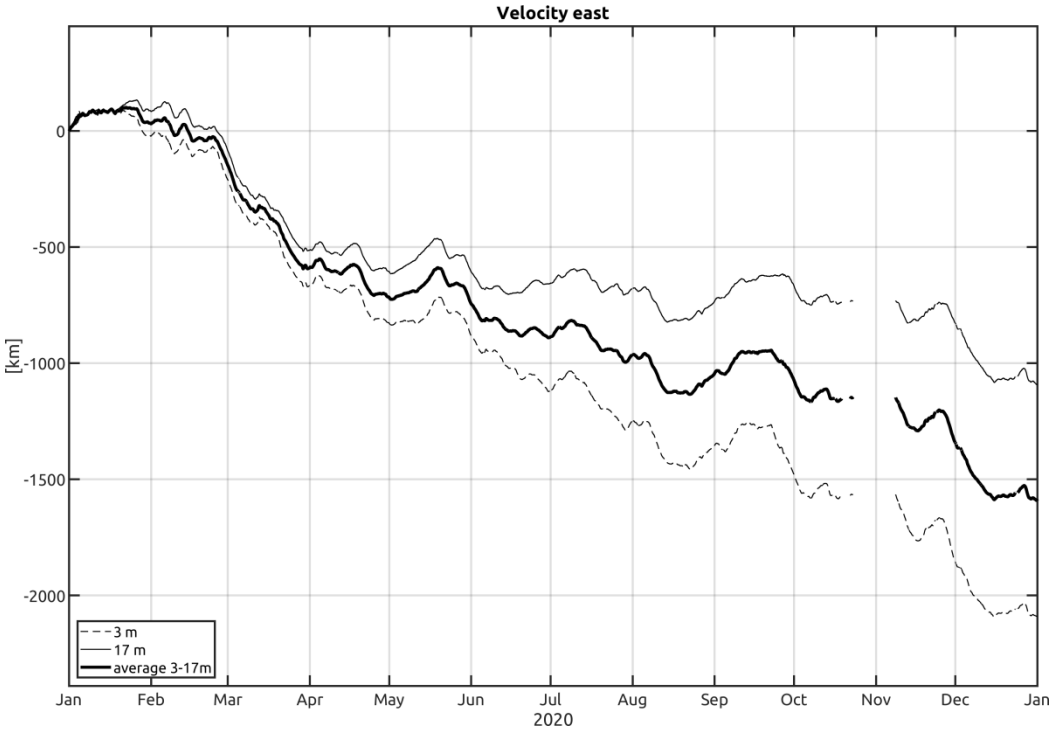

Fig. 11: East component of the progressive vector diagrams of the current in 3 m depth (solid line), the vertical averaged current (thick line), and the currents in 17 m depth (dashed line) at the Darss Sill in 2020.

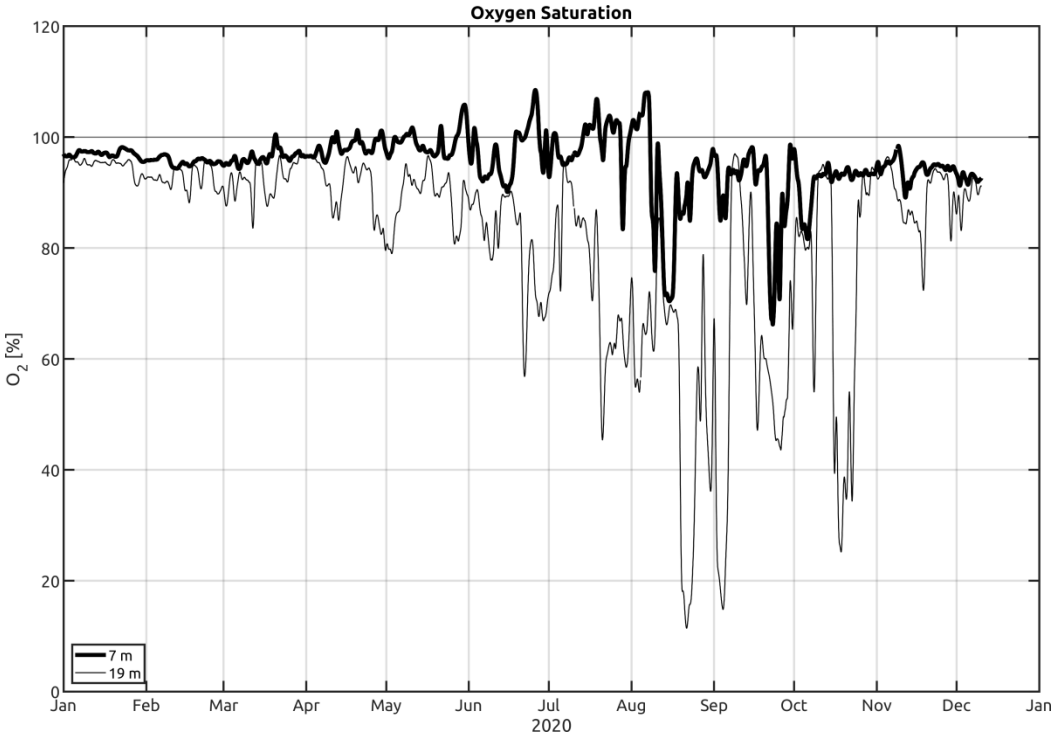

Fig. 12: Oxygen saturation measured in the surface and bottom layer at the Darss Sill in 2020.

3.2.3 An upwelling event

In the second week of August, the wind turned to easterly directions, but stayed calm. During the following two weeks, the surface temperature at Darss Sill dropped by 4 K (Fig. 9). At the same time, the oxygen saturation fell below 20%. The change in water mass property was caused by an upwelling event (Fig. 12), bringing colder, low oxygen near-bottom waters from the western Arkona Basin to Darss Sill.

To get a spatial impression of the western Baltic Sea, we analysed a numerical model's results with 600 m spatial resolution (GRÄWE et al., 2015). A snapshot of the surface temperature is shown in Fig. 13. Here, we present the conditions on the 17th August. Although the model underestimates the upwelling's total extend, one can clearly see that large parts of the coast from Hiddensee up to Fehmarn were affected by this event. Even upwelling filaments, generated at the northern coast of Fehmarn, were advected as far west as Kiel.

The upwelling lasted from 8th August until 22nd August. During the upwelling, the bottom oxygen conditions worsened. The oxygen saturation dropped from 70% to values below 20% (Fig. 12). Likely, the water masses originated from the western Arkona Basin. The low oxygen saturation points towards stagnant water, which can only found in the Arkona Basin or the Mecklenburg Bight. Since the latter is downstream of the upwelling, this potential origin can be excluded.

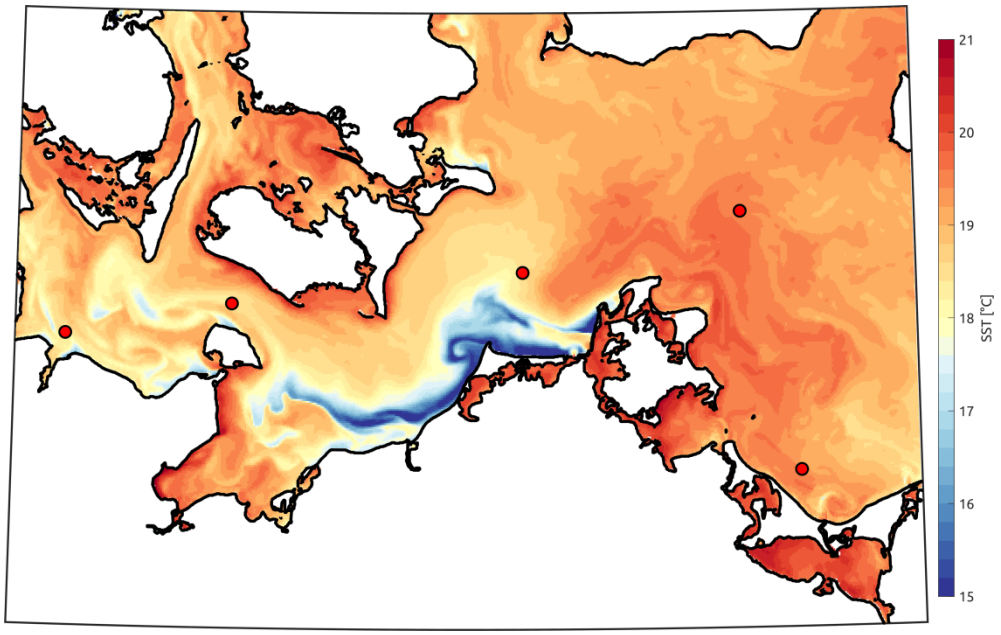

Fig. 13: Modelled sea surface temperature on 17th August in the western Baltic Sea. The red dots mark the location of the MARNET stations.

3.3 Observations at the MARNET monitoring buoy "Arkona Basin"

3.3.1 Temporal development until summer

The Arkona Basin monitoring station (AB) described in this chapter is located almost 20 nm north-east of Arkona in 46 m water depth. The monitoring station in the Arkona Basin supplied complete records during the year 2020. As described in chapter 3.2, the optode-based oxygen measurements at the monitoring station were corrected with the help of the Winkler method, using water samples collected and analysed during the regular MARNET maintenance cruises. Due to some ongoing validation, the oxygen data for December are still missing.

Fig. 14 shows the time series of water temperature and salinity at depths of 7 m and 40 m, representing the surface and bottom layer properties. Corresponding oxygen concentrations plotted as saturation values as in the previous chapter, are shown in Fig. 15.

Similar to the Darss Sill measurements, also at station AB, the first three months of the year were characterised by an anomalous warm surface layer (see also Fig. 10). The lowest daily mean temperatures of the year, approximately 5.05 °C, were reached on 27.01. (Fig. 14), about 0.3 K higher than the minimum temperatures measured 20 days earlier at the Darss Sill. While the local atmospheric fluxes largely determine the surface temperatures in the Arkona Basin, those at the Darss Sill are more strongly affected by lateral advection, which may explain the observed differences.

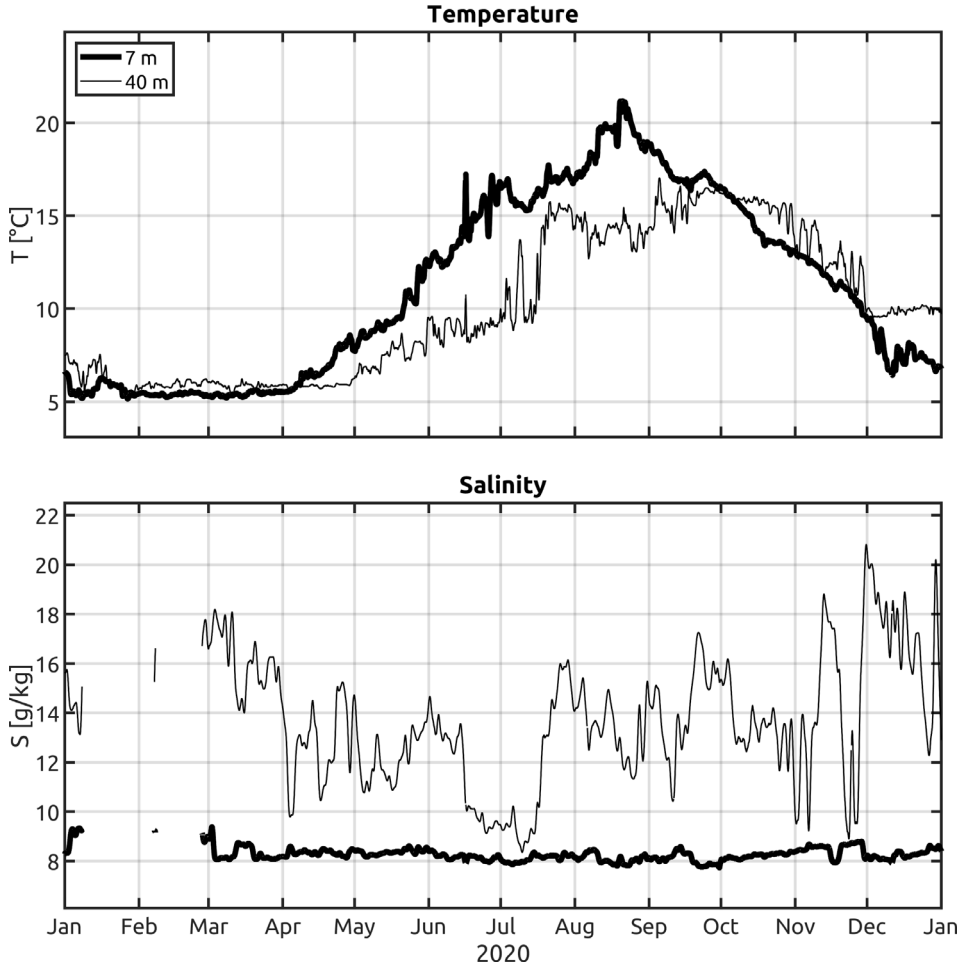

Fig. 14: Water temperature (above) and salinity (below) measured in the surface layer and near-bottom layer at the station AB in the Arkona Basin in 2020.

The water mass properties in the bottom layer during the first two weeks of 2020 were determined by the aftermath of small inflow events in the second half of December 2019. Peak salinities in the bottom waters reached 18 g/kg. Since the maximum salinities at Darss Sill were reaching 17 g/kg, during the end of 2019, the water masses must originate from Drogden Sill. Nearly stagnant temperatures around 5-6 °C suggest that the near-bottom region was decoupled from direct atmospheric cooling. The slowly decaying salinities indicate the draining of the bottom pool of salty and dense inflow waters through the Bornholm Channel (Fig. 14). The oxygen demand due to respiration is usually small during this time of the year due to low water temperatures, and oxygen concentrations therefore did not fall below approximately 80% of the saturation threshold (Fig. 15).

During March, the entire water column was homogeneous in temperature. Only a haline stratification existed. With the end of April and the beginning of May, two wind events with gust larger than 25 m/s, some mixing happened in the Arkona Basin. The slight thermal stratification collapsed. Additionally, the bottom salinity dropped to 11 g/kg in the bottom waters, close to the near-surface values.

After this event, the wind calmed down. Until the mid of July, a thermal stratification could build up with a maximum temperature difference between surface and bottom of 8 K. The two-layer

flow lead to a decoupling of well oxygenised surface waters from the stagnant bottom waters. End of June, the near bottom oxygen saturation dropped to 60% (Fig. 15).

At the end of June, a bloom lead to an oxygen-oversaturation of up to 120% (Fig. 15). At the same time, the oxygen saturation in the lower half of the water column started slowly to decline. Due to the double stratification (halocline and thermocline) shielding effect and low vertical mixing, no new oxygen could arrive from the well-saturated surface waters.

Starting in mid-July, water masses with higher salinities arrived at AB. Peak salinities reached 16 g/kg. At the same time, the near-bottom temperature increased by 5 k to 15 °C. Since the bottom water at Darss Sill (two weeks earlier) had temperatures of 12 °C and salinity of 14 g/kg, the newly arrived water likely originated again from Drogden Sill. Although salinity and temperature increased, the oxygen values further declined. Thus, stagnant water approached AB.

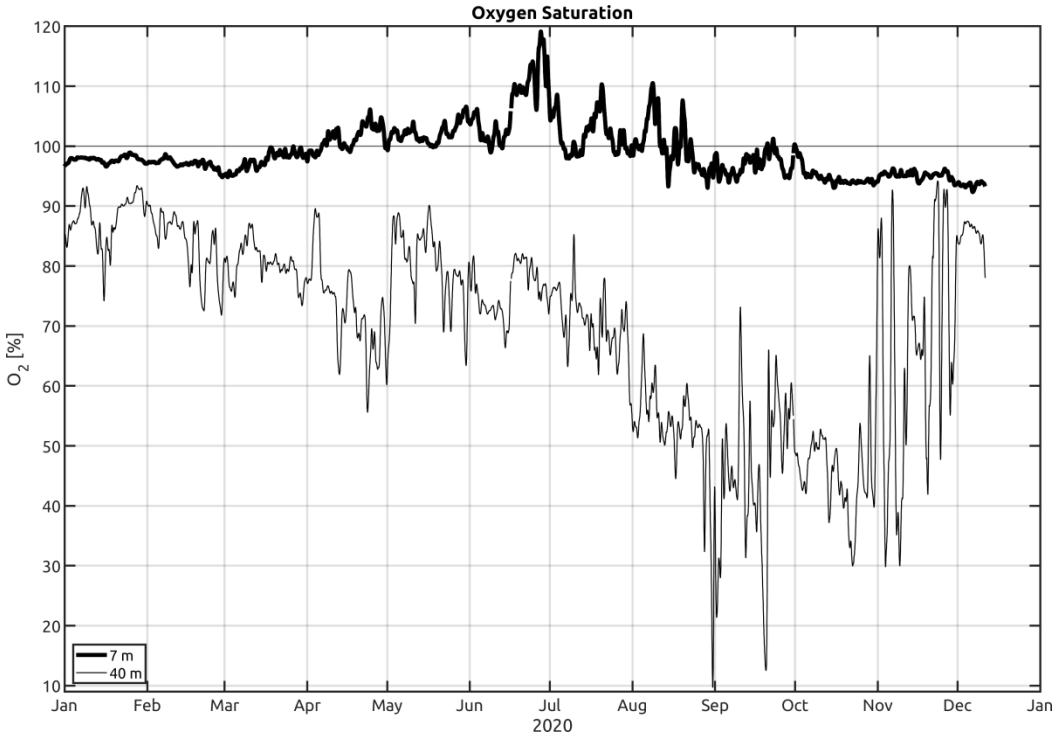

Fig. 15: Oxygen saturation measured in the surface and bottom layer at the station AB in the Arkona Basin in 2020.

3.3.2 Cooling in autumn

After the warmest day, 21st August, the surface and bottom waters started to cool down. Until the start of December, the bottom waters showed a nearly linear decline, indicating that vertical diffusion was the main driver of the cooling.

At the beginning of November, some highly saline waters reached Arkona Buoy. Peak salinities of 19 g/kg were observed. Since the measurements at Darss Sill only showed peak values of 16 g/kg (Fig. 9), part of the arriving water took the path through the Öresund. The same holds for the arrival of water masses with salinities of 21 g/gk, at the beginning of December. Indeed, the

numerical model indicates two inflows at Drogden Sill. Via this pathway, freshly oxygenised water entered the Arkona Basin. The oxygen saturation recovered from 30% to nearly 90% (Fig. 15). For the entire December, the near-bottom temperature stayed nearly constant, indicating that the bottom waters again decoupled from the surface waters and that the inflow had passed the station to propagate further into the Bornholm Basin.

3.4 Observations at the MARNET monitoring buoy "Oder Bank"

The water mass distribution and circulation in the Pomeranian Bight have been investigated in the past as part of the TRUMP project (TRansport und UMsatzprozesse in der Pommerschen Bucht) (v. BODUNGEN et al., 1995; TRUMP, 1998), and were described in detail by SIEGEL et al. (1996), MOHRHOLZ (1998) and LASS, MOHRHOLZ & SEIFERT (2001). For westerly winds, well-mixed water is observed in the Pomeranian Bight with a small amount of surface water from the Arkona Basin admixed to it. For easterly winds, water from the Oder Lagoon flows via the rivers Świna and Peenestrom into the Pomeranian Bight, where it stratifies on top of the bay water off the coast of Usedom. As shown below, these processes have an important influence on primary production and vertical oxygen structure in the Pomeranian Bight.

The Oder Bank monitoring station (OB) is located approximately 5 nm north-east of Koserow/Usedom at a water depth of 15 m, recording temperature, salinity, and oxygen at depths of 3 m and 12 m. The oxygen measurements were validated with the help of water samples taken during the regular maintenance cruises using the Winkler method. After the winter break, the monitoring station OB was brought back to service relatively late in the year, on 9th July 2020. Starting from that date, the station provided a continuous time series of all parameters until 8th December, when it was again demobilised to avoid damage from floating ice.

Temperatures and salinity at OB are plotted in Fig. 16; associated oxygen readings are presented in Fig. 17. Similar to the other MARNET stations, the maximum temperatures that were reached during the summer period were lower than in 2018 (the maximum temperature at OB 24.8 °C), but comparable with the years 2010, 2013, and 2014, when temperatures of up to 23 °C were observed at station OB. In 2020, the maximum hourly mean temperature reached on 10th August 22.5 °C, similar to 2019. As in the previous years, surface temperatures at the monitoring station OB were significantly larger compared to those at the deeper and more energetic stations in the Arkona Basin and the Darss Sill (see Fig. 10 and Fig. 14), which reflects the shallower and more protected location of this station.

On average years, there is also a dynamical reason for the more substantial warming of the surface layer at station OB, related to the suppression of vertical mixing due to the transport of less saline (i.e., less dense) waters from the Oder Lagoon on top of the more salty bottom waters (e.g. LASS et al., 2001). However, during 2020 the precipitation over most of the Oder catchment was like in 2019: lower than the long-term mean. The missing rain leads to lower water levels in the Oder until late autumn. Thus, the Oder plume's impact in the Pomeranian Bight was of less dynamical importance in 2020.

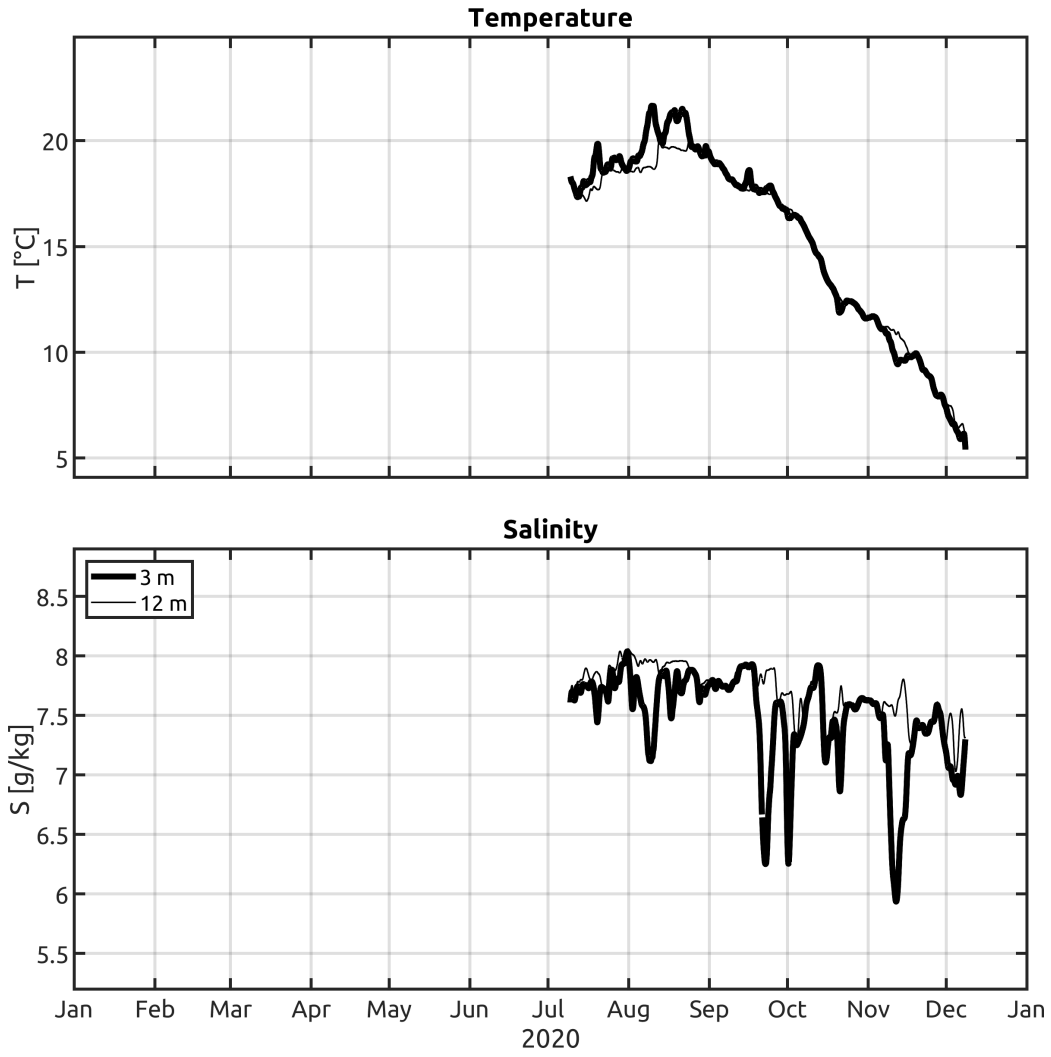

Fig. 16: Water temperature (above) and salinity (below) measured in the surface layer and near-bottom layer at the station OB in the Pomeranian Bight in 2020.

With the start of service in July, a temperature and haline stratification developed. The temperature gradient between the surface and bottom layers varied around 2 K. During August, peak values of 5 K were reached.

The upwelling at Darss Sill (see Sec. 3.2.3), caused by prolonged easterly winds during August, had little consequence for the Pomeranian Bight. At first, thermal stratification was weak at Oder Bank. Secondly, the station is too far away from the coast, such that the upwelled water could arrive. Moreover, the model results (Fig. 13) indicate no significant upwelling. However, some smaller filaments are visible close to the outflows of the Oder Lagoon.

From an ecological perspective, the most important consequences of the build-up of stratification and the suppression of turbulent mixing in June were the decrease in near-bottom oxygen concentrations due to the bottom layer's decoupling from direct atmospheric ventilation. Their impact on the Pomeranian Bight's oxygen budget becomes evident from Fig. 17, showing oxygen concentrations at depths of 3 m and 12 m. For August, a distinct correlation can be identified between increasing oxygen saturation in the surface layer and a decrease in the near-

bottom layer, reflecting the effects of primary production and the oxygen demand from remineralisation, respectively.

The lowest near-bottom oxygen concentrations (see Fig. 17) in 2020 were observed at the end of August, with hourly saturation values as low as 65%. With the onset of a slow atmospheric cooling and some stronger winds, the thermal stratification vanished, and near-bottom oxygen levels recovered to 95% saturation.

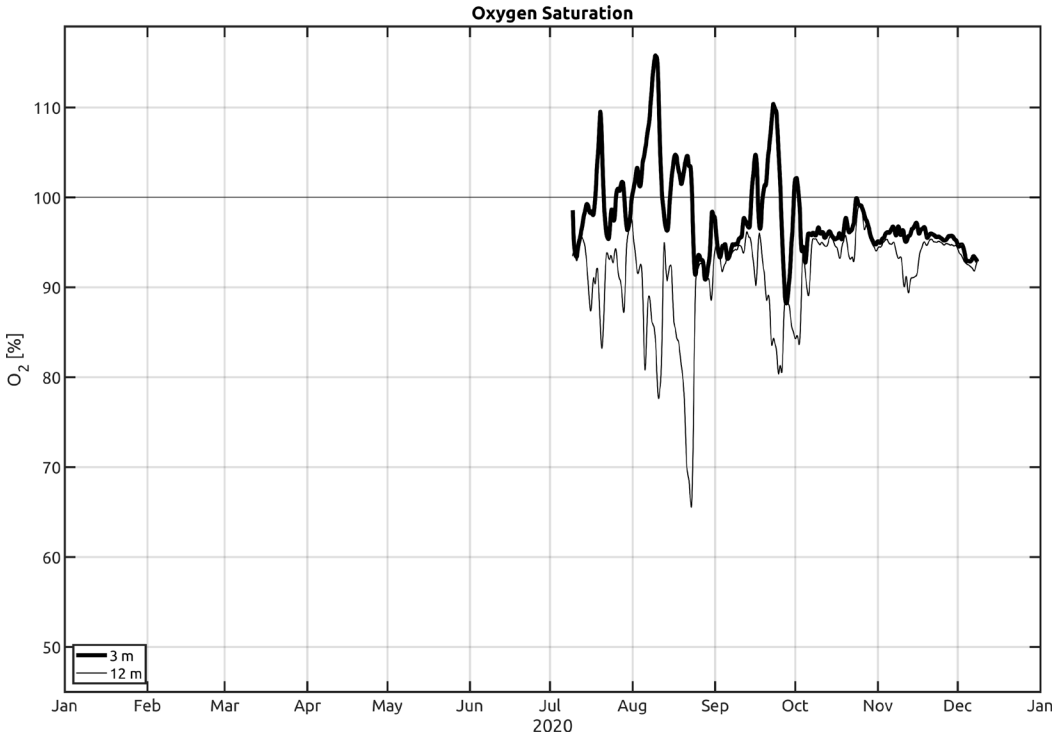

Fig. 17: Oxygen saturation measured in the surface and bottom layer at the station OB in the Pomeranian Bight in 2019.

Finally, it is worth noting that the increase in primary production of biomass in the Oder Lagoon, induced by the lateral transport of lagoon water to station OB, is likely to have resulted in the super-saturated oxygen concentrations that were observed in the surface-layer during all of the above events (Fig. 17). Highest near-surface oxygen concentrations approximately 15% above the saturation level were found in August. In addition, the lagoon water is known to export high nutrient concentrations towards the station. This may have resulted in locally increased production rates, which may explain the increased oxygen concentrations in the surface layer. The correlation between the oxygen increase in the surface layer and the decrease in the near-bottom layer points to increased oxygen consumption rates induced by freshly deposited biomass decay ("fluff").

3.5 Marine Heatwaves

Heatwaves that occur over land are well known for having adverse impacts on human health, infrastructure and agriculture. Less attention has been paid to analogous episodes in the ocean,

dubbed marine heatwaves (MHWs). Still, interest in these transient events is growing as their potentially dramatic ecological and economic impacts1 have become clear.

In 2020, two of the longest MHWs occupied the western Baltic Sea. As shown in Fig. 10, the SST climatology deviations were with +3 K over several months already indicative of the MHWs.

MHWs were identified from daily SST time series in the Arkona Basin, based on the dataset of REYNOLDS et al., 2007. A set of metrics was calculated to characterise their intensity and duration. Following Hobday et al., 2016, an MHW is defined as a discrete prolonged anomalously warm water event. "Discrete" means an identifiable event with recognisable start and end dates; "prolonged" implies a duration of at least 5 days, and "anomalously warm" measures temperatures relative to a baseline climatology and threshold. Periods when daily temperatures were above a threshold based on the seasonally varying 90th percentile for at least five consecutive days, were identified as MHW events. Events with a break of less than 2 days were considered a single event. The climatologically mean and threshold was calculated for each calendar day from the pool of daily SSTs within an 11-day window centred on the calendar day of interest across all years (within the climatology period). The climatology and threshold were smoothed by applying a 31-day moving average. The intensity of a MHW is defined as the area enclosed by the 90th percentile and the actual SST time series.

To illustrate the occurrence of MHW, we show in Fig. 18 time series of SST, climatology and 90th percentile of the SST. The red filled areas mark MHW. One can identify the MHW in July 2018, enclosing the highest SST values recorded since 1982. However, in 2020, two of the longest MHWs occupied the western Baltic Sea. The first MHW started 28th November 2019 and lasted until 10th May 2020. The duration was record-breaking 165 days (see Table 7). In sync with the most extended duration, the MHW also had the highest intensity recorded so far. Besides two short MHWs during summer, a further MHW started on 21st September 2020 and lasted until 6th February 2021. This MHW was only slightly shorter, with 139 days of duration. Nevertheless, the intensity was close the MHW at the beginning of the year (Table 7). Please note that those two MHW occurred in winter.

At present, the impact of MHW (and especially of winter MHWs) on the western Baltic Sea's biogeochemistry is still unclear. Whereas summer MHW have likely only an impact on the surface mixed layer, bounded by the thermocline, winter MHW occurs during well-mixed conditions. Since no or only weak thermal stratification exists, the MHW leaves an imprint on the bottom water. Thus, the nutrient availability and oxygen saturation in early spring are affected by the anomalous warm bottom waters.

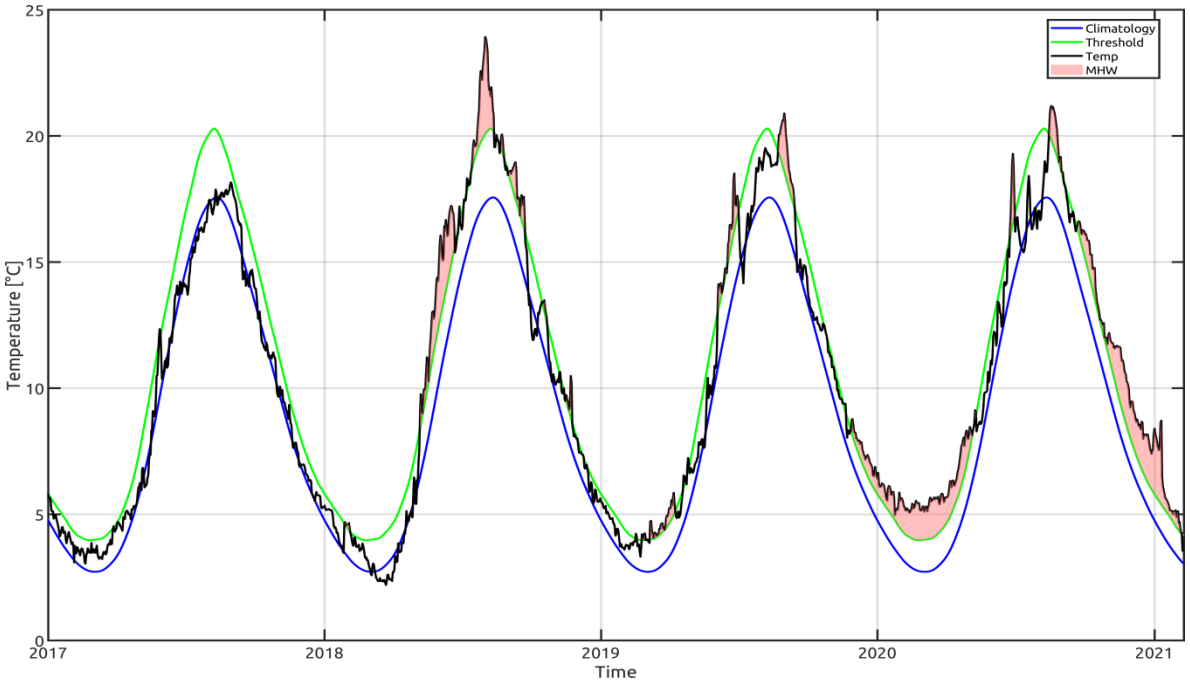

Fig. 18: The SST climatology (blue), 90th percentile MHW threshold (green), and SST time series (black). The red filled areas indicate the periods associated with MHWs. The climatology was built for the national reference period 1981-2010 and is based on REYNOLDS et al., 2007.

Table 7: Listing of the 10 longest MHW in the western Baltic Sea. Given are the start and stop date, the duration in days and the intensity in Kelvin.

Rank		Start	Stop	Duration	Intensity
1.	**2019**	28.11.2019	10.05.2020	165	360
2.	**2020**	21.09.2020	06.02.2021	139	338
3.	**1990**	20.01.1990	19.04.1990	90	161
4.	**2014**	10.10.2014	25.12.2014	77	173
5.	**2006**	26.11.2006	28.01.2007	64	116
6.	**2015**	06.11.2015	06.01.2016	62	115
7.	**2018**	07.05.2018	21.06.2018	46	174
8.	**2006**	21.09.2006	03.11.2006	44	126
9.	**2005**	04.10.2005	14.11.2005	42	93
10.	**2006**	01.07.2006	05.08.2006	36	168

4 Results of the routine monitoring cruises: Hydrographic and hydrochemical conditions along the thalweg

The routine monitoring cruises carried out by IOW provide the basic data for the assessments of hydrographic conditions in the western and central Baltic Sea. In 2020, monitoring cruises were performed in February, May, July, September and November. Usually also in March a cruise is performed. However due to the Covid19 pandemic restrictions this cruise was cancelled. To compensate this to some extent the September cruise that covered only the German waters was added.

4.1 Water temperature

Snapshots of the temperature distribution along the Baltic talweg transect obtained during each cruise are depicted in Fig. 19 and Fig. 20. This data set is complemented by monthly observations at central stations in each of the Baltic basins carried out by Sweden's SMHI. Additionally, continuous time series data are collected in the eastern Gotland Basin. Here the IOW operates two long-term moorings that monitor the hydrographic conditions in the deep water layer. The results of these observations are given in Fig. 21 and Fig. 24.

The surface temperature (SST) of the Baltic Sea is mainly determined by local heat flux between the sea surface and the atmosphere. In contrast, the temperature signal below the halocline is detached from the surface and the intermediate winter water layer and reflects the lateral heat flows due to salt-water inflows from the North Sea and diapycnal mixing. The temperature of the intermediate winter water layer conserves the late winter surface conditions of the Baltic till the early autumn, when the surface cooling leads to deeper mixing of the upper layer.

In the central Baltic, the development of vertical temperature distribution above the halocline follows with some delay the annual cycle of atmospheric temperature (cf. chapter 2). As in the previous year the winter of 2019/2020 started very mild. The January and February 2020 depicted extreme positive temperature anomalies of +3.6 K and +3.9 K, respectively. Also during March and April the mean air temperature was considerably warmer (+1.9 K and +2.0 K) than the long term mean. Thus the surface cooling of the Baltic was strongly reduced. The sea surface temperatures remained well above the density maximum, except of some parts of the Bothnian Bay and the Gulf of Finland. The extreme high temperatures are also reflected by the low maximum ice coverage of 36 000 km², which was the lowest observed ice coverage during the last 300 years. The higher than normal air temperature was continued after the spring. Only the May depicted air temperatures close the long term mean. The air temperatures remained at a higher than normal level for the rest of the year. From June to December 2020, the monthly air temperature anomaly ranged between +1.5 and +2.5 K (cf. chapter 2). Only the month of July interrupted the series with a temperature anomaly of -0.7 below the long term mean.

The deep water conditions in the central Baltic in 2020 were mainly controlled by subsequent minor inflow events of 2016 to 2020 (MOHRHOLZ, 2018). The most recent barotropic inflow events were observed in December 2019 and February 2020.

The February cruise was the only one in 2020 that was not affected by Covid-19 pandemic and supplied a comprehensive picture of the winter conditions. At the beginning of February the weak winter cooling of the surface layer has reduced the surface temperatures in the Baltic to 5 to 6 °C, only. As a result of the extreme warm winter conditions (compare chapter 2), surface temperatures were also high above the long term mean for February. The lowest surface temperatures of about 5 to 5.2 °C were observed on the Belt Sea and the shallow areas of the Mecklenburg Bight. This was more than 3 K above the climatological mean of 1.8 °C, and also above the high temperature of February of 2018. Surface temperatures in the Arkona Sea were considerably higher than in the Belt Sea. At the central station TF0113 the SST was about 5.6 °C (climatological mean 1.9 °C). In the entire Baltic the surface temperatures were well above the density maximum. Thus, the temperature driven convection forced by surface cooling was still ongoing. In the central Baltic the temperature driven mixing has homogenized the surface layer and the remains of former winter water layer completely, as it is usually observed in February. This was possible, since the winter water layer was only weak developed in the previous year. In contrast to normal years the temperature gradient between the surface and halocline layer was very low. The main thermocline at station TF271 in the eastern Gotland Sea was found at a depth of 58 m, and coincides with the permanent halocline. The well mixed surface layer reached down to 28 m depth. The temperature in the surface layer was 5.05 °C. Below 38 m the temperature increased slightly. Generally, the surface temperatures in the central Baltic between 4.95 and 5.4 °C were about 3 K above the long term average and exceed the extreme warm temperatures in February 2016 and 2018 by 1 K.

The temperature distribution below the halocline reflects the impact of the inflow events of saline water from the North Sea. A minor inflow in November 2019 transported about 50 km³ of warm saline water into the western Baltic. It was followed by two minor inflows in January and February 2020 with a total volume of 114 km³ of saline water. These inflows dominated the bottom temperature distribution in the Arkona and the Bornholm Basin. Waters of the November and January inflows covered a 20m thick bottom layer in the centre of the Arkona Basin, with a bottom temperature of 6.2 °C. In 2019 baroclinic late summer inflows have transported larger amounts of warm water into the western Baltic. The halocline of the Bornholm Basin was still occupied by theses warm saline water. The maximum temperature in the halocline of the Bornholm Basin was about 10.2 °C. Below 50 m depth the Bornholm Basin depicted in February a very patchy temperature distribution. The bottom layer is covered by the cool saline waters from the November inflow and the tip of the cooler January inflow in the western Bornholm basin. These inflows have not reached the Slupsk Sill. In the Bornholm Deep (TF0213) the bottom temperature was about 8.4 °C. Parts of warm summer water were shifted eastward into the Slupsk channel and further into the eastern Gotland Basin. Due to mixing with ambient water in the Slupsk Furrow the temperature of the inflowing water patches decreasing eastward. In the Slupsk Furrow bottom water temperatures of 9.1 to 9.5 °C were observed. Between the eastern outlet of the Slupsk Furrow and the entrance of the eastern Gotland Basin some warm water plumes were observed in the bottom layer. These plumes spread eastward and were originated from pulse like overflows of the eastern sill of Slupsk Furrow. Due to their relatively high density the warm water penetrated the permanent halocline in the Gotland Basin and interleaves at depths of 100 to 120 m. The deep water in the Gotland Basin was still covered by the warmer inflows of the recent

years. However, the bottom temperature at station TF 0271 has recently decreased to 7.2 °C, about 0.4K above the value observed in February 2019. The bottom water temperature in the Farö Deep of 7.2 °C has slightly increased since the last year. This compares to the temperature in the eastern Gotland Basin at 120m, which is the sill depth between both locations. Thus, the bottom water of the Farö Deep was replaced by eastward spreading waters from the Gotland Basin.

Due to the first "lock down" of the Covid-19 pandemic no monitoring cruise was performed in March 2020. Thus, there is no information about the temperature evolution in early spring in the Baltic.

The unusual high air temperatures and the above average solar radiation during March and April caused a strong warming of the surface water observed in May. The surface temperatures ranged between 10.6 °C in the Kiel Bight, 9.1 °C in the Arkona Basin and in the Bornholm Basin, and 7.4 °C in the eastern Gotland Basin. The SST was well about the climatological mean values for May, but lower than in May 2018. In the western Baltic there was a strong gradient in SST from west to east, whereas the temperature distribution was more uniform in the Baltic Propper. The seasonal thermal stratification was well established in the western Baltic, in contrast to a weaker vertical temperature Gradient in the eastern Gotland basin. The thermocline depth varied between 25 and 40 m along the thalweg transect, with a decreasing trend from southwest to northeast. In contrast to the previous years the winter water layer was thin and patchy in the central Baltic. The core temperature of winter was exceptionally high, since the SST was well above the temperature of maximum density during the entire winter season. In the eastern Gotland Sea, the minimum temperature of intermediate winter water was 5.2 °C, which was 1.4 K higher than in May 2019, and 2.7 K higher than in May 2018. The minimum temperature of 4.8 °C was observed in the intermediate layer at the southern rim of the eastern Gotland basin. In the Bornholm Basin and the Slupsk Furrow winter water layer depicted a very patchy structure, and was only weak pronounced.

Below the intermediate layer the temperatures increase with depth. In the halocline of the Bornholm Basin the remains of the warm inflow waters were mixed up with the colder water from winter inflows from November to February. Here the maximum temperature decreased slightly from 10.2 °C in February to about 8.3 °C. The bottom water temperature in the Bornholm Basin remained on the level from February with 8.3 °C. In the Slupsk Furrow the conditions changed significantly, since the warm deep water has left the Furrow towards the eastern Gotland Basin. The bottom water temperature in the Slupsk Furrow changed from 9.6 °C in February to 7.8 °C in May. The warm water patches observed in the southern and eastern Gotland basin in February were completely mixed up by isopcnal mixing. The mixed water formed a warm intermediate layer between 100 and 150 m depth. Its core temperature was about 7.5 to 7.5 °C. Unfortunately, the stations north of the eastern Gotland Basin were not measured due to bad weather conditions.

In the second half of July the surface temperature in the Baltic has reached its annual maximum. The negative air temperature anomaly in June hampered the ongoing unusual warming of the surface layer that was observed in winter and spring. It leads to normal summer SST, and established the typical summer thermal stratification throughout the Baltic Sea. The seasonal thermocline was found at depths between 25 m and 30 m, and separated the warm layer of surface water from the cooler intermediate water. The temperatures in the Arkona Basin reached

16.0 °C in a surface layer of 15 m thickness. Below this mixed layer warm waters with temperature of about 15 °C covers the Basin down to 30 m. At station TF213 in the Bornholm Basin an SST of 16.3 °C was recorded on 18th July, which was more than 6 K less than in the extreme warm July 2018. In the eastern Gotland Basin a SST 17.0 °C was observed in a very thin surface layer at station TF271. There the temperature decreased to 15.8 °C in 10 m depth. For this location the climatological mean value for July is 16.0 °C. Generally, in the central Baltic the SST was close to the long term mean, and not that warm as during two previous summers.

Below the surface layer the minimum temperatures in the intermediate water were about 5.2 °C in the eastern Gotland Basin, and 4.8 °C in the northern Gotland Basin, which caused a strong vertical temperature gradient between 25 and 50 m. In the Bornholm Basin and the Slupsk Furrow was no pronounced winter water layer was observed. the core temperature of intermediate layer was unusual high about 6 °C. During the summer minor barotropic and baroclinic inflow events transported warm saline water into the Arkona Basin. This water mass formed a warm bottom layer in the entire Arkona Basin, with bottom temperatures up to 15.6 °C. This water body has not passed the Bornholmgat till July. The bottom layer of the Bornholm Basin was still covered with water from the autumn/winter inflows of the previous year. At the central station TF0213 the bottom temperature was about 8.3°C. In the Slupsk Furrow considerably lower temperatures of 7.6 °C were observed. The deep water conditions in the central Baltic remain mainly unchanged. The weak diapycnal mixing in the Basin smoothed the vertical temperature gradients in the deep water layer near the warm core of inflow water. The bottom temperature in the eastern Gotland Basin was slightly reduced to at 7.2 °C.

The western Baltic was covered by an additional cruise in the end of September 2020. The temperature distribution was similar to July. The SST was about 15 to 16 °C. The ongoing inflow of warm saline water from the North sea has continued and filled the Arkona Basin with a 16 m thick layer of warm and saline water. At station TF0113 a bottom temperature of 16 °C was observed. Only a waek intermediate layer of 14.8 °C was detected.

In November 2020 the temperature distribution depicted the autumnal cooling and the erosion of the seasonal thermocline in the surface layer. Due to the ongoing positive air temperature anomaly, the SST observed in November 2020 was still higher than normal. The surface mixed layer has deepened to 40 to 45 m in the western Baltic and to 40 to 50 m depth in the eastern Gotland Basin. In the Arkona Basin surface temperatures between 11 °C and 12 °C were observed. Also in the Bornholm Basin the SST of 11.6 °C was still high at station TF213. This was about 2.5 K above the climatological mean for November. Unfortunately the Slupsk Furrow and the northern Gotland Basin were not covered during the November cruise, due to bad weather conditions. In the eastern Gotland Basin a slightly lower surface temperature was found. The station TF271 depicted a surface temperature of 10.6 °C, which exceed the climatological mean also by 2 K. The deepening of thermocline reduced the vertical extent of the intermediate winter water layer in the central Baltic to a thin layer of 25 m to 30 m thickness, with minimum temperatures of 5.5 °C. In the Bornholm Basin only no intermediate winter water was found. As seen in September, the inflow events in the summer and autumn brought warm saline water into the western Baltic. This water spreads from the Arkona basin into the halocline of the Bornholm Basin and further eastward. Maximum temperatures in this water body of 13.0 °C and 11.5 °C

were observed in the Arkona Basin and Bornholm Basin, respectively. The deep water temperature conditions in the Gotland basin remained unchanged compared to July.

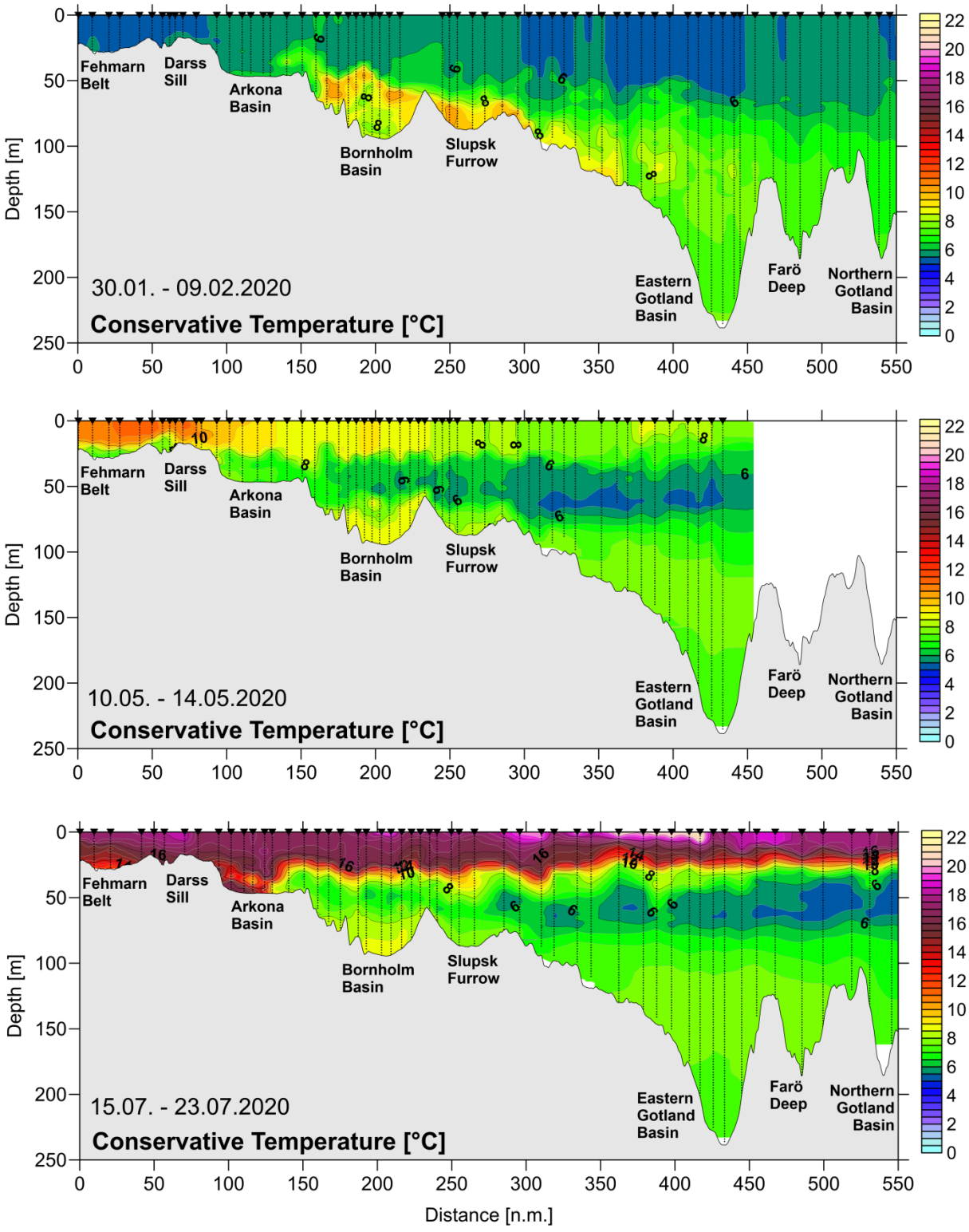

Fig. 19: Temperature distribution along the talweg transect through the Baltic Sea between Darss Sill and northern Gotland Basin for February, May, and July 2020.

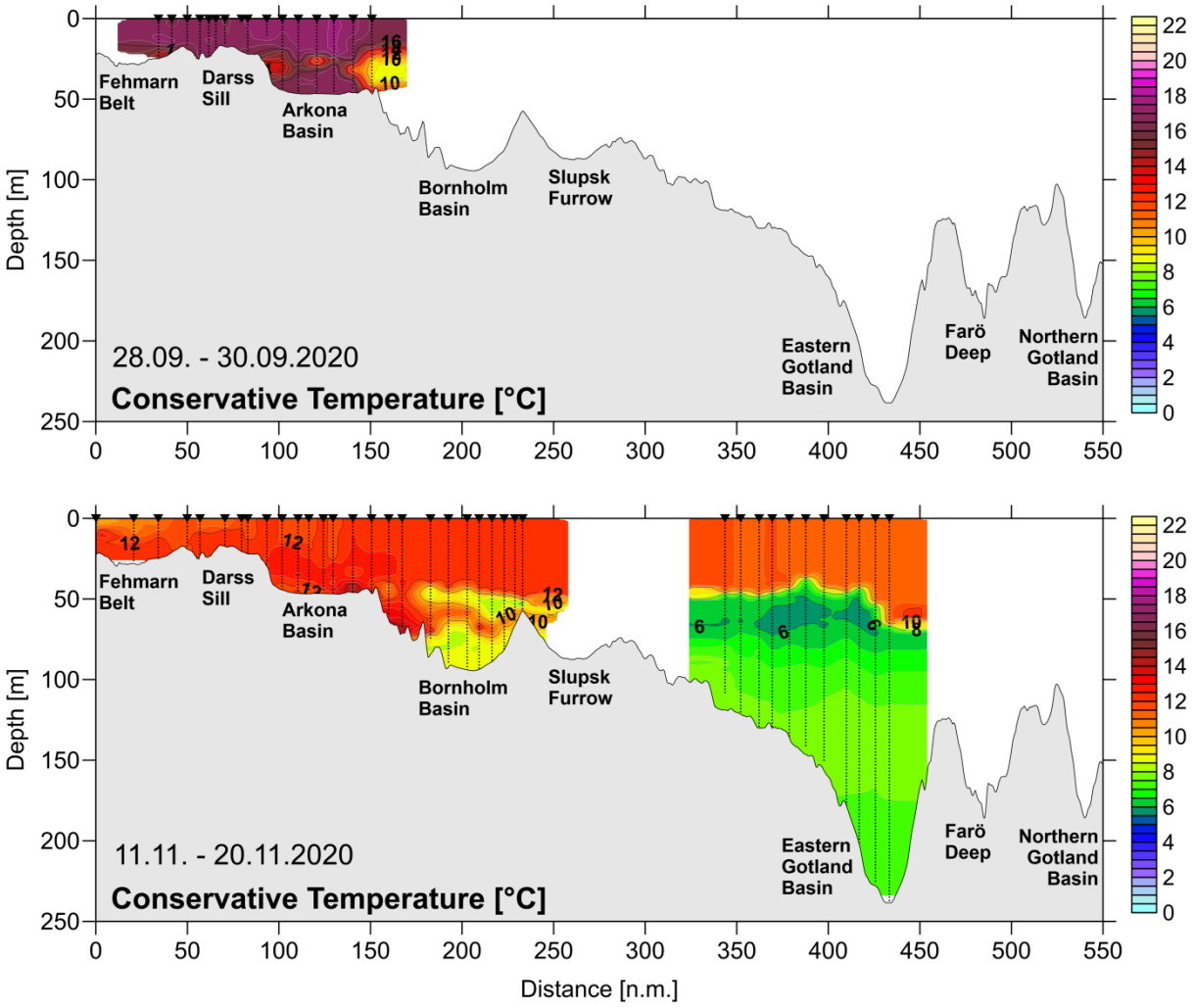

Fig. 20: Temperature distribution along the talweg transect through the Baltic Sea between Darss Sill and northern Gotland Basin for September and November 2020.

As part of its long-term monitoring programme, IOW operates hydrographic moorings near station TF271 in the eastern Gotland Basin since October 2010. In contrast to the Gotland Northeast mooring, operational since 1998 and from where the well-known 'Hagen Curve' is derived, the mooring at TF271 also collects salinity and oxygen data. The gathered time series data allow the description of the development of hydrographic conditions in the deep water of the Gotland Basin in high temporal resolution. This time series greatly enhances the IOW's ship-based monitoring programme. Figure 21 shows the temperature time series at five depths in the deep water of the eastern Gotland Basin between July 2018 and November 2020. Till December 2019 the temperature stratification in the deep water is characterized by a downward increasing temperature. Afterwards, the temperature gradient vanished below 190 m, and changed its sign in the water column above. However, the temperature difference between 140 m depth and 190 m was very weak with about 0.1 to 0.2 K. In the entire year 2020 no new pulse of warm or cold water intrusion occurred deep water of the Gotland basin. The inflow events of the inflow period 2019/2020 were not dens enough to reach the deep layers. Thus the deep water temperature remained in 2020 constantly at 7.2 °C. Which is relatively high compared to the recent decades.

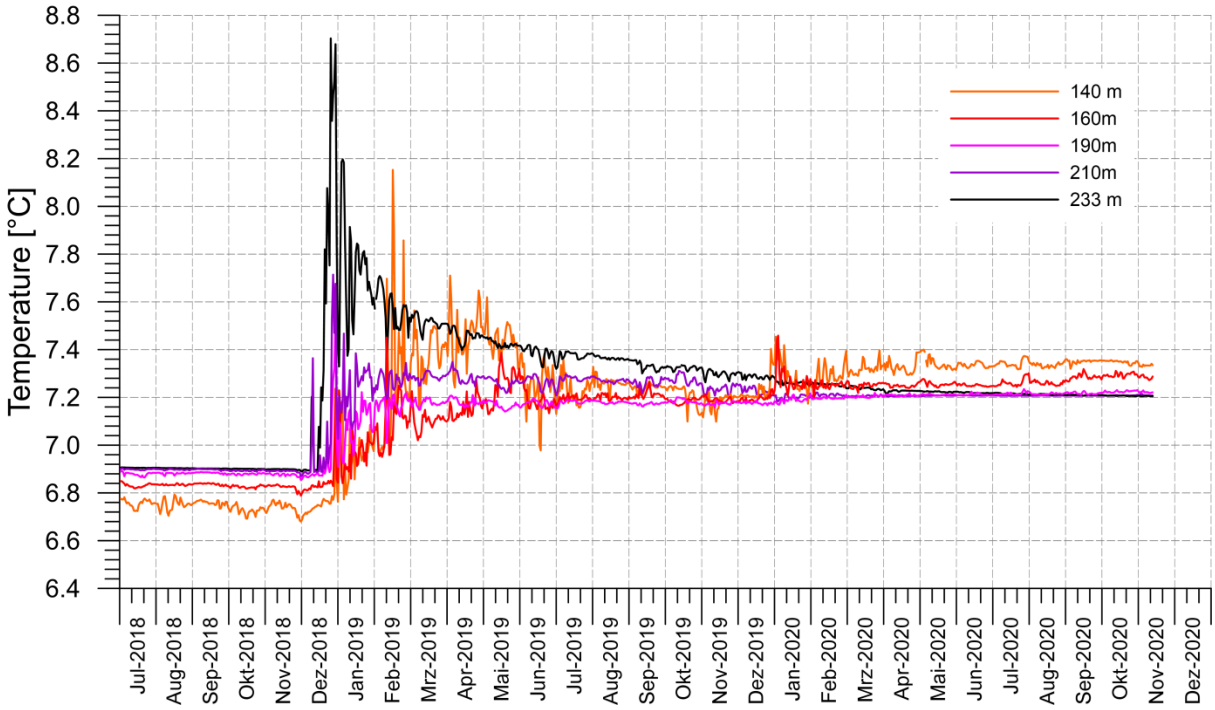

Fig. 21: Temporal development of deep water temperature in the Eastern Gotland Basin (station Tf271) from July 2018 to November 2020 (daily averages of original data with 10 min sampling interval).

Table 8.1 summarises the annual means and standard deviations of temperature in the deep water of the central Baltic based on CTD measurements over the past five years. With the exception of the Bornholm Basin the deep water temperatures in the entire Baltic increased in 2020 compared to the previous year. This continued the increasing trend since the extreme Christmas MBI in 2014. In the eastern Gotland Basin the increase was very weak and can attributed to vertical mixing processes. The increase in the Farö Deep, Landsort deep, and the Karlsö Deep was caused by the spreading of warmer water from the halocline layer of the eastern Gotland basin which was fed by the warm saline summer and autumn inflows of 2019.

In the Bornholm Basin the deep water temperature was slightly decreasing due to the lower temperature of the inflowing water in autumn and winter. The standard deviations of temperature fluctuations in 2019 were on a usual level.

Table 8: Annual means and standard deviations of temperature, salinity and oxygen concentration in the deep water of the central Baltic Sea: IOW- and SMHI data (n= 5-26).

Table 8.1: Deep water temperature (°C; maximum in bold).

Station	Depth m	2016	2017	2018	2019	2020
213 (Bornholm Deep)	80	7.06 ±0.63	7.06 ±0.28	7.81 ±1.49	**8.65 ±0.12**	8.45 ±0.29
271 (Gotland Deep)	200	7.06 ±0.12	7.05 ±0.15	6.89 ±0.01	7.20 ±0.07	**7.21 ±0.01**
286 (Fårö Deep)	150	6.56 ±0.06	6.83 ±0.15	6.70 ±0.04	7.05 ±0.18	**7.24 ±007**
284 (Landsort Deep)	400	5.92 ±0.10	6.14 ±0.19	6.27 ±0.03	6.37 ±0.15	**6.60 ±0.27**
245 (Karlsö Deep)	100	5.28 ±0.09	5.53 ±0.06	5.67 ±0.12	5.64 ±0.12	**5.83 ±0.11**

Table 8.2: Deep water salinity (maximum in bold).

Station	Depth m	2016	2017	2018	2019	2020
213 (Bornholm Deep)	80	**18.26 ±0.40**	17.40 ±0.46	16.64 ±0.32	16.63 ±0.27	16.34 ±0.34
271 (Gotland Deep)	200	**13.35 ±0.09**	13.30 ±0.04	13.17 ±0.03	13.16 ±0.03	13.03 ±0.03
286 (Fårö Deep)	150	12.35 ±0.12	**12.58 ±0.07**	12.50 ±0.12	12.46 ±0.08	12.39 ±0.03
284 (Landsort Deep)	400	11.12 ±0.13	11.29 ±0.19	**11.41 ±0.05**	11.33 ±0.06	11.34 ±0.16
245 (Karlsö Deep)	100	10.00 ±0.16	10.28 ±0.11	**10.44 ±0.21**	10.35 ±0.24	10.40 ±0.18

4.2 Salinity

The vertical distribution of salinity in the western and central Baltic Sea during IOW's five monitoring cruises is shown in Fig. 22 and Fig. 23. Salinity distribution is markedly less variable than temperature distribution, and a west-to-east gradient in the surface and the bottom water is typical. Greater fluctuations in salinity are observed particularly in the western Baltic Sea where the influence of salt-water inflows from the North Sea is strongest. The duration and influence of minor inflow events is usually too small to be reflected in overall salinity distribution.

Only combined they can lead to slow, long-term changes in salinity. The salinity distributions shown in Fig. 22 and Fig. 23 are mere 'snapshots' that cannot provide a complete picture of inflow activity. In 2020 the evolution of salinity distribution was mainly controlled by the minor barotropic inflows in autumn and winter 2019/2020 and the baroclinic inflows in late summer and autumn 2020. However, none of the inflows could be completely covered by the IOW monitoring cruises. The salinity at the Darss Sill was well below 17 g/kg during all cruises, although there were significant volumes of high saline water observed in the Fehmarn Belt. It is not possible to produce meaningful statistics on inflow events, by using only the monitoring cruises. The analyses of the sea level changes and the salinity observations in the western Baltic revealed three minor barotropic inflows in December 2019 (1.0 Gt salt), January 2020 (0.8 Gt salt), and February 2020 (1.4 Gt salt), which transported about 3.3 Gt salt into the western Baltic. A smaller event was observed in November 2020 (0.5 Gt salt). During summer and autumn the water exchange with the North Sea was controlled mainly by barocline inflows.

At the beginning of February a saline bottom water body was detected in the Fehmarn Belt, that can be attributed to the January inflow. At the time of the cruise the inflow waters have not passed the Darss Sill. The maximum salinity in the Fehmarn belt was only 19.1 g/kg. In the Arkona Basin a thin saline bottom layer of 5 m thickness and a maximum salinity of 18.7 g/kg was found, which consisted of the of the December inflow waters. Above the bottom water a second saline layer of 10 to 15 m thickness was observed. Its mean salinity was about 15 g/kg. As indicated by the temperature distribution a part of the inflow waters has passed the Bornholmgat, and reached the western Bornholm Basin and the replaces the former warm bottom waters. The bottom salinity in the Bornholm deep was about 17.2 g/kg. The halocline layers of Bornholm Basin were covered with saline water from the inflows in autumn 2019, illustrated by the several warm water patches. The halocline depth was at 55 m, close to the sill depth of the Slupsk Sill. Unfortunately the stations near the sill could not be covered, due to bad weather. It remained unclear whether there was an active overflow of the sill. The Slupsk Furrow is filled with warm saline water from the autumn inflows. The shallow halocline exceeds the sill depth at the eastern edge of the furrow. Thus, the halocline water of the Slupsk Furrow spreads into the southern Gotland Basin. After the inflow series of the recent years the salinity in the deep water of the central Baltic Sea was still at a high level in 2020. The bottom salinity in the Gotland Deep was of 13.2 g/kg was. This was only 0.17 g/kg less than in February 2019, and still close to the overall maximum of 13.6 g/kg observed after the extreme inflow event in 1951. The 12 g/kg isohaline lay at a depth of around 110m, after 118m in February 2019. This points to an inflow of saline water into the halocline layer. The 13 g/kg isohaline was found at 188 m depth, nearly 20m deeper than one year before. Thus, thus the inflow waters did not reach the deeper layers, were vertical mixing is the dominating process the slowly lowered the deep water salinity. The bottom salinity in the Farö Deep was 12.52 g/kg, indicating an ongoing stagnation in the bottom waters of the central Baltic.

In May the small saline bottom water body in the Fehmarn Belt indicated an outflow situation. The maximum salinity of only 19.0 g/kg was restricted to a very thin bottom layer. At the Darss Sill the bottom salinity was only 12.6 g/kg. And also the saline bottom water pool in the Arkona Basin was nearly vanished. The halocline was found at 35 to 40m depth in the centre of the basin. The bottom salinity of 14.5 g/kg was extremely low, much lower than in March. The halocline

depth in the Bornholm Basin was 55m, equally the sill depth of the Slupsk Sill. A tilt of the halocline near the sill forced an overflow of warm saline water into the Slupsk Furrow. The bottom salinity in the Bornholm Basin decreased slightly to 16.6 g/kg in the central part of the basin. Compared to February 2020, the saline deep water volume in the Slupsk Furrow was significantly reduced due to the eastward advection of saline water above eastern sill depth of the furrow. However, the bottom salinity in the furrow remained at 13.7 g/kg. No changes of deep water conditions were observed at station TF271 (Gotland Deep). There the bottom salinity was nearly unchanged at 13.15 g/kg. The 13 g/kg isohaline dropped from 188 m in February to a depth of 191 m. The 12 g/kg isohaline changed their depth from 110 m to 124 m, due to the more even distribution of inflow water in the halocline layer.

In July the observed salinity distribution in the western Baltic points to an early state of a baroclinic summer inflow, which enhance the stratification in the Fehmarn Belt. A strong halocline between 10 to 20 m depth separated the brackish surface water from the saline inflow at the bottom, where a salinity of 23 g/kg was measured. However, the inflow had not passed the Darss Sill were the bottom salinity was at a low level of only 9.8 g/kg. The pool of saline bottom water in the Arkona Basin was moderately filled with warm water from a previous baroclinic inflow. The maximum bottom salinity was about 18.3 g/kg. In the center of the Basin the warm and saline bottom water layer was 8m thick. In the Bornholm Basin mixing with overlaying water caused a slight dilution of deep water. However, the bottom salinity remained at 16.6 g/kg. The halocline depth in the Basin was found at 60m, well below the depth of the Slupsk Sill. The saline deep water pool in the Slupsk Furrow has been partly refilled. The bottom salinity was slightly reduced to 13.6 g/kg. At the eastern rim of the furrow an active overflow of upper halocline water into the Gotland basin was visible. In the central Baltic basins again no significant changes were observed. The depth of the 13 g/kg isohaline in the Gotland deep was at 196m, slightly deeper than in May. The bottom salinity in the Gotland Deep and the Farö Deep was 13.13 g/kg and 12.54 g/kg, respectively. The surface salinity in the central Baltic decreased according its usual seasonal cycle, and was at 7.17 g/kg in the eastern Gotland Basin.

In September 2020 the barocline inflows continued. The halocline in the Fehmarn Belt was still high at 10 to 12 m depth. The bottom salinity there was 21.4 g/kg. The saline bottom pool in the Arkona Basin was further filled up. The halocline was found near 30 m depth, but the bottom salinity decreased slightly to 17.8 g/kg.

In November 2020 a weak barotropic inflow signature was visible in the Belt Sea. The bottom salinity at the entrance of the Fehmarn Belt amounted to 24.4 g/kg. The tip of the first less saline water was detected at the Darss Sill. This water had a salinity of 14 g/kg and do not match the formal criteria for an barotropic inflow. In the Arkona Basin warm and high saline water from the baroclinic summer/autumn inflows still covered the bottom layer. The maximum bottom salinity has significantly increased to 19.3 g/kg. However, it covers only a thin layer of maximum 10m vertical extent. The halocline depth was at 35 m depth. The warm saline water has reached the halocline layer of the Bornholm basin, but did not reached the bottom of the Basin. Since July the bottom salinity in the basin decreased significantly to 15.7 g/kg. The halocline depth in the Bornholm Basin rose to 55 m, which compares to the sill depth of the Slupsk Sill. The deep water conditions in the eastern Gotland Basin remained nearly unchanged since July 2020. The bottom

salinity decreased very slowly in the Gotland Deep to 13.11 g/kg. The depth of the 13 g/kg isohaline in the Gotland deep was at 192 m, slightly shallower than in July.

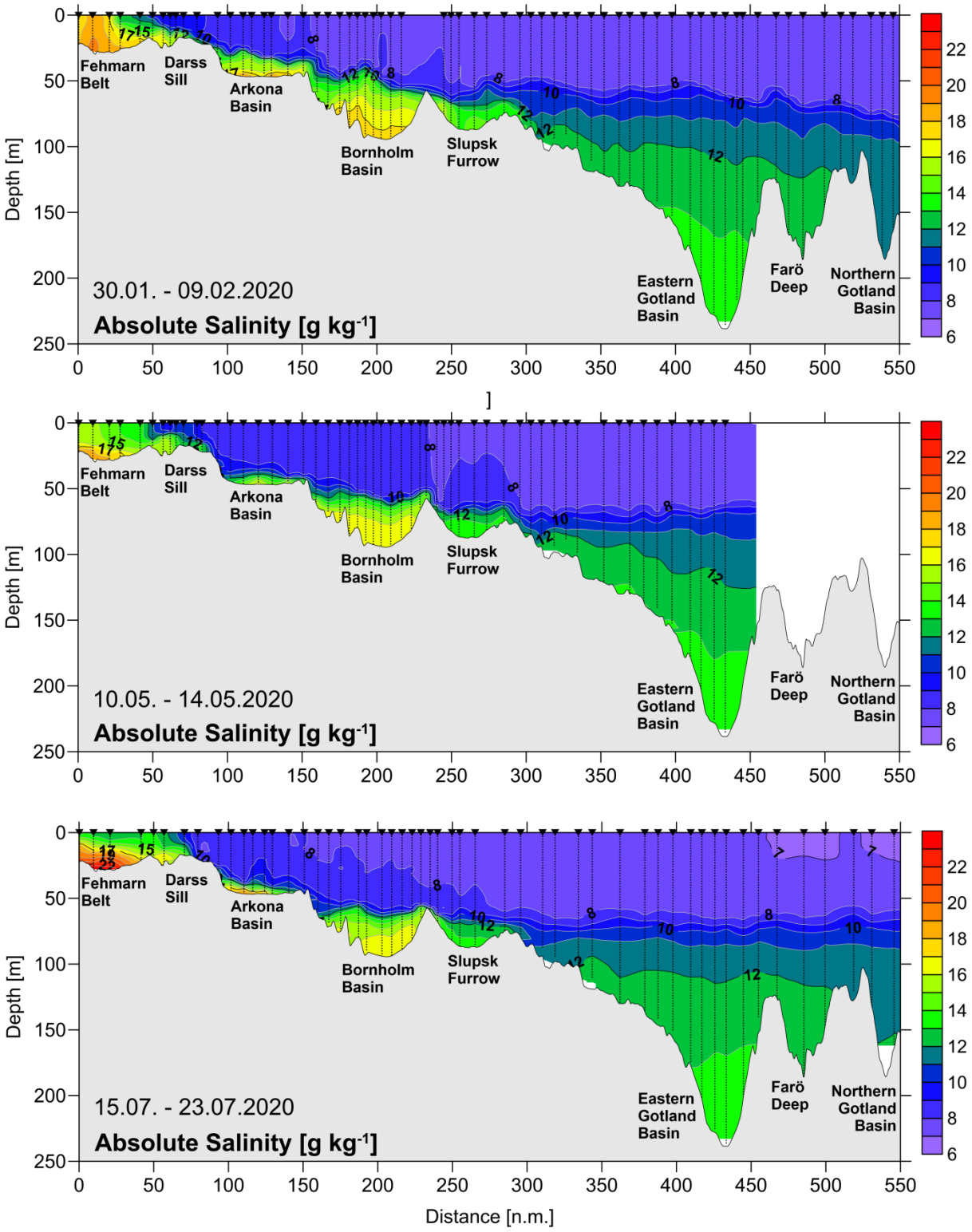

Fig. 22: Salinity distribution along the talweg transect through the Baltic Sea between Darss Sill and northern Gotland Basin for February, May, and July 2020.

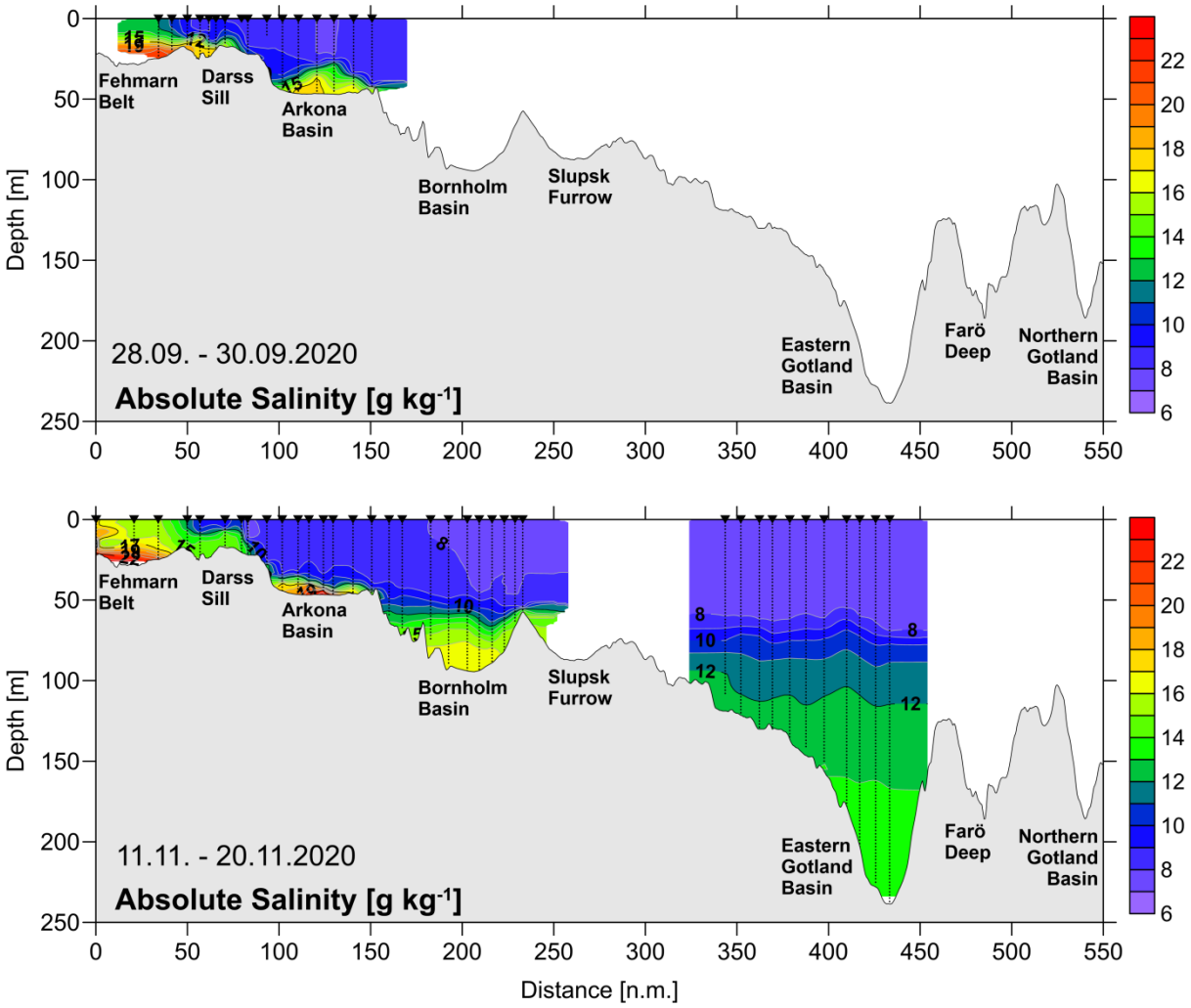

Fig. 23: Salinity distribution along the talweg transect through the Baltic Sea between Darss Sill and northern Gotland Basin for September and November 2020.

Table 8.2 shows the overall trend of salinity in the deep water of the Baltic in the past five years. After the series of inflow events in 2014 to 2016 the bottom salinity in the Gotland Deep and Farö Deep reached its maximum in 2016 and 2017. Although, warm saline waters from summer and autumn inflows 2018 reached the deep layer of the Gotland basin in December 2018 no permanent change in salinity stratification was observed at the central station TF271. In 2020 the deep water salinity in both basins dropped only slightly due to mixing by 0.13 g/kg and 0.05 g/kg in the Gotland Deep and the Farö Deep, respectively. In the Karlsö Deep and Landsort Deep the deep water salinity reached its maximum values of the past five year period in 2018. In 2020 deep water salinity in both Basin remained nearly at the level of 2019. In the Bornholm Basin the mean deep water salinity decreased slightly in 2020. However, also here the salinity was still high. The high standard deviation of salinity in the Bornholm basin points to rapid fluctuations, caused by particular inflow events.

As previously no clear trend emerges over the past five years for salinity in the surface layer of the Baltic. Table 8.3 summarises the variations in surface layer salinity. Compared to the values in 2019, surface layer salinity in the Bornholm Basin, the eastern Gotland Basin, the Farö Deep and the Karlsö Deep increased slightly by about 0.2 g/kg. This may be caused by the slow upward

mixing of saline water from the deep water body, which has a very high salinity compared to the long term mean. Usually, the long term changes in the surface salinity depict a time lag of about ten years to the deep water salinity. The surface salinity in the Landsort Deep increased only by 0.06 g/kg. However, this difference might be biased as result of the very few observations from this location in 2020. The standard deviations of surface salinity are close to the level with those of the long term average.

Table 8.3: Annual means of 2016 to 2020 and standard deviations of surface water salinity in the central Baltic Sea (minimum values in bold, n= 4-26). The long-term averages of the years 1952-2005 are taken from the BALTIC climate atlas (FEISTEL et al., 2008).

Station	1952-2005	2016	2017	2018	2019	2020
213 (Bornholm Deep)	7.60 ±0.29	7.75 ±0.26	**7.46 ±0.20**	7.53 ±0.08	7.63 ±0.11	7.80 ±0.18
271 (Gotland Deep)	7.26 ±0.32	**6.89 ±0.34**	7.33 ±0.22	7.09 ±0.27	7.19 ±0.25	7.33 ±0.16
286 (Fårö Deep)	6.92 ±0.34	**6.63 ±0.33**	7.13 ±0.43	6.92 ±0.34	6.78 ±0.33	7.07 ±0.29
284 (Landsort Deep)	6.75 ±0.35	6.57 ±0.16	6.54 ±0.34	6.59 ±0.32	**6.52 ±0.26**	6.58 ±0.50
245 (Karlsö Deep)	6.99 ±0.32	6.98 ±0.17	6.93 ±0.18	7.06 ±0.18	**6.89 ±0.24**	7.16 ±0.12

Fig. 24 shows the temporal development of salinity in the deep water of the eastern Gotland Basin between July 2018 and December 2020, based on data from the hydrographic moorings described above. As seen in the temperature data there were no significant changes of the saline stratification during the year 2020. The stratification, established after the arrival of warm waters from the summer and autumn inflows 2018, did not change significantly. The weak vertical mixing in the basin led to a slowly decreasing salinity in the entire deep water body, and in a slight reduction of the vertical salinity gradient.

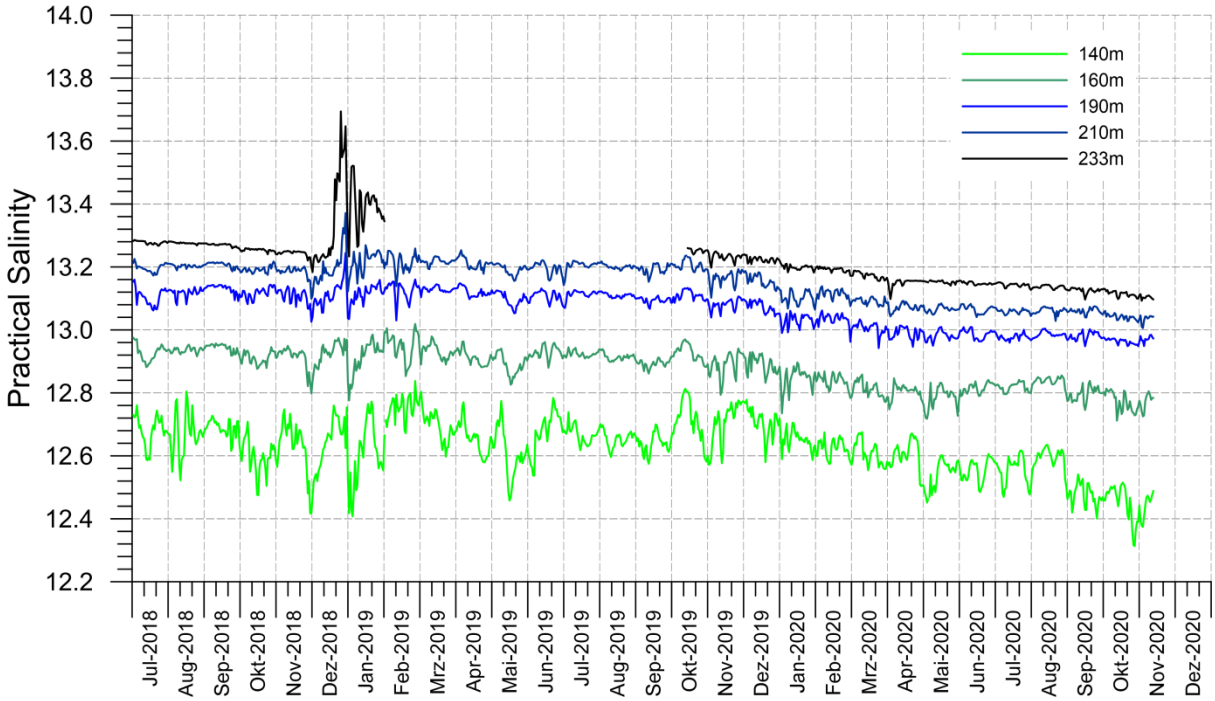

Fig. 24: Temporal development of deep water salinity in the Eastern Gotland Basin (station TF271) from July 2018 to November 2020 (Daily averages of original data with 10 min sampling interval).

4.3 Oxygen distribution

A precondition for the survival of higher marine life is the presence of sufficient oxygen. Low oxygen concentration appears especially problematic at the sea floor for demersal fish and zoobenthos organisms. For the Baltic Sea, it is a natural phenomenon that only Major Baltic Inflows (MBI) supply oxygen to the deep eastern Gotland Basin and subsequently further Northwest reaching the western Gotland Basin. However, after a few years of stagnation, the water below the permanent halocline turns into anoxic and then to euxinic conditions, hostile to life. This reflects the consumption of oxygen during the mineralization of organic matter, and subsequently of other oxidants, especially of sulphate as a major constituent of Baltic Sea seawater. Thereby, sulphate is converted to poisonous hydrogen sulphide and turns bottom areas into dead zones fostered by eutrophication (DIAZ & ROSENBERG 2008). The lack of oxygen is evaluated by using the HELCOM oxygen debt indicator for the deep basins below the halocline to figure out a potential deviation from a "good environmental status" (HELCOM 2013).

Recently it is recognized that also shallow Baltic Sea areas are more often subjected to temporally low oxygen values. "Shallow areas" in this context are regions, in which the water column is too shallow to establish a permanent halocline, thus, usually shallower than 60 m. Excess nutrient supply to the Baltic Sea and internal mobilization processes of especially phosphorus primarily cause increased phytoplankton blooms. Subsequently, the episodic remineralization activity of accumulated organic matter on the sea floor is intensified. To observe and finally to recommend measures, the bottom water oxygen concentration in shallow areas is aimed to be characterized by an indicator that appropriately describes the oxygen condition also

for these areas apart from the central deep basins. In surface waters as well as in shallow areas, the gas exchange with the atmosphere maintains an elevated oxygen content of seawater. Thus, oxygen is usually close to saturation that is mainly controlled by temperature. The situation changes, when a stable thermocline develops separating oxygenated surface waters from the waters below. Then, assimilation and dissimilation processes that change the oxygen content in seawater are mainly separated and in deeper waters, without contact to the atmosphere, oxygen concentration clearly declines by respiration in summer. Strong temperature and/or salinity changes hinders mixing between the bottom and upper waters. Lasting oxygen consumption during organic matter degradation can lead to total depletion of oxygen. Denitrification and subsequent reduction of sulphate result in the building of toxic hydrogen sulfide (shown as negative oxygen), which is worsening the conditions.

We generally use ml/l as the standard unit for oxygen concentration, however also mg/l was used in Fig. 26. In this case a conversion formula to ml/l is provided in the figure caption. In the hydrographic analysis of oxygen displayed in Fig. 27/Fig. 28 we use the chemical oceanographic unit µmol/kg, in comparison to Fig. 19/Fig. 20 of temperature and Fig. 22/Fig. 23 of salinity.

A general decrease of the oxygen concentration in deep waters of the five selected Baltic Sea deeps (Table 8.4 - Oxygen) was observed at respective reference depths after the MBI of December 2014. The choice of reference depths in the middle of the respective deep waters secure annual averages basically unbiased from episodic smaller inflows that frequently occur in the depth range of the pycnocline and partly in the bottom layer but disappear soon. At Gotland Deep station the decline of oxygen continued since 2016 and showed in 2020 an accumulation of hydrogen sulfide equivalent to 4.13 ml/l oxygen at 200 m depth. Further north and west the highest oxygen or lowest hydrogen sulfide values were determined in 2017. In subsequent years, ongoing accumulation of hydrogen sulphide was recorded (given as negative oxygen). Only the Bornholm Deep received enough oxygenated waters that scattered around an annual average oxygen concentration of about 1 ml/l in 80 m depth between 2016 and 2020. Fårö Deep received some weakly oxygenated waters likely via the Gotland Sea intermediate waters and remained at an oxygen status of above -2 ml/l in 150 m in 2020 with some variability during the year.

The annual average oxygen concentration in the Landsort Deep decreased from -1.49 ml/l in 2019 to -2.19 ml/l in 2020, and at Karlsö Deep from 1.95 to -2.28 ml/l in 2020 (Table 8.4). The oxygen maxima of the last five years of the Bornholm Sea and the eastern Gotland Sea were the values from 2016 and for the northern and western deeps, Fårö Deep, Landsort Deep and Karlsö Deep, the values of 2017, which were as well the consequences of the MBI 2014/2015 (Table 8.4).

Table 8.4: Annual means of 2016 to 2020 and standard deviations of deep water oxygen concentration (ml/l; hydrogen sulphide is expressed as negative oxygen equivalents; maximum in bold).

Station	Depth/m	2016	2017	2018	2019	2020
213 (Bornholm Deep)	80	**1.30 ± 0.93**	0.90 ±0.83	0.16 ±0.37	0.97 ±1.50	0.89 ±1.34
271 (Gotland Deep)	200	**0.55 ±0.26**	0.13 ±0.11	-0.85 ±0.50	-2.48 ±1.18	-4.13 ±1.30
286 (Fårö Deep)	150	-0.05 ±0.23	**0.34 ±0.33**	-0.73 ±0.42	-1.74 ±0.41	-1.42 ±0.64
284 (Landsort Deep)	400	-0.98 ±0.23	**-0.41 ±0.31**	-0.57 ±0.40	-1.49 ±0.25	-2.19 ±0.45
245 (Karlsö Deep)	100	-0.93 ±0.47	**-0.75 ±0.66**	-1.89 ±0.72	-1.95 ±1.25	-2.28 ±0.65

In the surface water the seasonal cycle of the water temperature controlled the oxygen concentration mainly by oxygen's solubility (upper panel of Fig. 25). However also deep mixing or upwelling may cause deviations. The highest value of 8.9 ml/l oxygen was recorded in 2020 in the central eastern Gotland Sea in May. The March cruise at usually lower sea surface temperatures and higher oxygen values was cancelled in 2020. Lowest values of below 6 ml/l were observed in surface waters of the Mecklenburg Bight in November caused by deep mixing in a windy period. The oxygen values slightly increased in the Belt Sea, Odra Bight and the Bornholm Sea in surface waters after the summer, during autumn cooling in November.

The bottom water of the shallow western Baltic Sea showed a similar seasonal pattern as the surface water (lower panel of Fig. 25). The maximum oxygen concentration occurred in May influenced by the prevailing temperature and the oxygen release by the spring bloom. However, no data were taken in March. The western Baltic Sea showed a decreasing oxygen concentration from May to July 2020 that recovered in the Belt Sea and the Odra Bight in autumn. But for the Mecklenburg Bight and the Arkona Sea, no recovery of the bottom water oxygen is observed in November. In contrast, it further decreased from 5.7 ml/l and 5.1 ml/l in July to 5.1 ml/l and 4.5 ml/l in November 2020, respectively. In the Bornholm Sea the bottom water oxygen concentration was close to 1 ml/l in February and May. Only few data were obtained in Gotland Sea that reflect almost stable sulphidic conditions during 2020. The bottom water in the central eastern Gotland Sea showed a decline from February -6.9 ml/l to -7.8 ml/l oxygen equivalents of hydrogen sulphide in November with a weak improvement in May of 6.1 ml/l through the year 2020. In comparison, the situation in the northern and western Gotland Sea bottom waters appeared relatively stable with values of about 2 ml/l, however, based on few data only.

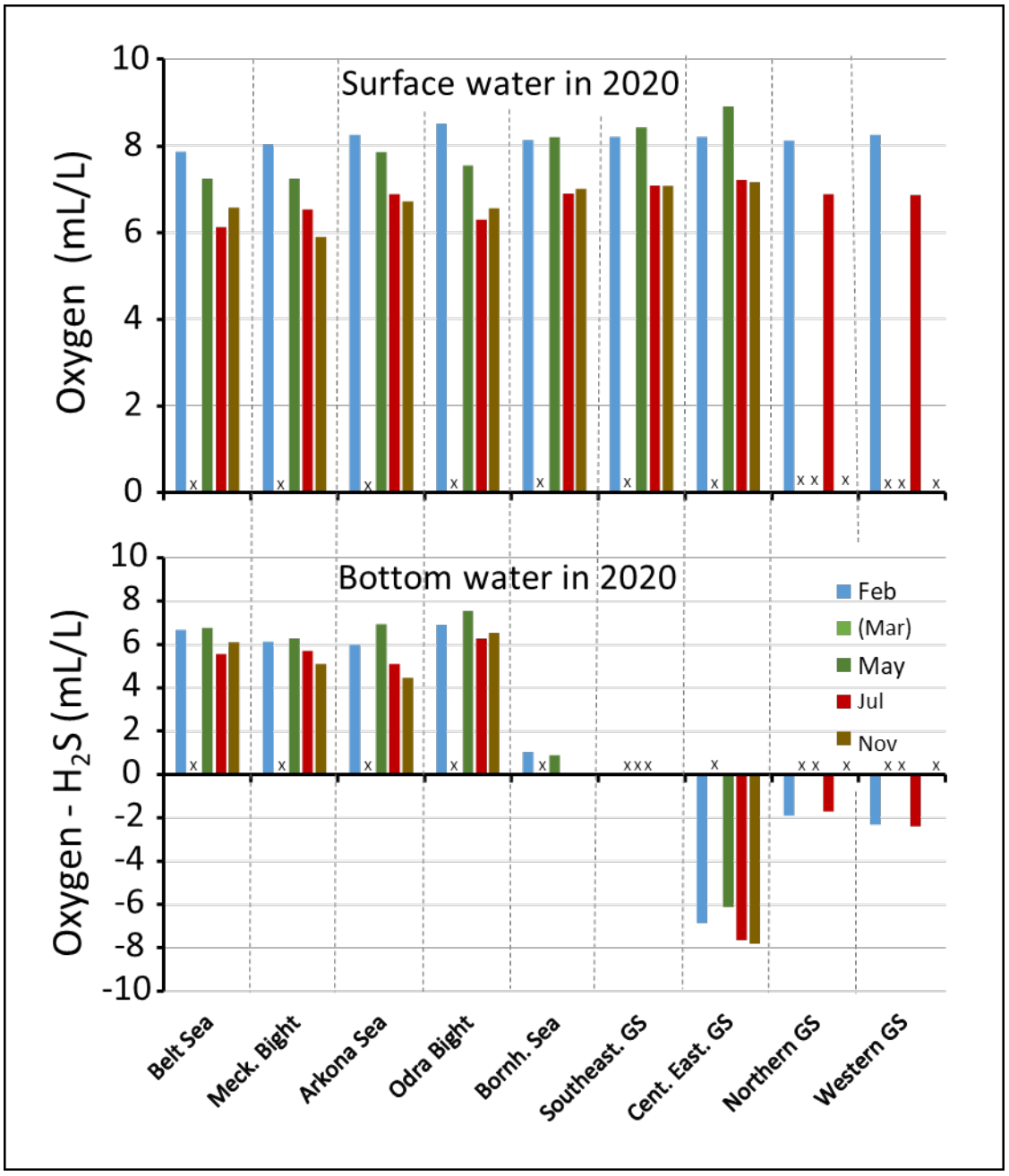

Fig. 25: Comparison of average oxygen concentrations in surface waters (upper panel, including O2-sensor data) and average oxygen/hydrogen sulfide concentrations in bottom waters (lower panel, without sensor data) of the studied Baltic Sea areas of February to November 2020: Belt Sea, Mecklenburg Bight, Arkona Sea, Odra Bight, Bornholm Sea, southern Gotland Sea, central Eastern Gotland Sea, Northern Gotland Sea, and Western Gotland Sea.

A period most critical for oxygen concentration in bottom waters of the shallow Baltic Sea areas is the time at the end of summer/early autumn, when usually the strongest oxygen depletion is observed. Since IOW does not perform a monitoring campaign that covers that time period, we turn to the findings of the State Agency for Agriculture, Environment and Rural Areas Schleswig-Holstein (LLUR), which routinely measures near-bottom oxygen concentrations at that time of the year (LLUR 2020). Investigations in 2020 were conducted from September 8th to 17th. Near-bottom

oxygen concentrations were measured on 42 stations. Thereof, 30 stations showed a water depth deeper than 15 m (circles) and 12 station were between 7 and 13 m deep (squares, Fig. 26).

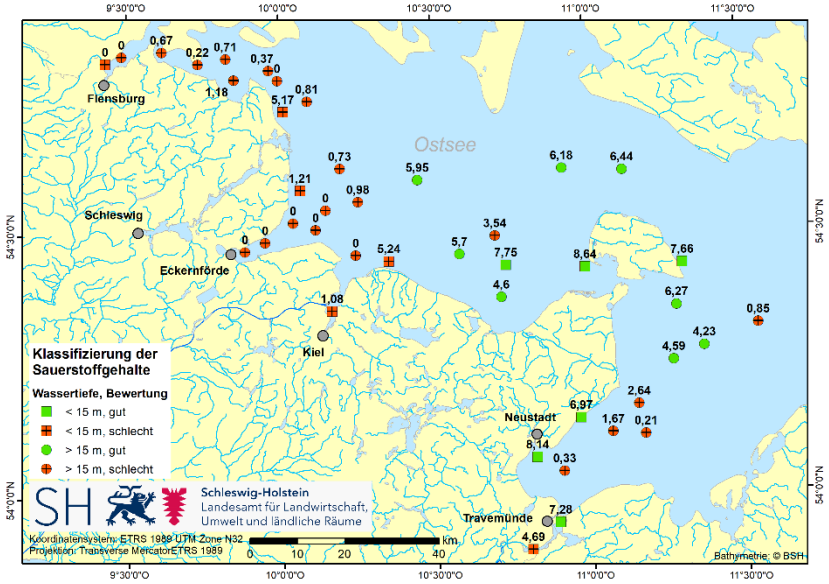

Fig. 26: Classified oxygen concentrations in the Belt Sea in September 2020 (LLUR 2020) – O2 [mg/l] x 0.7 = O2 [ml/l].

Measured bottom water oxygen concentrations are given at the respective sampling sites in Fig. 26. In September 2020, 22 of the 30 stations in deeper water (›15 m) showed values below the threshold value of 4 mg/l= 2.8 ml/l (73%). Thus, the oxygen status in September 2020 was slightly improved compared to September 2019 with 93 % of the deeper stations below the threshold (LLUR 2019). Moreover, at 6 of the 12 stations in shallower water (‹15 m) the oxygen concentration was below the threshold value of 6 mg/l=4.2 ml/l (50%), which is in agreement with 2019. For a more detailed analysis of the seasonal development of oxygen saturation, see the measurements from Darss Sill (chapter 3.2), the Arkona Basin (chapter 3.3), and Oder Bank (chapter 3.4).

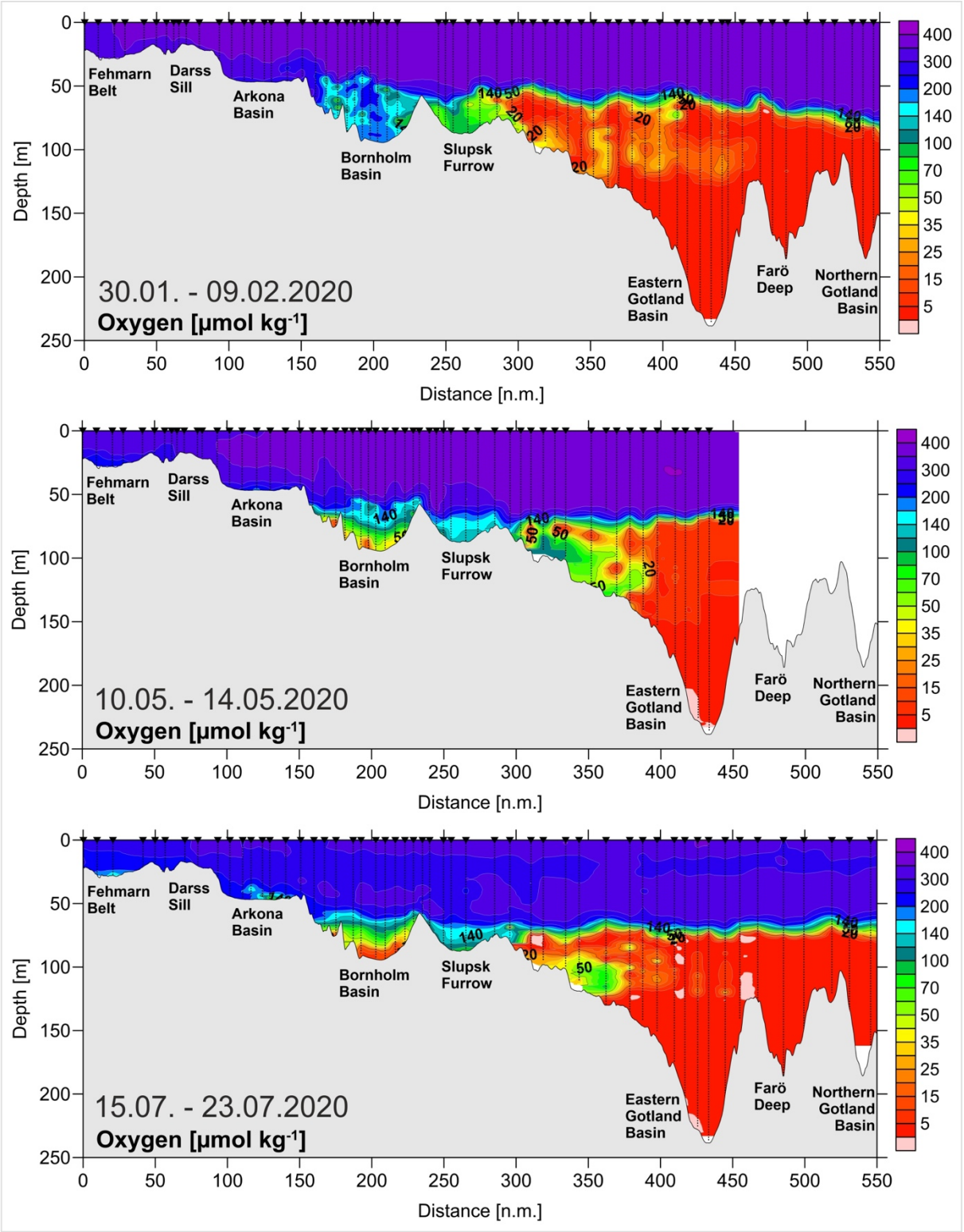

Fig. 27: Vertical distribution of oxygen (without H2S) during the February, May, and July cruises in 2020 between the Darss Sill and the northern Gotland Basin. Values below 1 µmol/kg could not be distinguished from 0 µmol/kg.

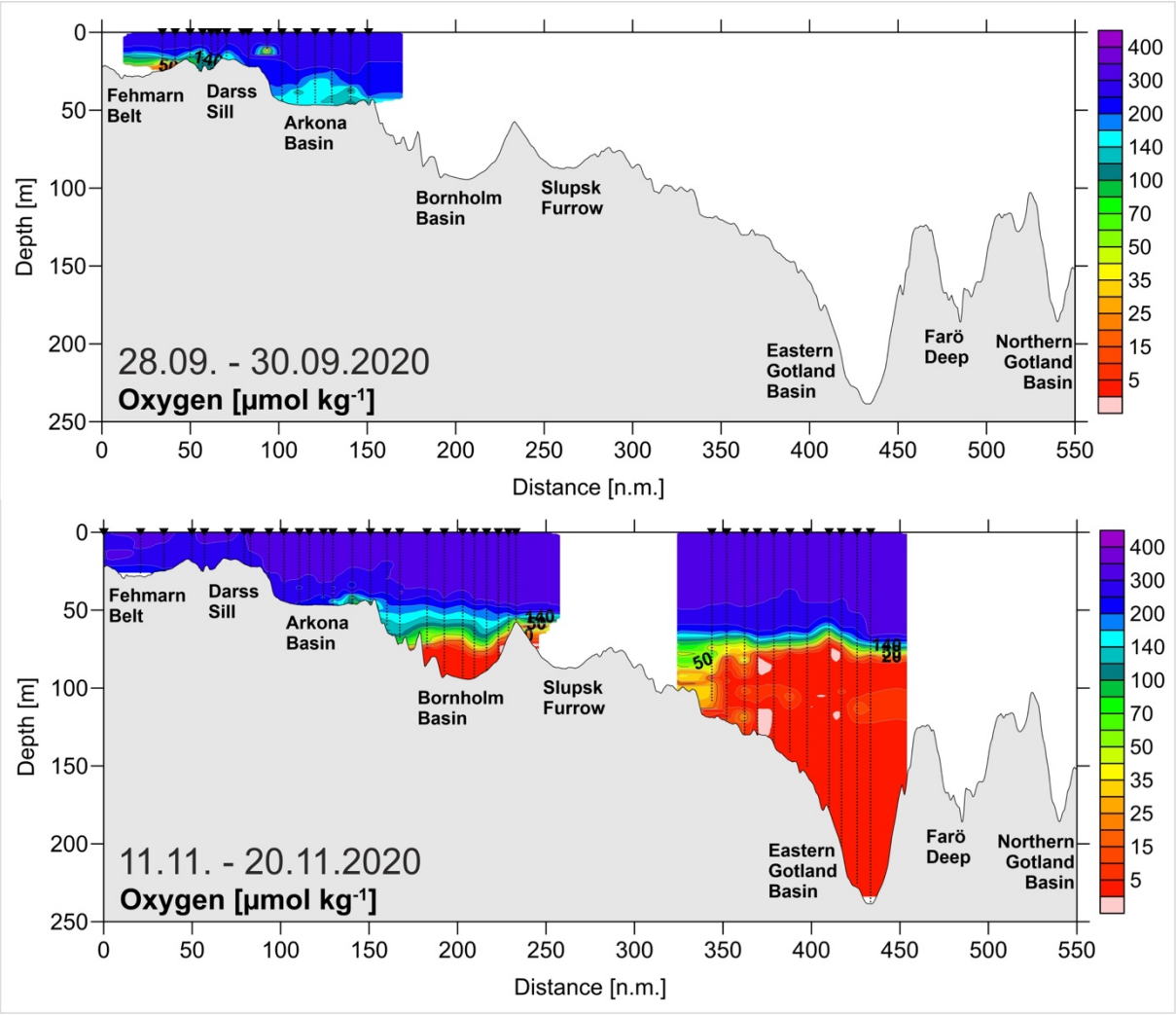

Fig. 28: Vertical distribution of oxygen (without H2S) during the September and November cruises in 2020 between the Darss Sill and the northern Gotland Basin. Values below 1 µmol/kg could not be distinguished from 0 µmol/kg.

Deep-water conditions of the central Baltic Sea deep basins are primarily influenced by the occurrence or absence of moderate and strong barotropic and/or baroclinic inflows. In February 2020 the slight remains of the inflow pulses of oxygenated water of the year 2019 were still visible. In February 2020 the eastern Gotland Basin showed values of up to 35 µmol/kg (about 0.82 ml/l) oxygen in the pycnocline between 80 and 120 m. Already some dense (8 °C and S=17-18) and oxygenated water (200 µmol/kg, about 4.53 ml/l) had entered the Bornholm Sea. The next campaign was in May that showed that the water had moved via the Słupsk Furrow to the southeastern Gotland Basin with oxygen concentrations of up to 120 µmol/kg (about 2.73 ml/l). The water inserted above 130 m depth in the central eastern Gotland Sea Basin. However, the oxygen was almost consumed in the central eastern basin until November. Only remains of 50 µmol/kg (about 1.15 ml/l) were still found above 100 m depth at the southern slope of the basin.

4.4 Nutrients: Inorganic nutrients

The eutrophication of the Baltic Sea remains a major concern despite many reduction measures that have been implemented in the last decades. In Germany, riverine inputs of total phosphorus declined between 2006 and 2014 by 14 %. In the same time-period, total nitrogen input decreased by 31 % (HELCOM 2018a). Despite this positive development, German territorial waters and bordering sea areas of the Baltic Sea remained hypertrophied by up to 50 % in the western and up to 100 % in the eastern part (HELCOM 2018b). To determine the effects of changes in nutrient inputs and to evaluate the results of reduction measures undertaken, the frequent monitoring of the nutrient situation is mandatory. Nutrients are core parameters since HELCOM established a standardized monitoring programme at the end of the 1970ies.

A drastic description of the consequences of eutrophication is given by DUARTE et al. (2009) "The effects of eutrophication include the development of noxious blooms of opportunistic algae and toxic algae, the development of hypoxia, loss of valuable seagrasses, and in general a deterioration of the ecosystem quality and the services they provide". According to the second "State of the Baltic Sea" report, 97 % of the Baltic Sea area is affected by eutrophication and 12 % is assessed as being in the worst status category (HELCOM 2018a).

Comparing the Pollution Load Compilation for the year 2010 (PLC-5.5) (HELCOM 2015) with that for 2014 (PLC-6) (HELCOM 2018b), **total waterborne and airborne inputs of nitrogen to the Baltic Sea** decreased from 977,000 megagrammes (Mg) to 826,000 Mg annually. For **phosphorus** the decline was given for 2006 to 2014 from annual 35,500 Mg to 31,000 Mg without accounting for the less important atmospheric deposition of about 2,100 Mg determined for 2010.

The 826,000 Mg total nitrogen that was delivered to the Baltic Sea shared between 27.1 % from the atmosphere, 3.5 % from direct sources and 69.4 % from rivers, correspondingly, of the 31,000 Mg of total phosphorous, 5.2 % were from direct sources and 94.8 % by riverine supply (HELCOM, 2018b). In turn, 61 % of the atmospheric deposition of total nitrogen to the Baltic Sea of overall 228,000 Mg originated from surrounding HELCOM countries, 8 % from Baltic Sea shipping (+ 5 % from North Sea shipping), 21 % from EU countries which are not HELCOM Contracting Parties, and the remaining 5 % from other countries and distant sources outside the Baltic Sea region in 2017 (GAUSS et al., 2020). Thereby, a major contribution of almost 35,000 Mg originates from agriculture in Germany, which is 25 % of the HELCOM countries atmospheric total nitrogen supply to the Baltic Sea of 140 000 Mg.

4.4.1 Surface water processes

Nitrate and phosphate concentrations in the surface waters of temperate latitudes exhibit a typical annual cycle with high concentrations in winter, depletion during spring and summer, and recovery in autumn (NAUSCH & NEHRING 1996, NEHRING & MATTHÄUS 1991). However, in recent years it appears more and more clear that nitrate is completely taken up by the spring bloom and replenished during late autumn and winter, whereas phosphate is significantly declining in April/May, but persists at low concentration almost throughout the summer. Thus, blooms of diazotrophic cyanobacteria, which use dinitrogen gas in addition to phosphate for growth, are always enabled.

Fig. 29 illustrates the annual cycle of nitrate and phosphate concentrations in surface waters at the stations Gotland Deep and Bornholm Deep in comparison to the surface water temperature development in 2020. For this purpose, the data of four monitoring cruises of the IOW were combined with data of the Swedish Meteorological and Hydrological Institute (SMHI) to get a better resolution of the seasonal patterns. In the central Baltic Sea, a typical phase of elevated nutrient concentrations usually develops during winter, which lasted two to three months (NAUSCH et al, 2008). In 2020, maximum nitrate concentrations were measured in the end of January/early February of 3.4 µmol/l in the central eastern Gotland basin and 2.9 µmol/l in the central Bornholm Sea, respectively. Maximum phosphate concentrations were determined in mid-March of 0.8 µmol/l at Gotland Deep and 0.9 µmol/l at Bornholm Deep site. The decline of nitrate started at the Gotland Deep station in mid-March and reached the detection limit in early May at a surface water temperature of 7.6 °C. At Bornholm Deep station nitrate already declined in second half of March and reached the detection limit in mid-April at 6.0 °C. The phosphate reserves lasted at both stations well during the summer of 2020. Only on 20th July, phosphate was below the detection limit at the Gotland Deep station. Thus, spring bloom in 2020 likely ended in the Bornholm Sea by mid-April, one month later than in 2019, and similarly to 2019 in the beginning of May in the eastern Gotland Sea. A significant increase of these basic major nutrients in the surface waters at both stations did not take place before early November. At that time, cooling to below 12 °C enabled wind induced mixing in a stormy period and a supply of nutrients from deeper layers. Mineralization processes at depth had caused an increase of nutrient concentrations that subsequently replenished the surface water until the end of the year.

The early exhaustion of nitrate at low temperatures likely caused availability of phosphate almost throughout the year 2020. Algae growth is nitrate limited and phosphate remains unused at prevailing spring temperatures. This is seen in a low dissolved inorganic nitrogen/phosphorus ratio (DIN/DIP) present in the winter surface water of the Baltic Sea. The favorable uptake ratio of about 16 was already shown by an early study of Redfield (REDFIELD et al., 1963) and was proven to be a valuable approximation many times thereafter. The DIN/DIP ratio (mol/mol) was determined from the sum of ammonium, nitrate, and nitrite concentrations versus the phosphate concentration. The surface water DIN/DIP ratio in the Baltic Sea in winter 2020 ranged between 6 and 11 mol/mol in the investigated sea areas. Closest to the ideal ratio were the data of Odra Bight and Mecklenburg Bight with N/P = 11 mol/mol. In 2019 the N/P-ratio in the Mecklenburg Bight was about 6 mol/mol only. A clear increase also happened in the western Gotland Sea from N/P = 3 to almost 8 mol/mol. Also for the Belt Sea, Arkona Sea, Bornholm Sea, central, southern, and northern Gotland Sea the N/P-ratio was higher in 2020 compared to 2019. However, these values appeared overall in the range of recent years (Fig. 30). This indicated again that nitrogen was a limiting factor, giving diazotrophic cyanobacteria an advantage compared to primary producer that depend on nitrate. However, a weak sign of improvement compared to recent years is also indicated. The exceptional high DIN/DIP ratio of about 20 mol/mol in the Odra Bank area from 2017-2019 was clearly lower in 2020 and similar to 2016.

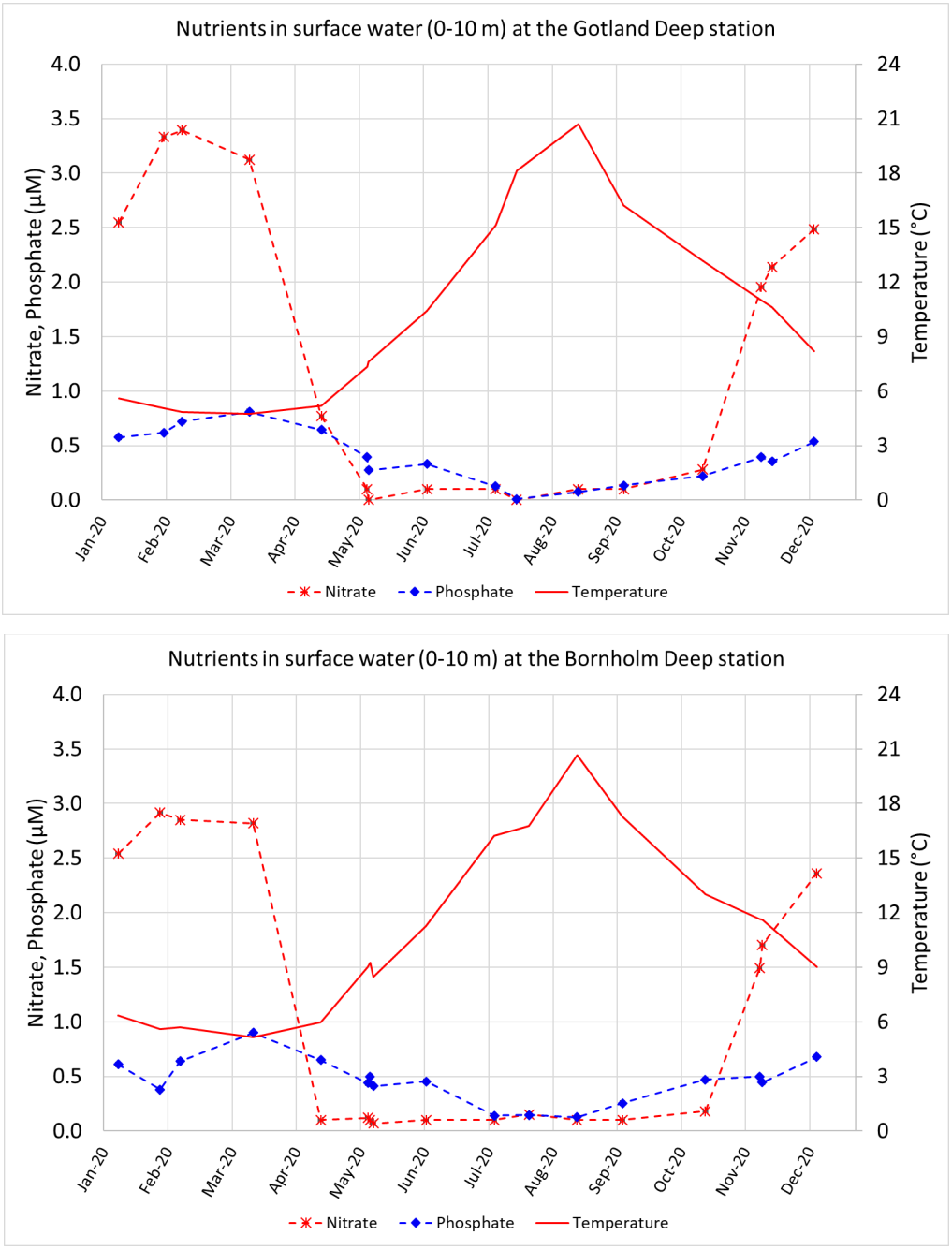

Fig. 29: Vertical distribution of oxygen (without H2S) during the September and November cruises in 2020 between the Darss Sill and the northern Gotland Basin. Values below 1 µmol/kg could not be distinguished from 0 µmol/kg.

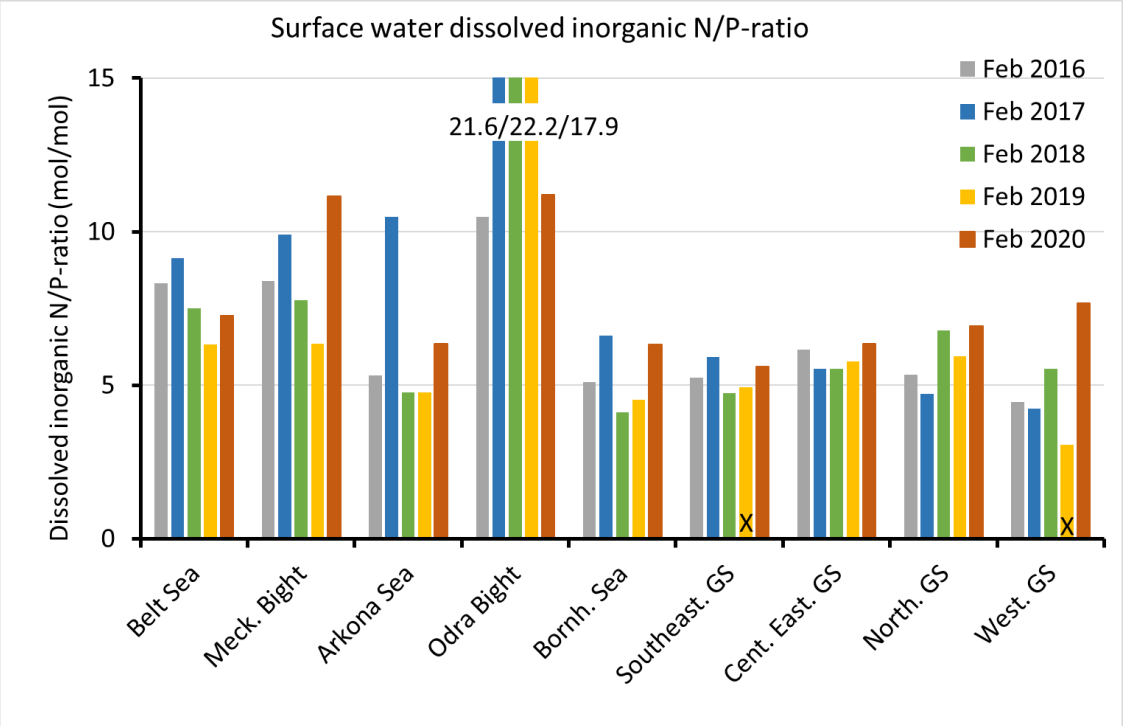

Fig. 30: Average dissolved inorganic nitrogen versus phosphate ratio in surface waters of selected Baltic Sea areas in February of 2016 to 2020; for the cross-marked bars the ammonium concentration (a minor contribution to DIN) was estimated. Three very high ratios from the Odra Bight are indicated as numbers to avoid prolonging the y-axis.

Table 9 shows winter phosphate and nitrate concentrations in surface waters for the February months of recent years. For phosphate, slightly lower values were determined for 2020 compared to previous years. Thus phosphate in 2020 reflects the minimum or is at least close to the minimum of the last five years. Most pronounced was the change on Fehmarn Belt Station from 0.42 µmol/l in 2019 to 0.26 µmol/l in 2020, a decrease by about one-third. On other stations the phosphate concentration decreased by at least 0.1 µmol/l like the Arkona Sea, Bornholm Deep, Fårö Deep and Landsort Deep. Phosphate in Gotland Sea surface water is relative stable in recent years. At Karlsö Deep station, a weak declining trend since 2017 from 0.91 µmol/l to 0.58 µmol/l in 2020 is recorded.

The nitrate concentration of the selected stations determined for February 2020 were generally in the range of previous years with a tendency, similarly as for phosphate to lower concentrations. For the Fehmarn Belt station a decline by 0.6 to 1.1 µmol/l nitrate, for Gotland Deep by 0.6 to 3.4 µmol/l, for Fårö Deep by 0.4 to 3.6 µmol/l, and Landsort Deep by 0.2 to 3.8 µmol/l nitrate were determined. However, at the Mecklenburg Bight station an increase was observed from 2.8 to 3.8 µmol/l. Also the Bornholm Deep station showed a slight change from 2.6 to 2.9 µmol/l nitrate. For Karlsö Deep the strongest increase from low nitrate concentrations in the last year of 1.2 µmol/l to a value of 3.6 µmol/l that was also found in 2018 and slightly lower before.

The changes during the last five years may indicate some declining tendencies of phosphate and to a lesser extent for nitrate, but statistically solid reductions of nutrient concentrations that have already been observed in coastal waters are up to now not reflected in the nutrients concentrations of the central Baltic Sea basins (NAUSCH et al. 2011b, NAUSCH et al. 2014). By comparison with nutrient target values elaborated in the TARGEV project (HELCOM 2013), a discrepancy is observed between the phosphate and dissolved inorganic nitrogen (DIN), basically nitrate in surface waters, in terms of reaching the targets. The target values of DIN and DIP winter concentrations are for the Kiel Bight 5.45/0.60 µmol/l, Mecklenburg Bight 4.24/0.50 µmol/l, the Arkona Sea 2.90/0.36 µmol/l, for the Bornholm Sea 2.52 0.32 µmol/l, and for the Eastern Gotland Basin 2.59/0.29 µmol/l, respectively. This indicates that the nitrate winter concentration (ammonium and nitrite reflect minor contributions) may stabilzes at or below the respective target values in the western Baltic Sea within this decade, but for phosphate it may need some more decades to reach the Good Environmental Status at business as usual. However, it has to be noted that the lower winter nitrate concentration could be significantly caused by increased anoxia in deep waters that could constitute a considerable nitrate sink by denitrification. Thus, it may be - at least partly - not a good sign.

Table 9: Mean nutrient concentrations in the surface layer (0-10 m) in winter in the western and central Baltic Sea (IOW and SMHI data).

Table 9.1: Surface water phosphate concentrations (µmol/l) in February (Minima in bold).

Station	2016	2017	2018	2019	2020
360 (Fehmarn Belt)	0.66 ± 0.04	0.54 ± 0.01	0.66 ± 0.02	0.42 ± 0.00	**0.26 ± 0.04**
022 (Lübeck Bight)	0.79 ± 0.15	**0.53 ± 0.09**	0.69 ± 0.00	-	-
012 (Meckl. Bight)	0.68 ± 0.01	**0.56 ± 0.00**	0.70 ± 0.00	0.58 ± 0.00	0.58 ± 0.00
113 (Arkona Sea)	0.64 ± 0.01	0.53 ± 0.00	0.67 ± 0.01	0.59 ± 0.00	**0.43 ± 0.01**
213 (Bornholm Deep)	0.67 ± 0.06	0.61 ± 0.06	0.65 ± 0.01	0.61 ± 0.02	**0.51 ± 0.03**
271 (Gotland Deep)	**0.67 ± 0.04**	0.70 ± 0.08	**0.67 ± 0.01**	0.68 ± 0.02	**0.67 ± 0.00**
286 (Fårö Deep)	0.65 ± 0.08	0.69 ± 0.01	0.64 ± 0.01	0.71 ± 0.01	**0.57 ± 0.01**
284 (Landsort Deep)	0.75 ± 0.01	0.79 ± 0.03	**0.59 ± 0.01**	0.70 ± 0.01	**0.59 ± 0.00**
245 (Karls Deep)	0.87 ± 0.09	0.91 ± 0.07	0.70 ± 0.01	0.65 ± 0.01	**0.58 ± 0.01**

Table 9.2: Surface water nitrate concentrations (µmol/l) in February (Minima in bold).

Station	2016	2017	2018	2019	2020
360 (Fehmarn Belt)	4.5 ± 0.5	3.2 ± 0.1	3.7 ± 0.0	1.7 ± 0.1	**1.1 ± 0.8**
022 (Lübeck Bight)	6.3 ± 0.1	**4.5 ± 0.7**	6.1 ± 0.0	-	-
012 (Meckl. Bight)	4.8 ± 0.1	4.4 ± 0.0	4.7 ± 0.3	**2.8 ± 0.1**	3.8 ± 0.0
113 (Arkona Sea)	3.2 ± 0.2	5.2 ± 0.0	2.8 ± 0.0	2.6 ± 0.0	**2.5 ± 0.0**
213 (Bornholm Deep)	2.8 ± 0.2	3.8 ± 0.1	**2.5 ± 0.0**	2.6 ± 0.1	2.9 ± 0.0
271 (Gotland Deep)	**3.4 ± 0.4**	3.9 ± 0.3	**3.4 ± 0.0**	4.0 ± 0.0	**3.4 ± 0.1**
286 (Fårö Deep)	**3.3 ± 0.5**	3.9 ± 0.1	3.9 ± 0.0	4.0 ± 0.0	3.6 ± 0.1
284 (Landsort Deep)	3.9 ± 0.0	**3.4 ± 0.2**	3.9 ± 0.0	4.0 ± 0.0	3.8 ± 0.0
245 (Karls Deep)	3.3 ± 0.3	3.3 ± 0.1	3.6 ± 0.0	**1.2 ± 0.1**	3.6 ± 0.1

4.4.2 Deep water processes in 2020

In central Baltic Sea deep waters, the nutrient distribution is primarily influenced by the occurrence or absence of strong barotropic and/or baroclinic inflows and, thus, by its oxygen/hydrogen sulphide concentrations in deep waters. Since the MBI 1014/2015 the accumulation of phosphate in the deep water of the central basins has continued. In the Gotland Deep at 200 m phosphate reached 5.1 µmol/l, almost 4 µmol/l in the Landsort Deep in 400 m depth, and 3.9 µmol/l phosphate in the Karlsö Deep at 100 m depth. Thus the Gotland Deep surpassed the pre-inflow annual average phosphate concentration of 4.50 µmol/l. The Fårö Deep received some oxygen in 2020, likely from the Gotland Sea intermediate water as mentioned before, and consequently showed some lower phosphate concentration of 3.4 µmol/l in 2020, compared to 4.0 µmol/l in 2019 (Table 11). During locally weak oxic water conditions phosphate could be bound to iron as well as to manganese and could be transported to the sediment by particles. The particles are dissolved during anoxia and then release the phosphate back to the water column. The Bornholm Deep showed some reduction in the annual average phosphate concentration at 80 m depth since the high value in 2018 of 4.73 to 2.88 in 2020. This is in agreement with its slight oxygen excess on average during 2020.

The fading of the MBI impact (NAUMANN et al. 2018) is also reflected in the depletion of nitrate in deep waters. Only the Bornholm Deep continued to accumulate nitrate in deep waters to a

concentration of 7.7 µmol/l in 2020, because of its weak oxic condition during this year. In the Fårö Deep an average nitrate concentration of 0.3 µmol/l at 150 m depth was determined for 2020 that was likely caused by the episodic oxygen supply mentioned before. At all other investigated sites at the selected reference depths the average annual nitrate concentration was below the detection limit (Table 10). An explanation is that anoxic conditions prevent mineralization of organic matter to nitrate. Instead, ammonium is formed and represents the end product of the degradation of biogenic material. Therefore, ongoing accumulation of ammonium in deep waters was recorded in Baltic Sea deep waters, in the Gotland Deep from 12.2 to 20.1 µmol/l, the Landsort Deep from 8.0 to 9.4 µmol/l, and the Karlsö Deep from 9.4 to 12.8 µmol/l between 2019 and 2020. In the Fårö Deep also for ammonium the slight oxygen supply is confirmed by a decrease of ammonium from 9.1 to 7.3 µmol/l between 2019 to 2020 in the reference depth. In the Bornholm Deep ammonium decreased since 2018 by episodic smaller inflow events from 1.9 in 2018 to 1.5 in 2019 and further to 0.4 µmol/l annual mean ammonium concentration in 2020 (Table 10). Fig. 31 illustrates the nutrient distributions in the water column on the transect between the Mecklenburg Bight and the Northern Gotland Sea in February, May, July and November 2020.

In summary, the stagnation period that has started in the Eastern Gotland Sea already in 2015, thus, shortly after the MBI of December 2014 was basically ongoing in 2020 and hydrogen sulphide is accumulating in deep waters (Table 8.4). This is accompanied by phosphate and ammonium increase and a depletion of nitrate (Table 10). Again in 2020 the Bornholm Sea and the southern Gotland Sea received pulses of oxygenated waters in the bottom range. Afterwards, plumes of water bearing oxygen residues were entrained all over the eastern Gotland Basin in the 80 to 120 m depth range and also influenced to nutrient concentrations in the Fårö Deep.

Table 10: Annual means and standard deviations for phosphate (Tab. 11.1), nitrate (Tab. 11.2) and ammonium (Tab. 11.3) in the deep water of the central Baltic Sea (IOW and SMHI data).

Table 10.1: Annual mean deep water phosphate concentration (µmol/l; Maxima in bold).

Station	depth/m	2016	2017	2018	2019	2020
213 (Bornholm Deep)	80	2.23 ± 0.29	2.51 ± 1.15	**4.73 ± 1.56**	3.78 ± 1.40	2.88 ± 1.03
271 (Gotland Deep)	200	2.56 ± 0.14	2.91 ± 0.92	4.08 ± 0.13	4.38 ± 0.25	**5.14 ± 0.34**
286 (Fårö Deep)	150	2.93 ± 0.22	2.49 ± 0.12	3.55 ± 0.68	**4.02 ± 0.45**	3.36 ± 0.42
284 (Landsort Deep)	400	3.25 ± 0.31	3.08 ± 0.22	3.12 ± 0.22	3.64 ± 0.57	**3.98 ± 0.24**
245 (Karls Deep)	100	**4.25 ± 0.34**	3.77 ± 0.24	3.63 ± 0.34	3.51 ± 0.29	3.89 ± 0.25

Table 10.2: Annual mean deep water nitrate concentration (µmol/l; Minima in bold).

Station	depth/m	2016	2017	2018	2019	2020
213 (Bornholm Deep)	80	10.4 ± 1.9	7.5 ± 2.3	**1.6 ± 1.5**	6.8 ± 2.9	7.7 ± 4.1
271 (Gotland Deep)	200	9.3 ± 0.7	1.8 ± 2.2	**0.0 ± 0.0**	**0.0 ± 0.0**	0.1 ± 0.1
286 (Fårö Deep)	150	1.4 ± 1.7	5.5 ± 3.5	**0.0 ± 0.0**	**0.0 ± 0.0**	0.3 ± 0.6
284 (Landsort Deep)	400	**0.0 ± 0.0**	**0.0 ± 0.1**	**0.0 ± 0.0**	**0.0 ± 0.0**	0.1 ± 0.0
245 (Karls Deep)	100	0.1 ± 00	0.1 ± 0.0	**0.0 ± 0.0**	**0.0 ± 0.0**	0.1 ± 0.0

Table 10.3: Annual mean deep water ammonium concentration (µmol/l; Maxima in bold).

Station	depth/m	2016	2017	2018	2019	2020
213 (Bornholm Deep)	80	0.2 ± 0.1	0.2 ± 0.3	**1.9 ± 2.4**	1.5 ± 3.1	0.4 ± 0.7
271 (Gotland Deep)	200	0.2 ± 0.0	0.8 ± 0.9	6.0 ± 2.3	12.2 ± 3.8	**20.1 ± 5.0**
286 (Fårö Deep)	150	2.0 ± 2.0	0.1 ± 0.0	3.6 ± 1.7	**9.1 ± 1.2**	7.3 ± 3.6
284 (Landsort Deep)	400	7.8 ± 3.3	3.8 ± 1.9	5.0 ± 2.2	8.0 ± 1.0	**9.4 ± 2.2**
245 (Karls Deep)	100	9.7 ± 1.7	8.4 ± 1.5	10.4 ± 2.9	9.4 ± 5.1	**12.8 ± 2.9**

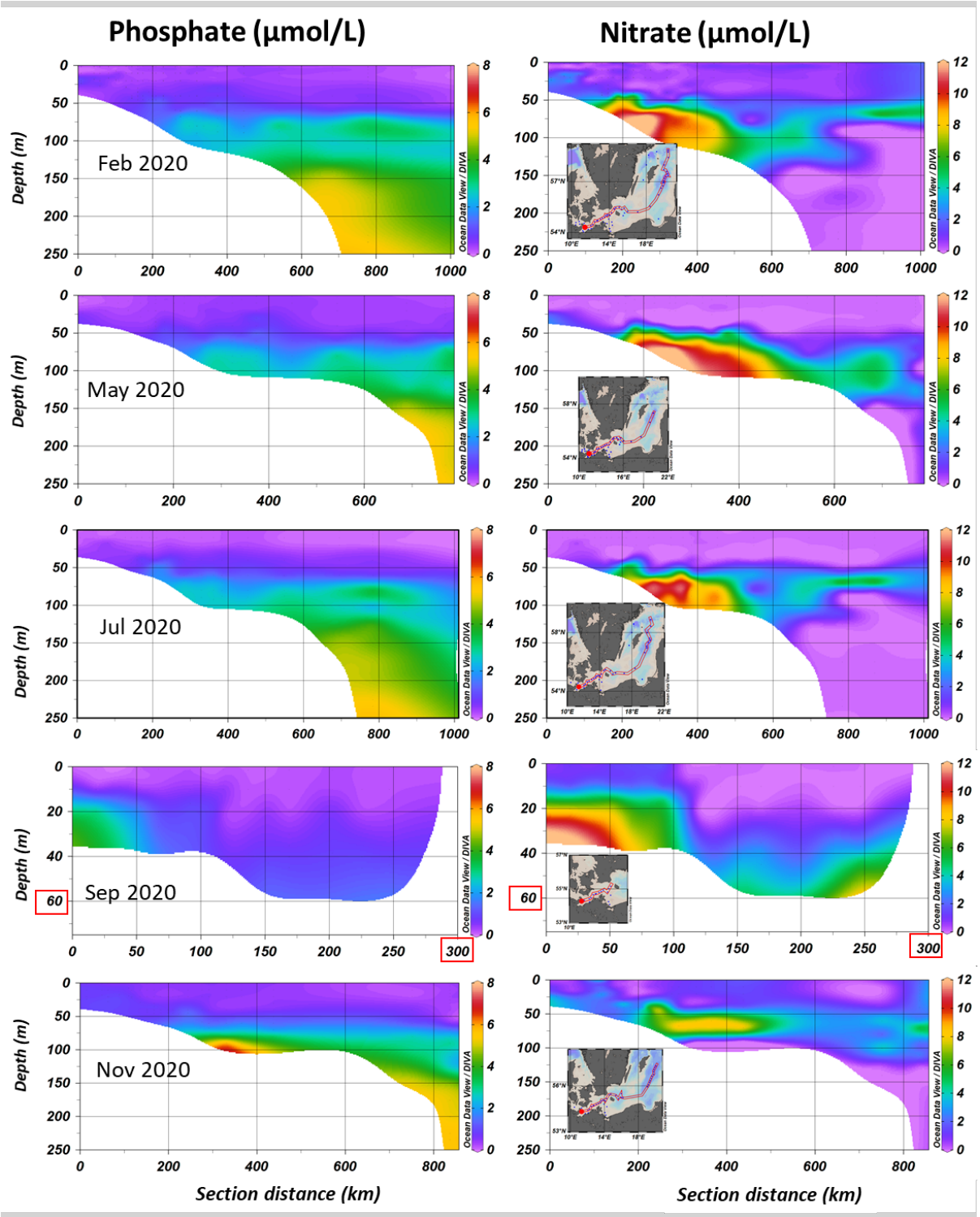

Fig. 31: Vertical distribution of phosphate (left column) and nitrate (right column) in 2020 between the Mecklenburg Bight and the northern Gotland Basin measured on the monitoring cruises in February, May, July and November; in September the transect was from Darss Sill to the Island of Bornholm with a maximum depth of 60 m (figure panels were prepared by using ODV 5, (SCHLITZER 2018).

In **surface water** a south-north gradient was documented in February from 2 to 4 µmol/l for nitrate and a patchy distribution of the phosphate concentration usually between 0.5 and 1 µmol/l with slightly higher values in the North. In May, nitrate was already depleted during the whole transect

down to 40-50 m depth. The depletion was maintained until November when breakup of the thermocline partly enabled deeper mixing. Only in the Darss Sill area, the surface water showed nitrate concentration of about 1 µmol/l in September. Phosphate showed a smooth decline from February until July/September 2020, but still mostly above the detection limit. In November phosphate almost reached 1 µmol/l again (Fig. 31).

Below 150 m (February) to 120 m (November) the nitrate and phosphate concentration in **deep waters** of the eastern Gotland basin were generally o µmol/l and about 4 - 6 µmol/l, respectively. Only in May some elevated values of about 1 µmol/l nitrate were determined in the depth range of 160-180 m. In the Bornholm Basin and the southern Gotland Sea nitrate was accumulating to more than 10 µmol/l and phosphate increased from 2 to 3 µmol/l until May. Locally elevated nitrate concentrations were measured in the depth range between 50 and 120 m throughout the eastern Gotland Basin of up to 6 µmol/l nitrate. The location of these filaments change clearly through the year. In contrast to nitrate, phosphate showed a distinct layering in February, May and July 2020 with phosphate concentrations of about 3 µmol/l in 100 m, 4 µmol/l in 150 m, and below about 170 m 4-6 µmol/l. In November phosphate had accumulated in bottom waters in the area of the Słupsk Furrow to a concentration of 5-6 µmol/l (Fig. 31).

4.5 Nutrients: Particulate organic carbon and nitrogen (POC, PON)

Organically bound carbon in the global ocean comprising around 1000 Pg C (FALKOWSKI & RAVEN 2013) outcompetes the carbon present in atmospheric CO2 (EMERSON & HEDGES 2008). For practical reasons, the water column OM is divided in dissolved organic matter (DOM) and particulate organic matter (POM) by filtration of seawater. Most of the OM is present in dissolved form (~662 Pg C, HANSELL et al., 2009), whereas POM constitutes the main pathway by which organic matter is channeled through the biological pump to depths (LE MOIGNE 2019). POM includes biomass from living microbial cells, detrital material including dead cells, fecal pellets, other aggregated material, and terrestrially-derived organic matter (KHARBUSH et al. 2020). In the Baltic Sea, the cycling and relative contributions of organic bound carbon and nitrogen are different to the global ocean compositions, reviewed in KULINSKI & PEMPKOWIAK (2012). The concentrations of organic matter in the Baltic Sea are elevated compared to open ocean waters, highest concentrations are found close to the rivers, indicating terrestrial sources. In the eutrophic, brackish marginal sea experiencing little exchange with the North Sea, the terrigenous OM accumulates and residence times of ~4.5 years for high molecular weight OM are determined for the Baltic Proper (BIANCHI et al. 1997, OSBURN & STEDMON 2011, DEUTSCH et al. 2012).

The relative contributions of dissolved organic carbon (DOC) and particulate organic carbon (POC) in the western Baltic Sea were 93.2±3.9 and 6.8±3.9 % including data from the stations TF0012 in the Mecklenburg Bight, TF0109 and TF0113 in the Arkona Basin, TF0213 in the Bornholm Basin, TF0360 at Fehmarn Belt and TFO5 close to Warnemünde since 1995. Nitrogen fractions were much more variable and comprised 73.6±11.9 dissolved organic nitrogen (DON), 13.6±7.2 % particulate organic nitrogen (PON), 9.8±12.2 % nitrate+nitrite, and 3.0±6.5 % ammonium. The values for the warm year of 2020 fit in with this and the long-term observations described by NAUSCH et al. (2008) for an extended dataset of the Baltic Sea.

POC and PON concentrations were highly correlated (1995 to 2020, Pearson's r=0.94, p<0.001, n=2653, Fig. 32) and little systematic seasonal variability. The particulate C/N ratios were for 2020 on average 7.2±0.5 for the bottom waters and 7.4±0.2 for the surface waters and thus only slightly below the long-term means of 7.6±0.6 (Fig. 33, Fig. 34). The overall 2020 C/N ratio of 7.1±1.2 was higher than the ratio for living plankton of 6.6 (REDFIELD 1934), indicating preferential nitrogen remineralization at some stations (SCHNEIDER et al. 2003). This is also supported by the fact that the lowest C/N values were detected at the northernmost deep station TF0213 in the Bornholm Basin.

In the photic surface waters, POC and PON concentrations are mainly controlled by the presence, growth and degradation of biological produced material (SZYMCZYCHA et al. 2017, WINOGRADOW et al. 2019). Although terrestrial inputs are a significant source of OM to the Baltic Sea regarding the dissolved fraction (NAUSCH et al. 2008, SEIDEL et al. 2017), the extremely weak correlation of salinity and POC indicated that terrestrial POC played a negligible role at the sampled stations (Pearson's r=0.07, p<0.001). POC and PON concentrations were elevated in the surface waters of all deep, stratified stations with depth › 40 m during May and July (Fig. 33). The seasonal POC and PON signal induced by primary production of phytoplankton was mostly visible down to the bottom water layers. Especially at TF0109 and to some degree at TF0113 in the Arkona Basin, the lower C/N ratios indicated less degraded material in the bottom layer compared to TF0213 with a depth of › 80 m, which can be attributed to the shorter sinking time in the Arkona Basin.

This signal is not always visible (depending on the sampling time and resolution) as degradation of the organic matter is fast. Resuspension of material from organic-rich sediments (LEIPE et al. 2011) and slowed degradation of the OM under anoxic conditions in the deep basins (ASMALA et al. 2018) also contribute to the variability of bottom layer Baltic Sea POM. Resuspension processes likely contribute to the POM at the shallow, mixed stations TF012, TFO5, and TF0360, where increased POC and PON concentrations in spring and summer were detected throughout the water column (Fig. 34). At Fehmarn Belt (TF0360), high POC and PON concentrations were also found in January. The high water temperatures of 2020 were not reflected in exceptional POC or PON concentrations compared to previous years, and the impact of marine heat waves on the Baltic Sea biogeochemistry remains to be resolved (see Chapter 3.5 - Marine Heat Waves).

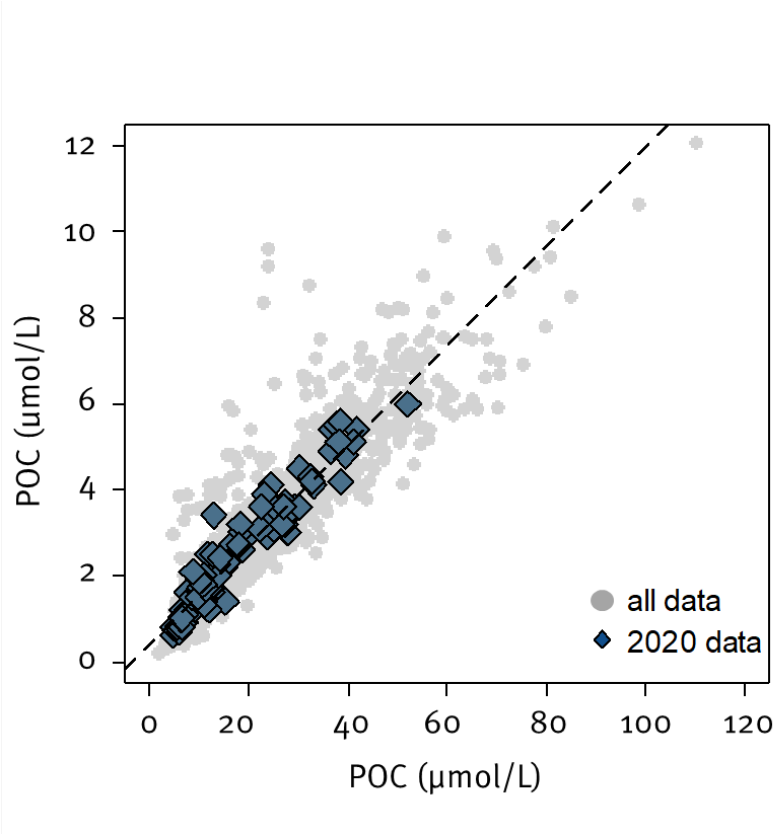

Fig. 32: POC versus PON concentrations for all data (gray dots, 1995-2019) and 2020 data in blue color. Dashed line denotes regression line.

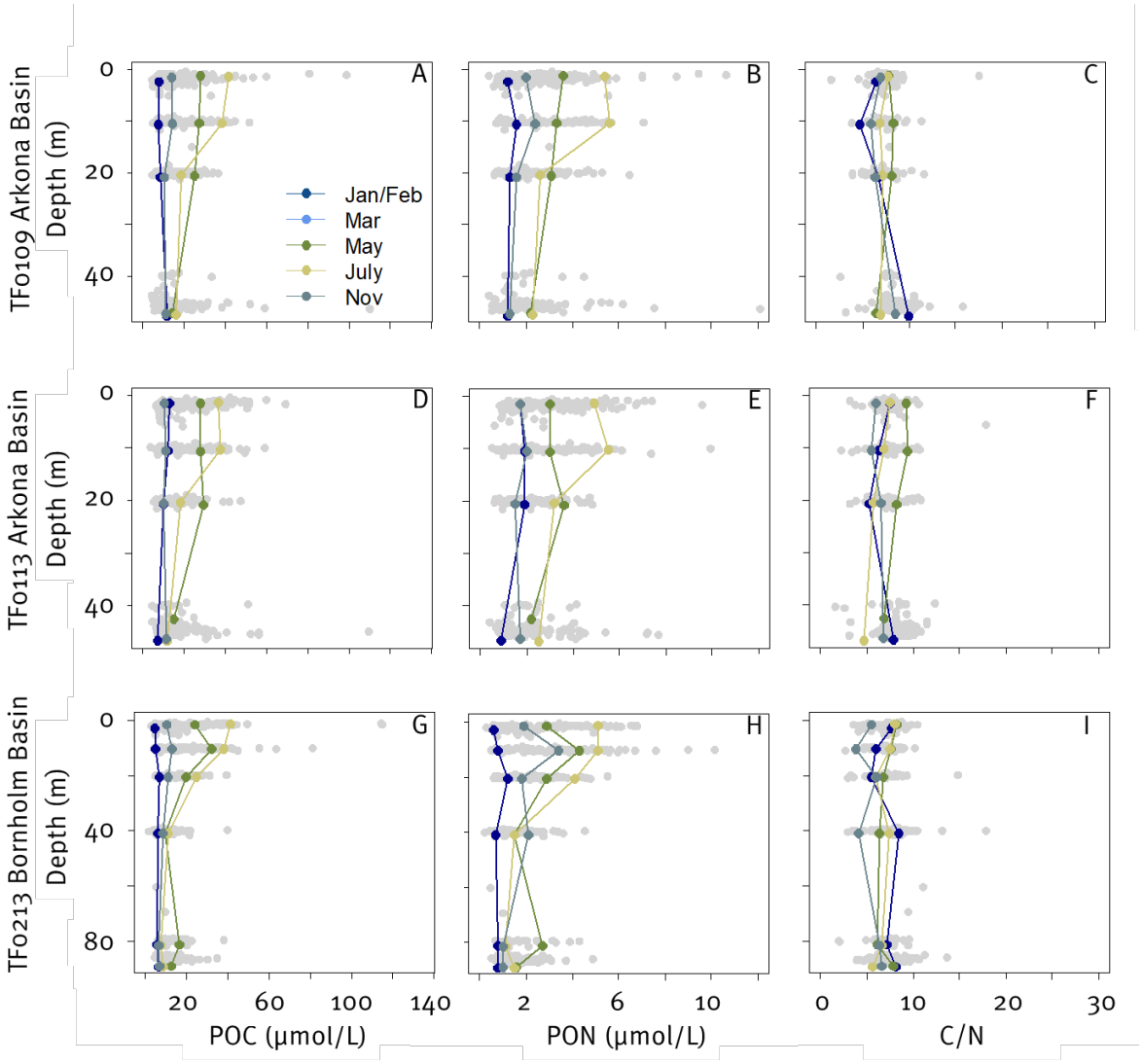

Fig. 33: POC, PON and particulate C/N ratio over depth at deep stations TF0109 (A-C), TF0113 (D-F) and TF0213 (G-I) in 2020 by month. Grey dots show range of historical data (1995-2019) from respective stations.

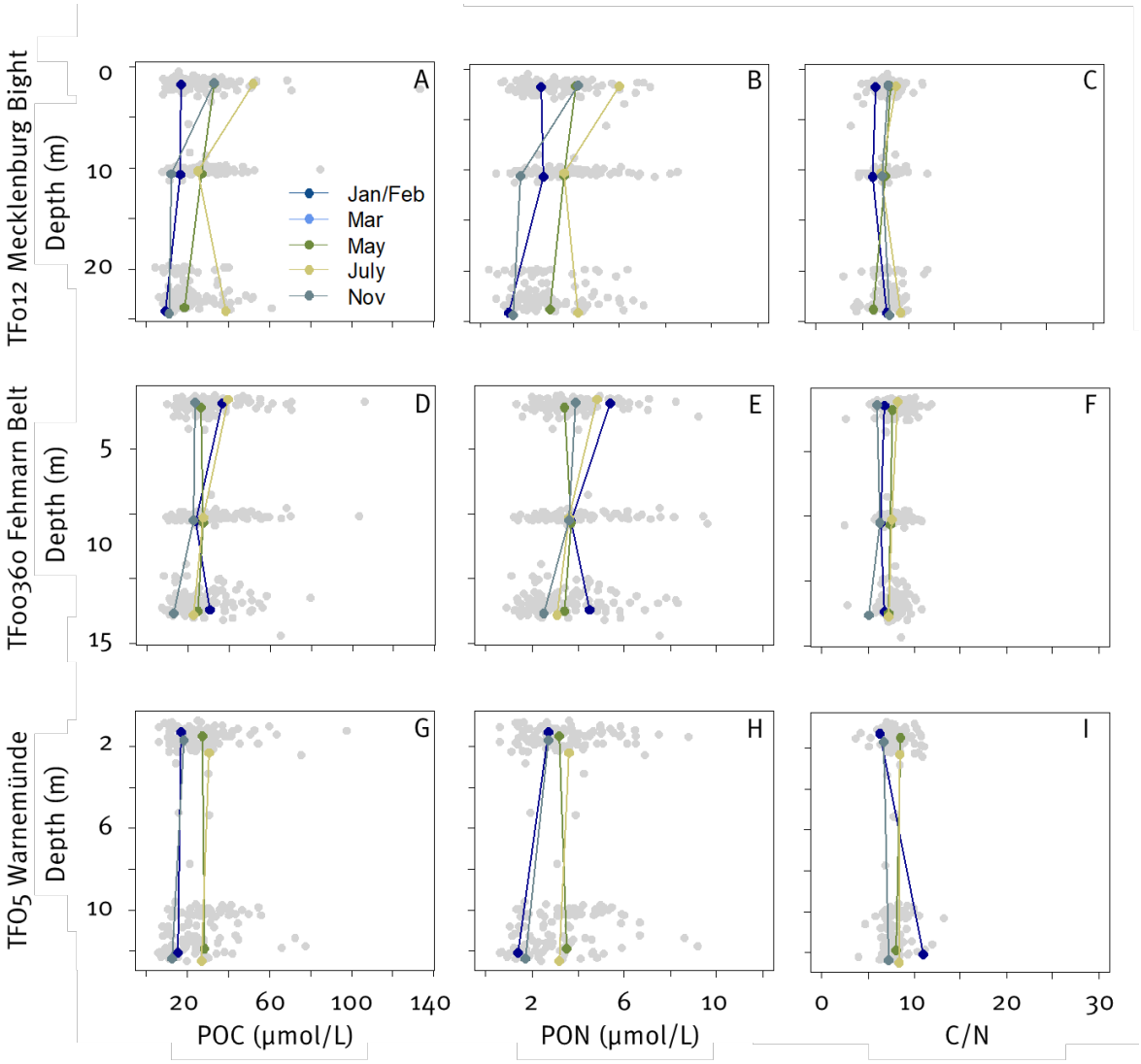

Fig. 34: POC, PON and particulate C/N ratio over depth at shallow stations TF012 (A-C), TF0360 (D-F) and TF05 (G-I) in 2020 by month. Grey dots show range of historical data (1995-2019) from respective stations.

4.6 Organic hazardous substances in surface water and sediment of the Baltic Sea in January/February 2020

The Baltic Sea is largely affected through contamination since the onset of the industrialization in the late 19th century. Riverine transport and atmospheric deposition are the main transport pathways of organic hazardous substances from land based sources in the catchment area into the Baltic Sea (HELCOM 2018c).

During the January/February 2020 surveillance, Baltic Sea surface sediments and water were sampled and analyzed for polycyclic aromatic (PAH) as well as chlorinated (CHC) hydrocarbons and also for organotin (OT) in surface sediment (Table 11). Herein, we report on the obtained data (for an overview see Fig. 35), continue time series data for the Mecklenburg Bight, Arkona Basin and the Pomeranian Bight. The results are assessed based on criteria of HELCOM as well as the Marine Strategy Framework Directive (MSFD) and the Water Framework Directive (WF).

Table 11: Analyzed compounds in Baltic Sea surface water and sediment samples obtained during the January/February 2020 observation.

Compound group	Subgroup	Determined substances
Chlorinated hydrocarbons	ICES-polychlorinated biphenyls (PCB_{ICES})	PCB28/31, PCB52, PCB101, PCB118, PCB153, PCB138, PCB180
	dichlorodiphenyl-trichloroethane (DDT) and metabolites	*p,p'*-DDT, *o,p'*-DDT dichlorodiphenyldichloroethylene (DDE): *p,p'*-DDE dichlorodiphenyldichloroethane (DDD): *p,p'*-DDD
		hexachlorobenzene (HCB)
Polycyclic aromatic hydrocarbons (PAH)	U.S. EPA PAH indicator compounds except naphthalene	acenaphthylene (ACNLE), acenaphthene (ACNE), fluorine (FlE), pheanthrene (PA), anthracene (ANT), fluoranthene (FLU), pyrene (PYR), benzo(*a*)anthracene (BAA), chrysene (CHR), benzo(*b*)fluoranthene (BBF), benzo(*k*)fluoranthene (BKF), benzo(*a*)pyrene (BAP), indeno(1,2,3-*cd*)pyrene (ICDP), dibenzo(*a,h*)anthracene (DBAH), benzo(*g,h,i*)perylene (BGHIP)
Organo-tins		monobutyltin (MBT), dibutyltin (DBT), tributyltin (TBT), triphenyltin (TPhT)

Samples were taken during the expedition EMB230 with RV "Elisabeth Mann Borgese" in January/February 2020. Surface water samples from sites in the Kiel Bight/Fehmarn Belt (T1), Mecklenburg Bight (T2), Arkona Sea (T3), Pomeranian Bight (T4), Bornholm Sea (T5), Central Baltic Sea (T6) as well as in the Eastern Gotland Sea (South and North, T7 and T8), and the Western Gotland Sea (T9) were obtained by transect sampling in the respective Baltic Sea area (Fig. 36).

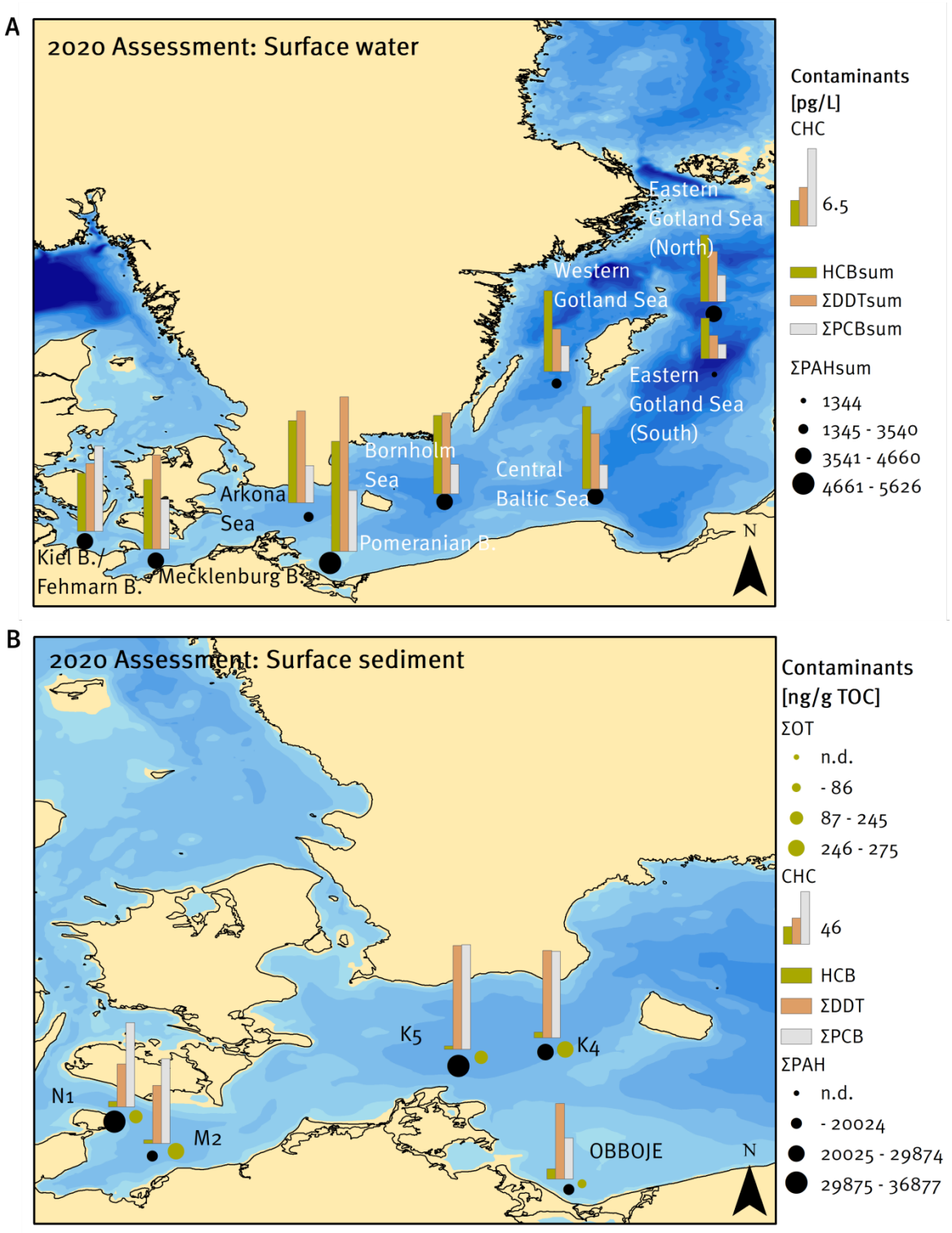

Fig. 35: Summary of obtained data for polycyclic aromatic hydrocarbons (PAH), chlorinated hydrocarbons (CHC) and organotin (OT) in Baltic Sea: A surface water and B surface sediment in January/February 2020. ΣPAHsum: summarized U.S. EPA PAH indicator compounds (exc. NAPH) in dissolved and particulate water fraction, HCBsum: summarized HCB concentration for dissolved and particulate water fraction, ΣDDTsum: summarized concentrations of DDT and metabolites in dissolved and particulate water fraction, ΣPCBsum: summarized concentrations of PCBICES of dissolved and particulate water fraction, ΣOT: sum of mono-, di- and tributyltin.

During the transect route a pump/filtration system was used to continuously pump surface water from 5 m below the surface through a GF/F filter and subsequently through an XAD-2 resin packed column with a flow rate of about 1.1 l/min for 4 to 6 hours. Sediment samples were taken at stations in the Fehmarn Belt (N1), Mecklenburg Bight (M2), Arkona Basin (K4, K5) and Pomeranian Bight (OBBOJE) using a multi corer for sampling (Fig. 36).

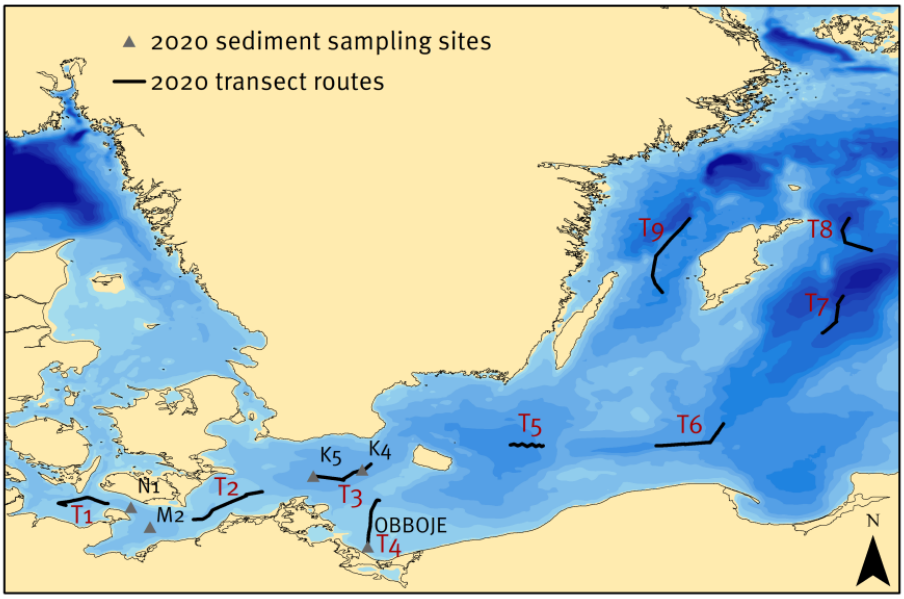

Fig. 36: Sediment sampling sites (gray triangles) and surface water sampling transect routes (solid lines) of the research vessel during the January/February 2020 monitoring. T1: Kiel Bight/Fehmarn Belt, T2: Mecklenburg Bight, T3: Arkona Sea, T4: Pomeranian Bight, T5: Bornholm Sea, T6: Central Baltic Sea, T7 Eastern Gotland Sea (South), T8: Eastern Gotland Sea (North), T9: Western Gotland Sea.

Chemical analysis of the CHC and PAH in the dissolved and particulate water fractions as well as in the sediment samples was conducted as described before (SCHULZ-BULL et al. 2011; KANWISCHER et al. 2020). Organotin compounds were analysed by GALAB Laboratories GmbH. All analyses followed accredited procedures.

4.6.1 Chlorinated Hydrocarbons: DDT and metabolites

The insecticide DDT has been used as a contact and feeding poison in agriculture and forestry since the 1940s. DDT technical formulations were mixtures of *o,p'* and *p,p'* congeners with *p,p'*-DDT as the predominant one. In the environment DDT degrades to the stable metabolites DDE and DDD. Due to their chemical stability and lipophilic properties, these contaminants accumulate in the tissues of animals and humans *via* the food chain. Due to their negative effects to non-target organisms, production and use of DDT is internationally restricted with the initial Stockholm Convention of 2004. However, in some countries DDT is still used, particularly for the control of disease-transmitting insects such as *Anopheles*.

DDT and metabolites in Baltic Sea surface water

In January/February 2020 concentrations of DDT and metabolites in Baltic Sea surface water ranged from 1.96 pg/L ΣDDT_{sum}[1] in the Eastern Gotland Sea (T7) to 13.06 pg/L ΣDDT_{sum} in the Pomeranian Bight (T4) (Fig. 37, Table Appendix 1). Bascially, ΣDDT_{sum} concentrations are higher in the western part of the Baltic Sea with highest concentrations in the Pomeranian decreasing to sites in the Gotland Sea.

Concentrations of ΣDDT_{part}[2] correlate with concentrations of suspended matter (SPM) (Fig. 37). Thus, the observed high SPM load at the Pomeranian Bight (about 1.1 mg/L) is accompanied with the highest particulate ΣDDT_{part} concentration of 5.96 pg/L. In contrast, the observed highest SPM concentration of about 1.6 mg/L in the Kiel Bight/Fehmarn Belt, which was caused by the beginning spring bloom at this site, does no gave rise to respective ΣDDT_{part} concentrations what is different to the obtained data for particulate PCB (see chapter 4.6.3 – surface water).

The observed concentrations of both dissolved and particulate DDT and metabolites in the Pomeranian Bight (T4) indicate a high pressure of DDT and metabolites in this area originating from the river Odra.

[1] ΣDDT_{sum}: summarized concentration of DDT congeners and their metabolites in particulate and dissolved fraction
[2] ΣDDT_{part}: summarized concentration of DDT congeners and their metabolites in particulate fraction

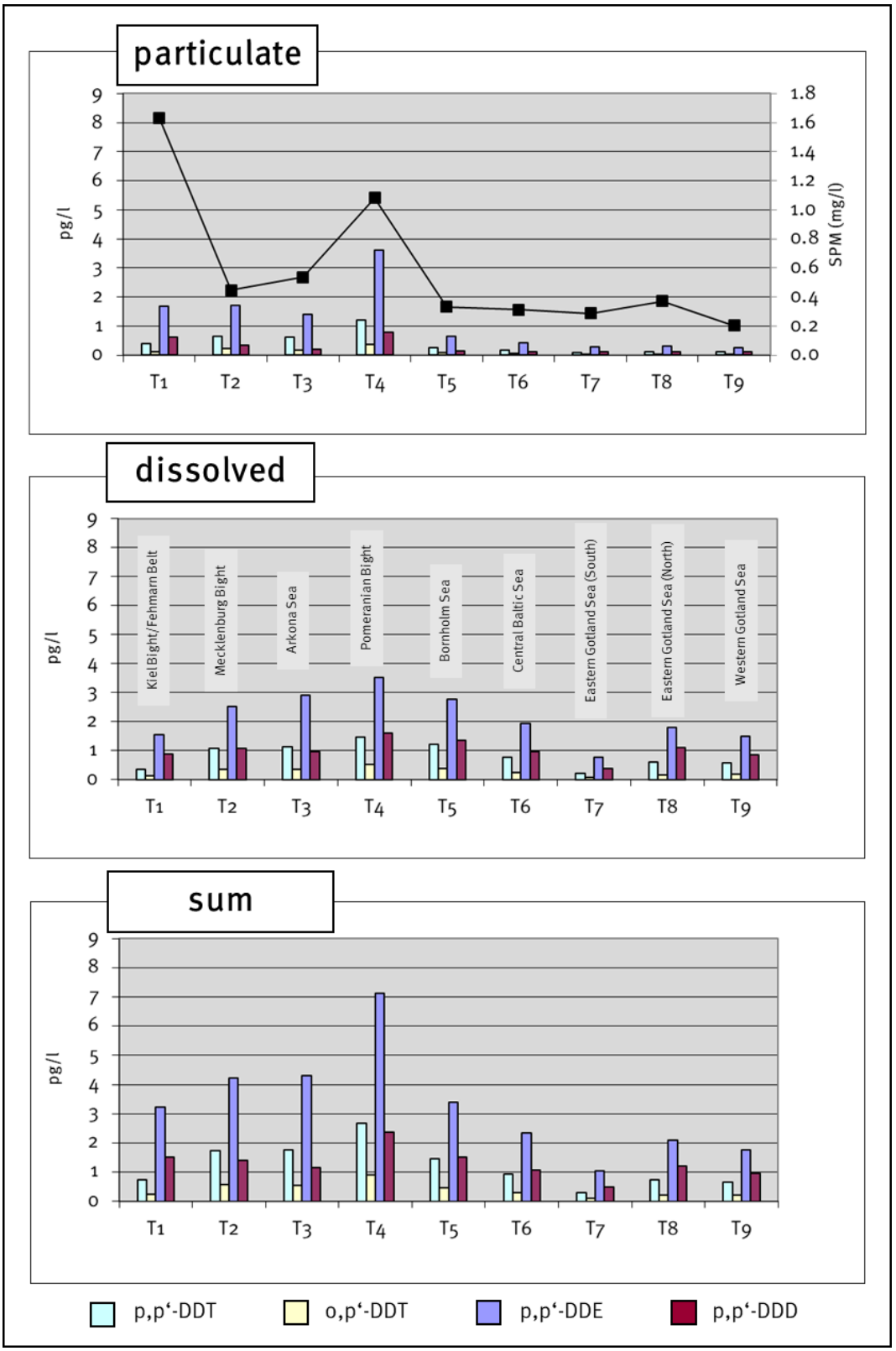

Fig. 37: Concentrations of DDT and metabolites in the dissolved and particulate fractions of Baltic Sea surface water samples of the January/February 2020 surveillance.

Concentrations of *p,p'*-DDE and *p,p'*-DDT of past winter observations are shown in Fig. 38 for the sites Mecklenburg Bight, Arkona Sea and Pomeranian Bight. Overall decreasing concentration trends of both compounds can be observed at these sites with higher annual variation for *p,p'*-

DDT than *p,p'*-DDE. The time series data for ΣDDT_{sum} identify the river Odra as particular source for particulate *p,p'*-DDT and *p,p'*-DDE contamination.

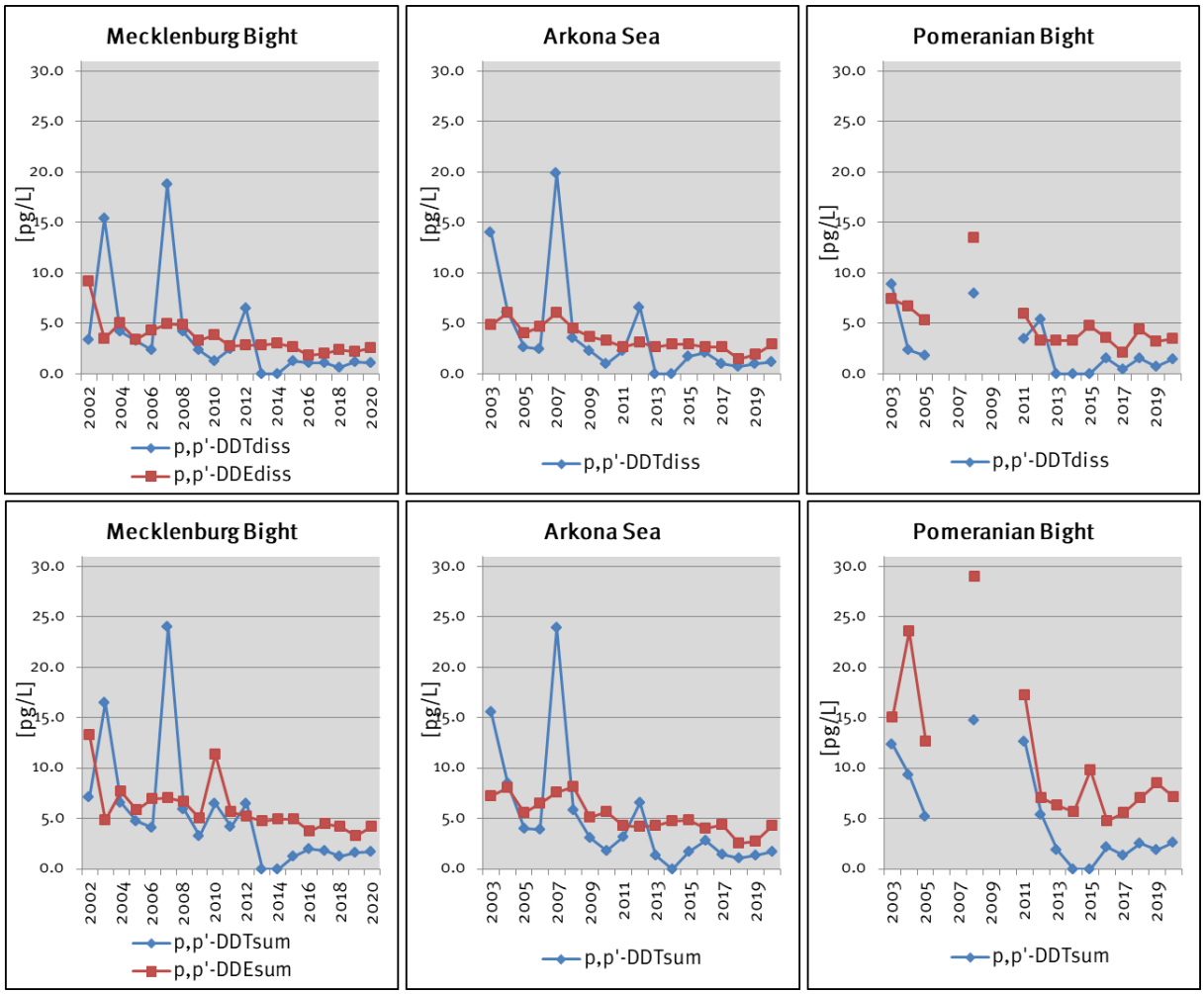

Fig. 38: Time series of p,p'-DDT and p,p'-DDE concentrations in surface water of the Mecklenburg Bight, Arkona Sea and Pomeranian Bight. Upper panel: dissolved fraction, lower panel: summarized dissolved and suspended fraction. Gaps in the time line indicate no sampling at the respective year; concentrations at "o ng/L" mean that the compound was not detected in the sample.

As observed in previous years, too, higher concentrations of the long-lived degradation product *p,p'*-DDE as compared to *p,p'*-DDT were recorded in the entire study area. This implies no recent input of DDT which is also reflected by *p,p'*-DDT/*p,p'*-DDE ratios which were below 0.5 at all sites (Table 12) (STRANDBERG ET AL. 1998).

Table 12: Ratios of p,p'-DDT/p,p'-DDE for the determined concentrations of DDT and metabolites in Baltic Sea surface water. [a] ratios were determined from summarized particulate and dissolved concentrations.

	T1	T2	T3	T4	T5	T6	T7	T8	T9
***p,p'*-DDT/*p,p'*-DDE** [a]	0.23	0.41	0.41	0.37	0.43	0.39	0.29	0.35	0.38

DDT and metabolites in Baltic Sea sediment

Obtained contents of DDT and metabolites in Baltic Sea surface sediment in January/February 2020 ranged from 37.6 ng/g TOC ΣDDT (≙ 445 pg/g DW) at station N1 at the Fehmarn Belt to 90.7 ng/g TOC ΣDDT (≙ 5597.1 pg/g DW) at station K5 in the Arkona Basin (Fig. 39, Table Appendix 4). Overall, highest ΣDDT contents were found at both Arkona Basin stations K4 (76.2 ng/g TOC, 4047 pg/g DW) and K5.

In contrast to Baltic Sea water, the predominant DDT metabolite in sediment is *p,p'*-DDD.

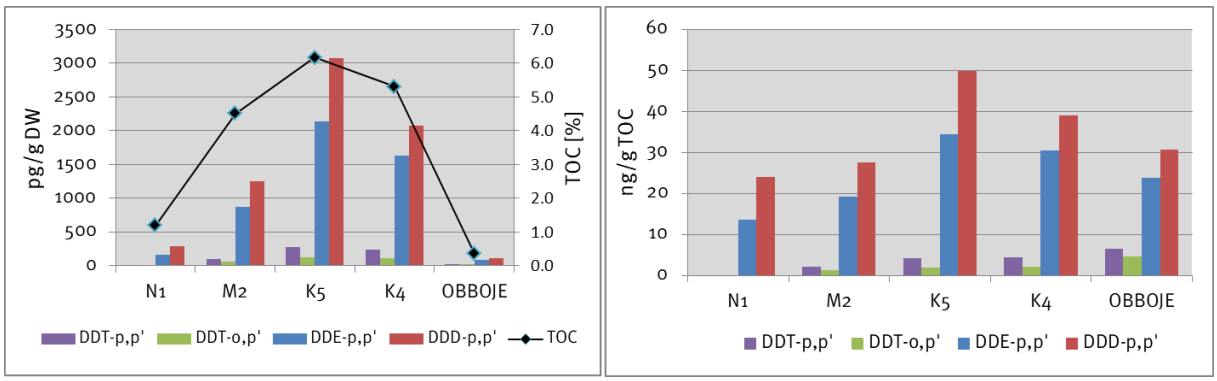

Fig. 39: Contents of DDT and its metabolites in Baltic Sea surface sediments in January/February 2020 in pg/g DW (left) and normalized to the organic carbon content in ng/g TOC (right).

Analysis of time series data for the long-lasting DDT metabolite *p,p'*-DDD shows that there are no trends in the Mecklenburg Bight, Arkona Basin and Pomeranian Bight during the investigated time period (Fig. 40). High variation of *p,p'*-DDE contents in the Pomeranian Bight indicates temporarily high entry from the river Odra, but also possible transportation of deposited pollutants.

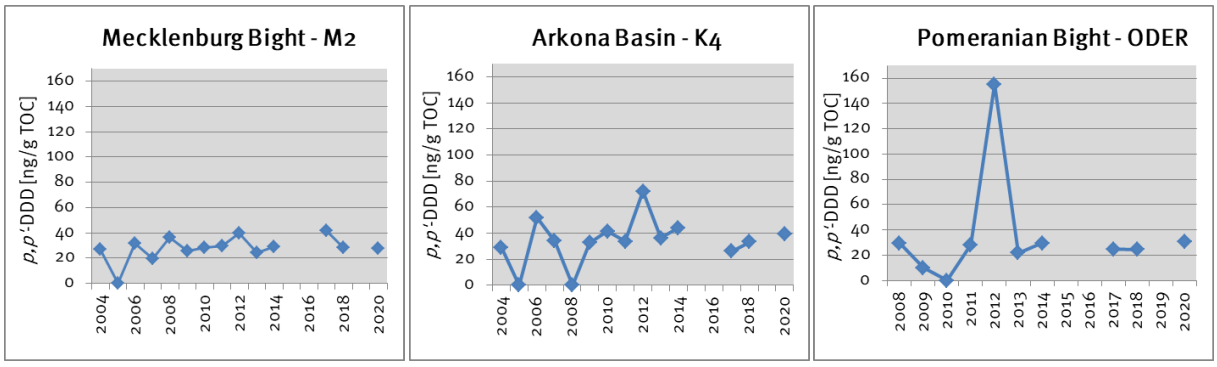

Fig. 40: Times series of p,p'-DDD contents in Baltic Sea surface sediments from 2004 to 2020 for the Mecklenburg Bight as well as the Arkona Basin and from 2008 to 2020 for the Pomeranian Bight. Gaps in the time line indicate no sampling at the respective year; concentrations at "0 ng/g TOC" mean that the compound was not detected in the sample.

4.6.2 Chlorinated Hydrocarbons: Hexachlorobenzene (HCB)

HCB is a fungicide which was mainly used for seed treatment and as wood preservative. It is persistent and toxic to aquatic organisms. Use and production of HCB is internationally banned by the Stockholm Convention of 2004.

HCB in Baltic Sea surface water

Observed concentrations for HCB_{sum}[3] in Baltic Sea surface water ranged from 3.43 pg/L HCB_{sum} in the Eastern Gotland Sea (South, T7) to 9.30 pg/L HCB_{sum} in the Pomeranian Bight (T4, Table Appendix 2). HCB was mainly found in the dissolved water fractions. Highest HCB concentrations at T4 indicate that the river Odra is a source for HCB in the Baltic Sea. Highest HCB_{part}[4] concentrations were found for the Pomeranian Bight and the Kiel Bight/Fehmarn Belt which is attributed to the high SPM concentrations at these sites.

Developments for dissolved HCB concentrations for the areas Mecklenburg Bight, Arkona Sea and Pomeranian Bight are shown in Fig. 41. The pattern depicts regularly increasing HCB concentrations from certain years such as from 2002, 2008 and 2016 which declined thereafter. This implies that HCB is periodically introduced into the Baltic Sea presumably by riverine inflow. Overall, since 2001 dissolved HCB concentrations have decreased only slightly which reflects the persistence of HCB in the marine environment. This time series data also indicates that the river Odra is a source for HCB, temporarily transporting very high HCB loads into the Baltic Sea, in particular through the particulate water fraction.

[3] HCB_{sum}: summarized HCB concentrations of particulate and dissolved fraction

[4] HCB_{part}: HCB concentrations in the particulate fractions

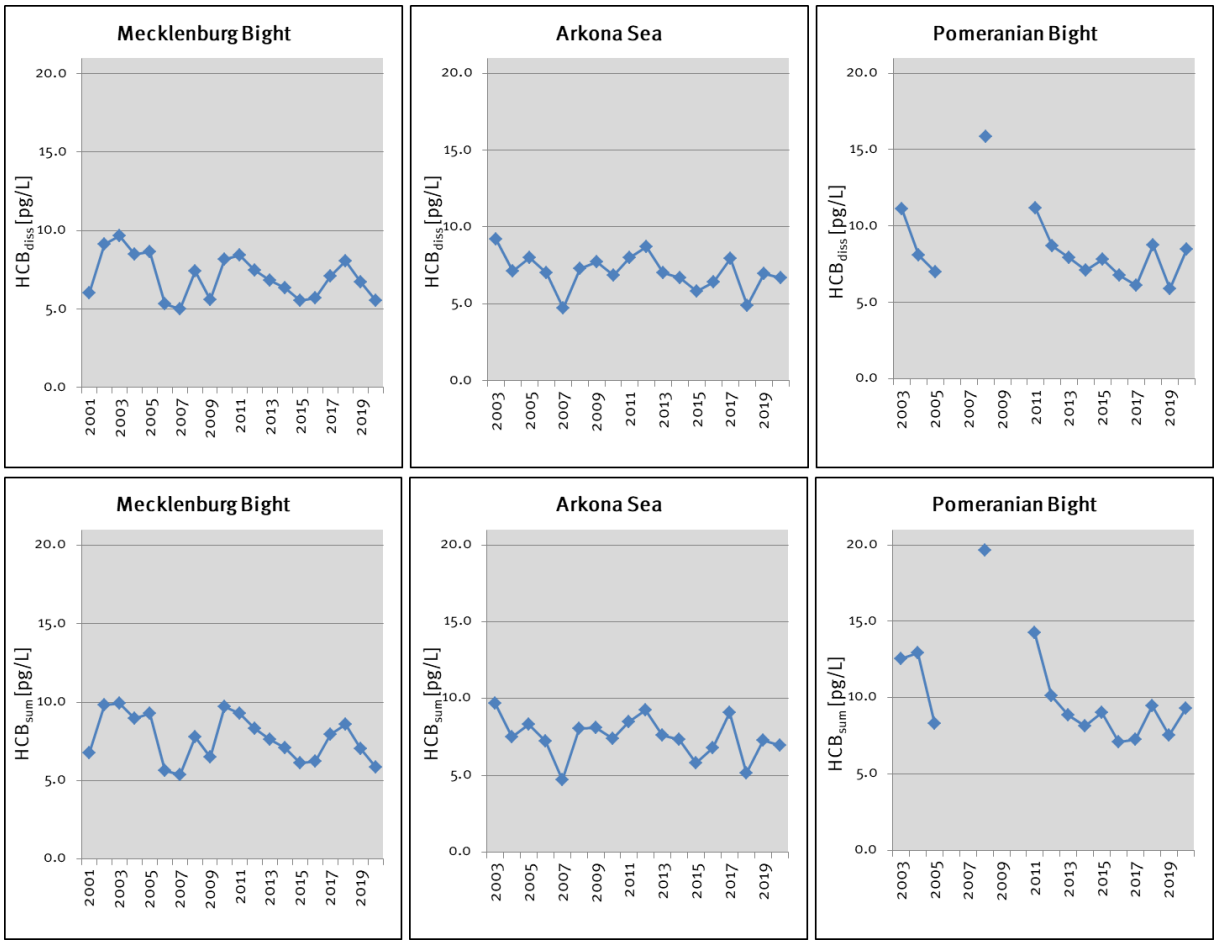

Fig. 41: Concentrations of HCB in Baltic Sea surface water of the Mecklenburg Bight, Arkona Sea and the Pomeranian Bight. Upper panel: dissolved water fraction, lower panel: summarized dissolved and suspended fraction. Gaps in the time line indicate no sampling at the respective year.

HCB in Baltic Sea sediment

Lowest HCB surface sediment contents of 3.1 ng/g TOC were observed at station M2 n the Mecklenburg Bight and K5 in the Arkona Basin, whereas the highest HCB content of 8.8 ng/g TOC were observed at the Pomeranian Bight (OBBOJE, Table Appendix 5).

HCB surface sediment contents since 2004 for stations in the Mecklenburg Bight, Arkona Basin and Pomeranian Bight are shown in Fig. 42. Decreasing trends for HCB contents cannot be observed for the surface sediment within the investigated time period, but particular high variations at the Pomeranian Bight.

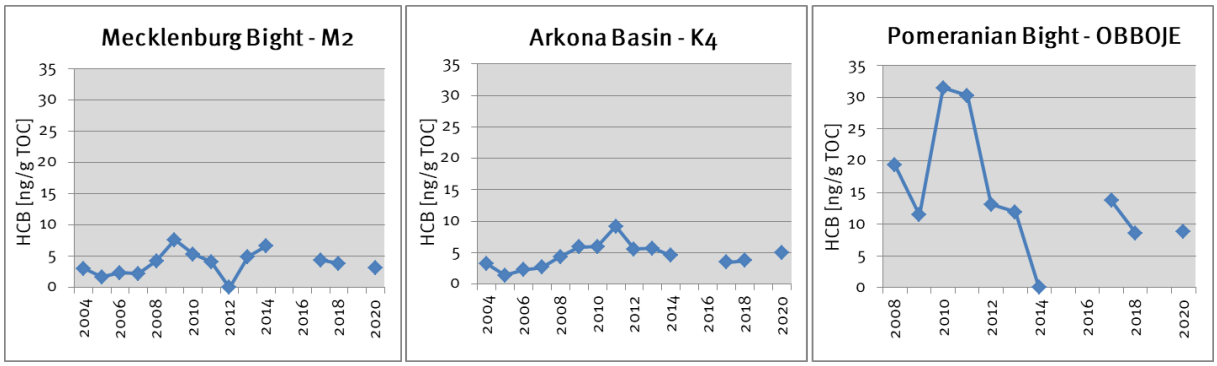

Fig. 42: Times series of HCB contents in surface sediments from 2004 to 2020 for the Mecklenburg Bight as well as the Arkona Basin and from 2008 to 2020 for the Pomeranian Bight. Gaps in the time line indicate no sampling at the respective year; concentrations at "0 ng/g TOC" mean that the compound was not detected in the sample.

4.6.3 Chlorinated Hydrocarbons: Polychlorinated Biphenyls (PCB)

Since the 1930s PCBs had been used as fluids in hydraulic systems, as lubricants and insulating and cooling fluids in transformers and electrical capacitors. Production and use of PCBs is internationally banned by the initial Stockholm Convention of 2004. Commercial PCB formulations usually consisted of a wide range of PCB congeners which differ in the number and position of substituted chlorine on the biphenyl rings. Seven PCB congeners were suggested as indicators for environmental monitoring by the International Council of the Exploration of the Sea (ICES, PCB_{ICES}).

PCB_{ICES} in Baltic Sea surface water

PCB_{ICES} concentrations of the surface water ranged from 1.22 pg/L ΣPCB_{sum}[5] in the Eastern Gotland Sea (South, T7) to 7.20 pg/L ΣPCB_{sum} at the site Kiel Bight/ Fehmarn Belt (T1) (Fig. 43, Table Appendix 2). Overall, ΣPCB_{sum} concentration decrease from sites in the western Baltic Sea (T1) to the Gotland Sea (T9) with noticeable concentrations at the Pomeranian Bight (5.15 pg/L ΣPCB_{sum}, T4).

The low chlorinated PCB congeners such as PCB28/31 were mainly found in the dissolved water fraction whereas higher chlorinated congeners, particularly PCB153 and PCB138, are associated to the particulate fraction. As observed for DDT and its metabolites, too (see chapter 4.6.1 – surface water), concentrations of particulate PCBs correlate to the SPM. Thus, highest concentrations for ΣPCB_{part}[6] were found at those sites with highest SPM concentrations, i.e., at the Fehmarn Belt/Kiel Bight with 4.29 pg/L ΣPCB_{part} (SPM 1.63 mg/L) and at the Pomeranian Bight with 2.51 pg/L ΣPCB_{part} (SPM 1.1 mg/L).

[5] ΣPCB_{SUM}: summarized concentrations of PCB_{ICES} congeners of the dissolved and particulate fraction
[6] ΣPCB_{part}: summarized concentrations of PCB_{ICES} congeners in the particulate fraction

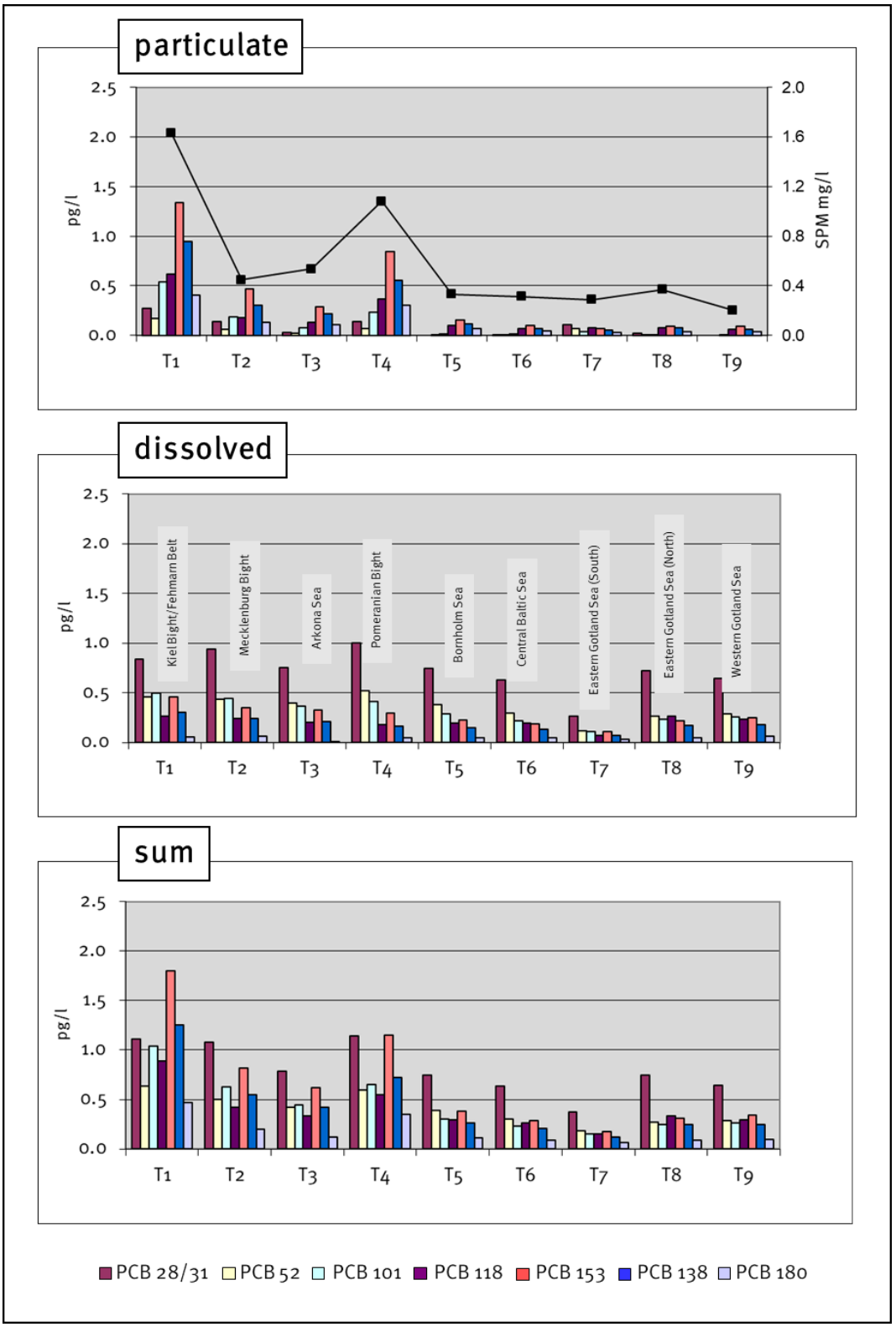

Fig. 43: Concentrations of PCB$_{ICES}$ in the particulate and dissolved water fractions of Baltic Sea surface water in January/February 2020.

Concentrations for PCBs in surface water in the study areas Mecklenburg Bight, Arkona Sea and Pomeranian Bight of past observations are shown in Fig. 44. At these sites concentrations for ΣPCB$_{diss}$ decreased continuously from up to about 20 pg/L to currently below 3 pg/L. The time

series data additionally show that suspended PCBs contribute significantly to the PCB load of Baltic Sea surface water, temporarily particularly at the Pomeranian Bight.

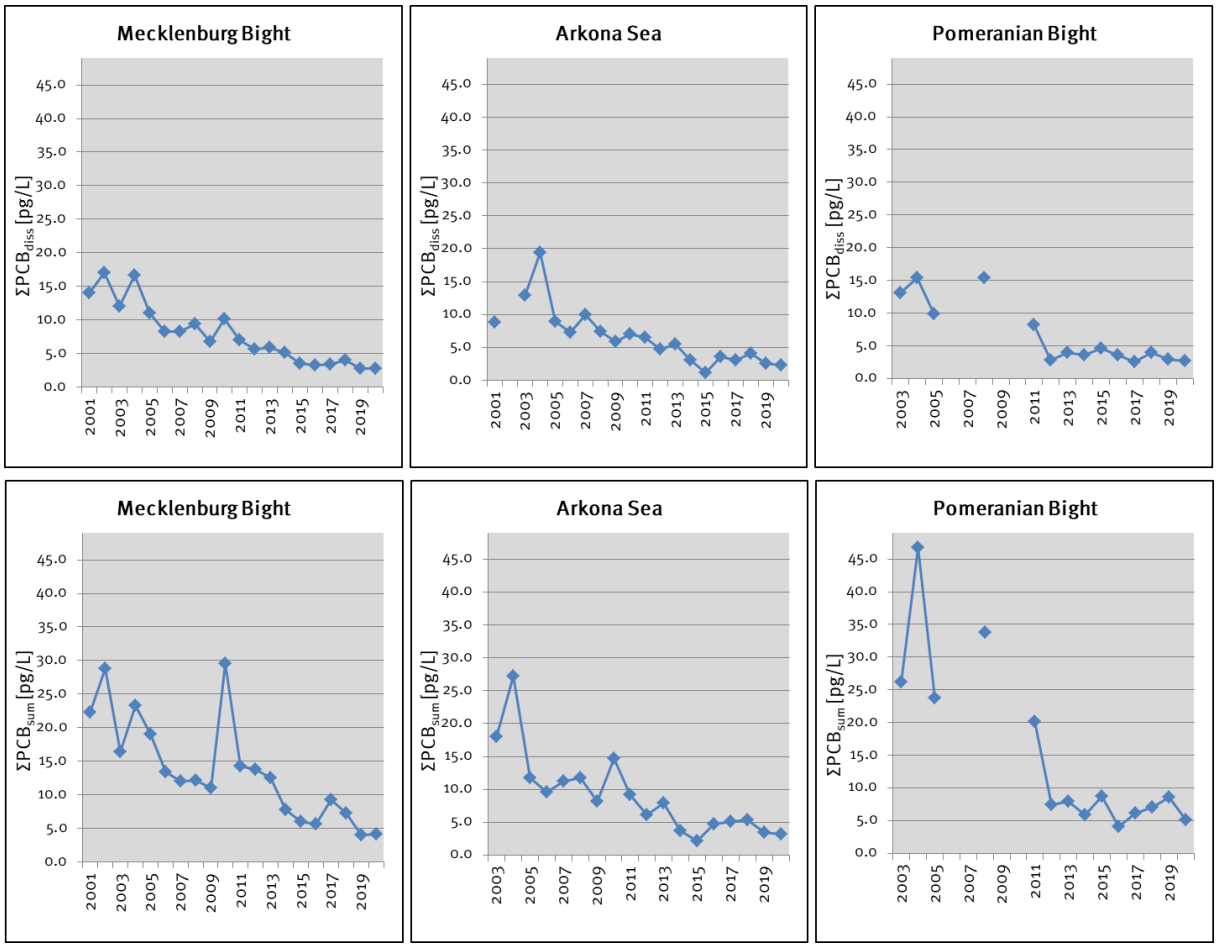

Fig. 44: Time series of ΣPCB$_{ICES}$ concentrations in Baltic Sea surface water at the Mecklenburg Bight, the Arkona Sea and in the Pomeranian Bight. Upper panel: dissolved fraction, lower panel: summarized dissolved and suspended fraction. Gaps in the time line indicate no sampling at the respective year.

PCB$_{ICES}$ in Baltic Sea surface sediment

PCB$_{ICES}$ contents ranged from 35.9 ng/g TOC ΣPCB$_{ICES}$ (≙ 126 pg/g DW) in the Pomeranian Bight (OBBOJE) to 91.3 ng/g TOC ΣPCB$_{ICES}$ (≙ 5637 pg/g DW) in the Arkona Basin at station K5 (Fig. 45).

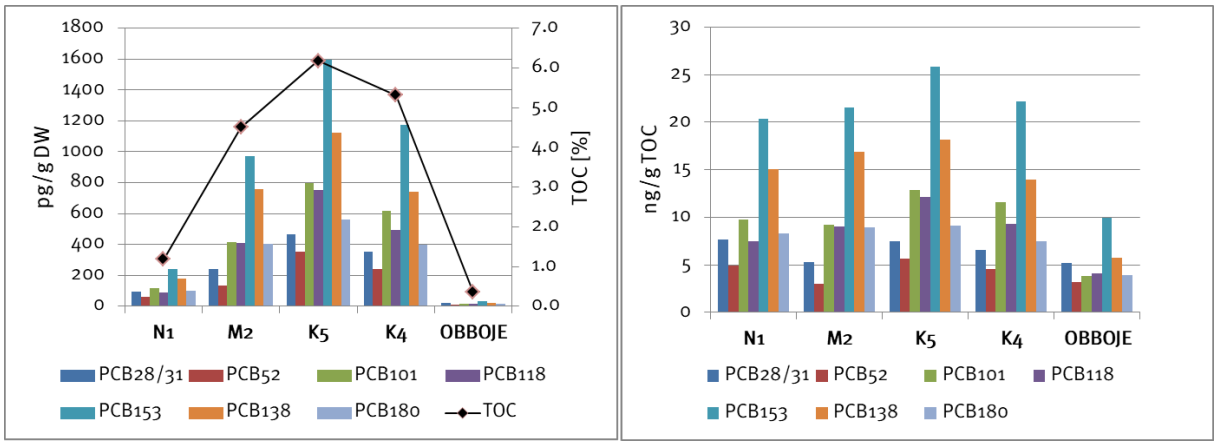

Fig. 45: Contents of PCB$_{ICES}$ in Baltic Sea surface sediments in January/February 2020 in pg/g DW (left) and normalized to the organic carbon content in ng/g TOC (right).

Time series data for PCB$_{ICES}$ contents depict no trends within the investigated time period, but particular high variations at the Pomeranian Bight (Fig. 46) pointing towards temporarily high PCB inputs through the river Odra and also transportation of PCB containing material. In this regard, it was reported that discharged contaminants are transported with the fluffy layer material of the Pomeranian Bight to the Arkona Basin and deposit there (WITT ET AL. 2001).

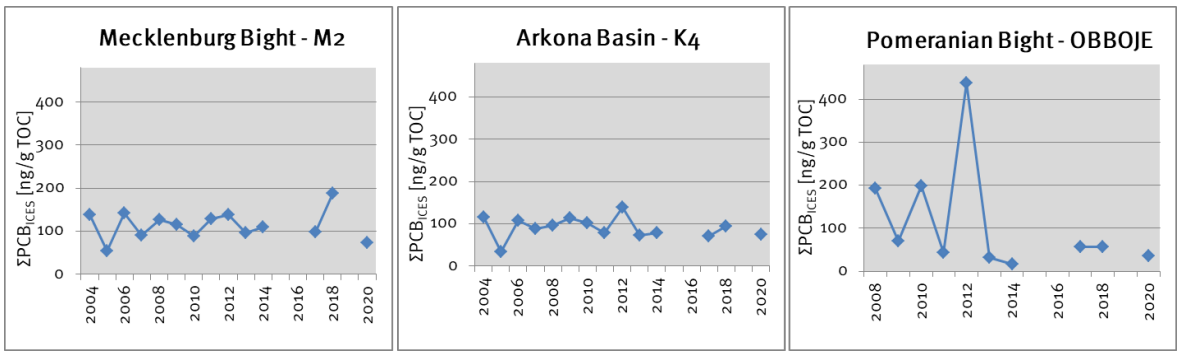

Fig. 46: Times series of ΣPCB$_{ICES}$ contents in surface sediments from 2004 to 2020 for the Mecklenburg Bight as well as the Arkona Basin and from 2008 to 2020 for the Pomeranian Bight. Gaps in the time line indicate no sampling at the respective year.

4.6.4 Polycyclic Aromatic Hydrocarbons

PAHs result from incomplete combustion of organic material. Therefore, they largely derive from industrial combustion processes such as from fossil fuel or wood combustion. Thus, the presence of these pollutants in the environment is strongly associated to anthropogenic activities. PAHs enter the marine environment particularly through oil spills from shipping, river discharges and the atmosphere. PAHs are persistent in the environment and have toxic, carcinogenic as well as reprotoxic properties.

PAHs belong to the main environmental pollutants; a number of 16 compounds – the U.S. EPA PAH indicator compounds – serve as representatives for PAH contamination in the environment (KEITH 2015) and, thus, are an inherent part of environmental surveillance.

PAHs in Baltic Sea surface water

ΣPAH_{sum}[7] concentrations ranged from 1344 pg/L in the Eastern Gotland Sea (South, T7) to 5626 pg/L at the Pomeranian Bight (T4, Fig. 47, Table Appendix 3) which is less by factors ranging from 1.5 to 5 compared to observed PAH data for the year 2019 (NAUMANN et al. 2020). PAH concentrations correlate to the SPM and, thus, highest ΣPAH_{part}[8] concentrations were determined at the sites of the Kiel Bight/Fehmarn Belt (T1, 1081 pg/L ΣPAH_{part}) and Pomeranian Bight (T4, 1099 pg/L ΣPAH_{part}). However, in contrast to the CHC, the Baltic Sea surface water PAH load predominantly associates to the dissolved water fraction.

[7] ΣPAH_{SUM}: summarized U.S. EPA PAH indicator compounds (exc. Naph) in particulate and dissolved fraction
[8] ΣPAH_{part}: summarized U.S. EPA PAH indicator compounds (exc. Naph) for dissolved fraction

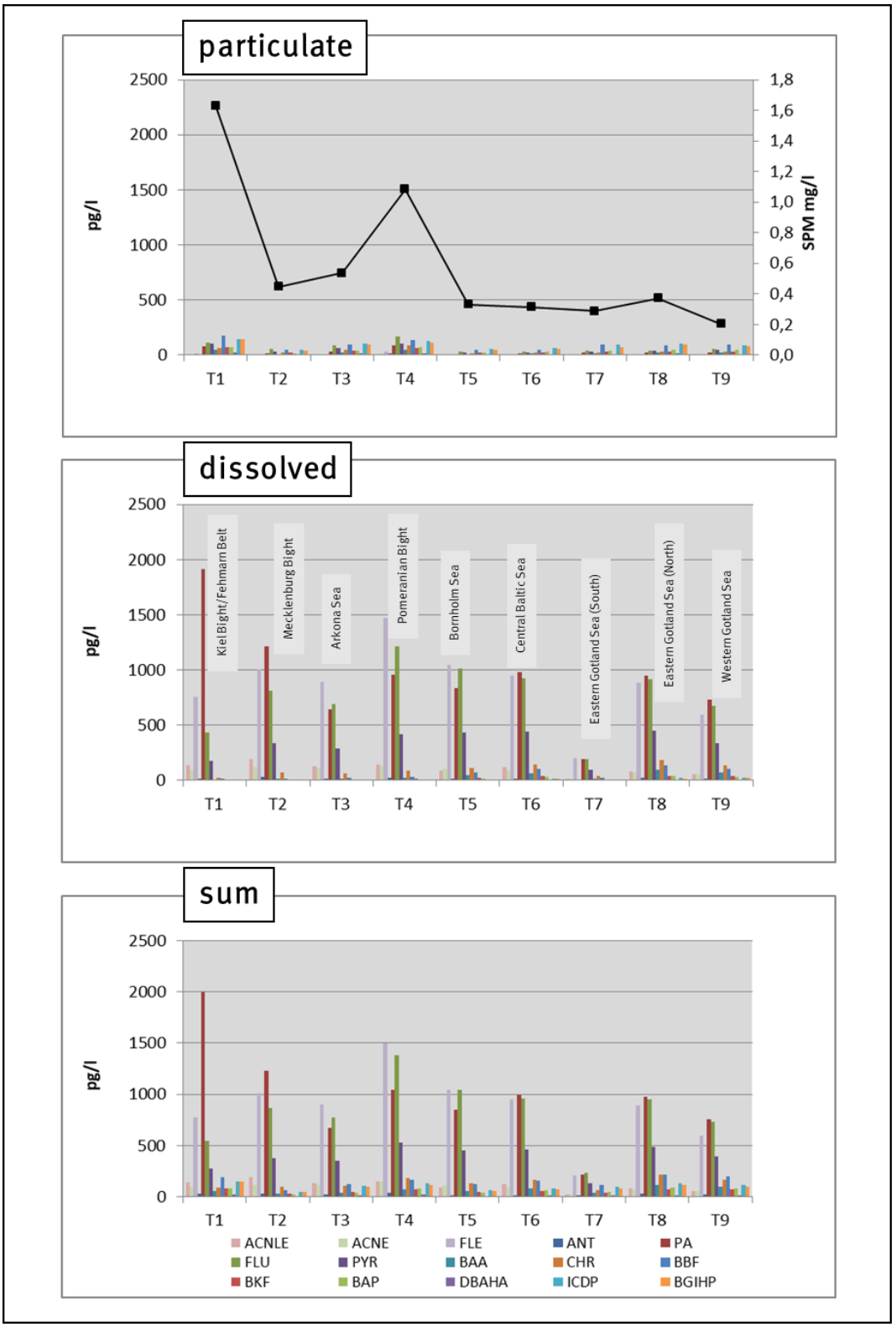

Fig. 47: Concentrations of PAHs in the dissolved and particulate fraction of Baltic Sea surface waters in January/February 2020.

Application of diagnostic ratios as described by YUNKER et al. 2002 or KATSOYIANNIS & BREIVIK 2014 to the observed PAH data revealed petrogenic and combustion as PAH sources for all investigated sites and additionally marine traffic as PAH source for the sites Pomeranian Bight

(T4), Bornholm Sea (T5), Central Baltic Sea (T6), the Eastern Gotland Sea (North) (T8) and the Western Gotland Sea (T9) (Table 13).

Table 13: Diagnostic ratios BAP/BGHIP and BAA/(BAA+CHR) for the identification of putative PAH sources in Baltic Sea surface water in January/February 2020. Boundaries: BAA/(BAA+CHR) ‹ 0.2: petrogenic PAH source, BAA/(BAA+CHR) › 0.35: combustion derived PAH; 0.2 ‹ BAA/(BAA+CHR) ‹ 0.35: mixed sources; BAP/BGHIP › 0.6: traffic derived PAH

	T1	T2	T3	T4	T5	T6	T7	T8	T9
BAP/BGHIP	0.52	0.46	0.41	0.71	0.68	0.87	0.59	0.74	0.86
BAA/(BAA+CHR)	0.40	0.22	0.26	0.29	0.30	0.33	0.36	0.35	0.38

Baltic Sea surface water concentrations for PAH since 2003 for the areas Mecklenburg Bight, Arkona Sea and Pomeranian Bight are shown in Fig. 48. The pattern depicts high variation of the PAH concentrations indicating temporally intense PAH sources. This data set also depicts the particular influence of the river Ordra on the particulate PAH load of Baltic Sea surface water. Overall, within this time period slightly decreasing concentrations can be observed for the Mecklenburg Bight, but not for the Arkona Sea and the Pomeranian Bight.

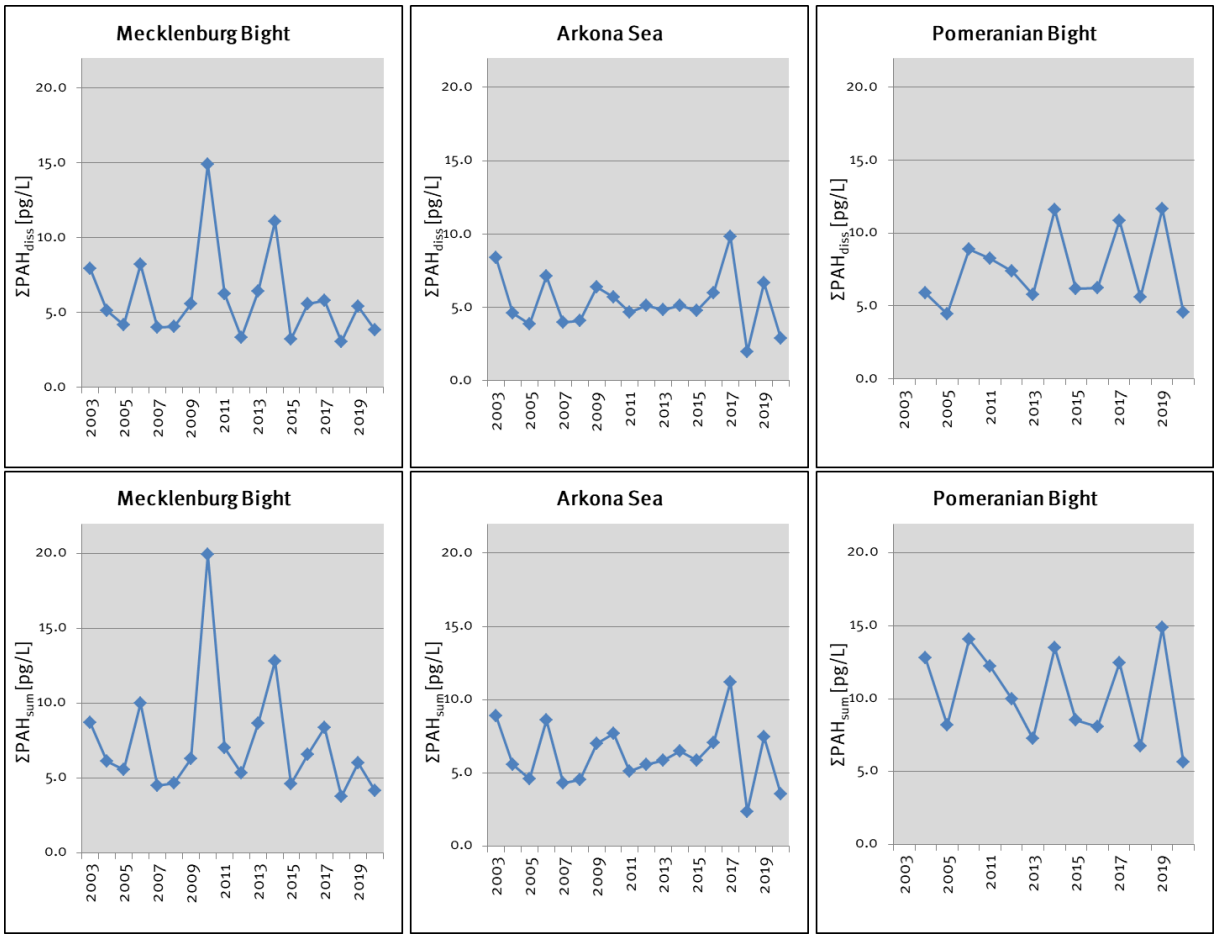

Fig. 48: Concentrations of ΣPAH in surface water of the Mecklenburg Bight, the Arkona Sea and the Pomeranian Bight. Upper panel: dissolved fraction, lower panel: summarized dissolved and suspended fraction.

PAHs in Baltic Sea sediment

Observed contents of ΣPAH in Baltic Sea surface sediment ranged from 16010 ng/g TOC (≙ 56.0 ng/g DW) at the site Pomeranian Bight (OBBOJE) to 36877 ng/g TOC (≙ 437 ng/g DW) at station N1 in the Kiel Bight/Fehmarn Belt and station K5 in the Arkona Basin (Fig. 49, Table Appendix 7).

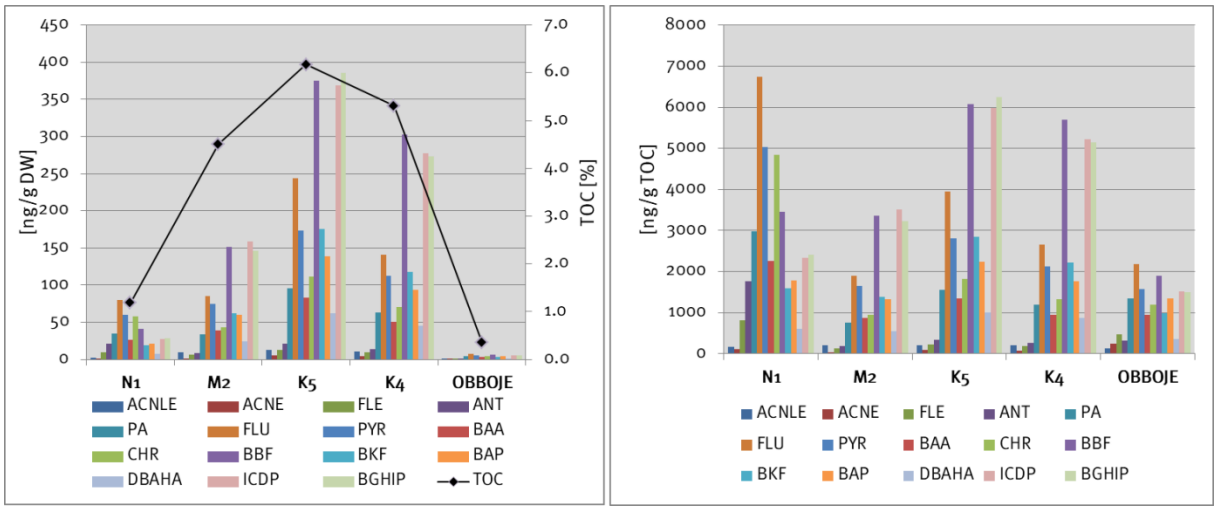

Fig. 49: Contents of U.S. EPA PAH indicator compounds in Baltic Sea surface sediments in January/Febuary 2020 in pg/g DW (left) and normalized to the organic carbon content ng/g TOC (right).

Time series data for PAH surface sediment contents depict no trends within the investigated time period, but particular high variations at the Pomeranian Bight (Fig. 50).

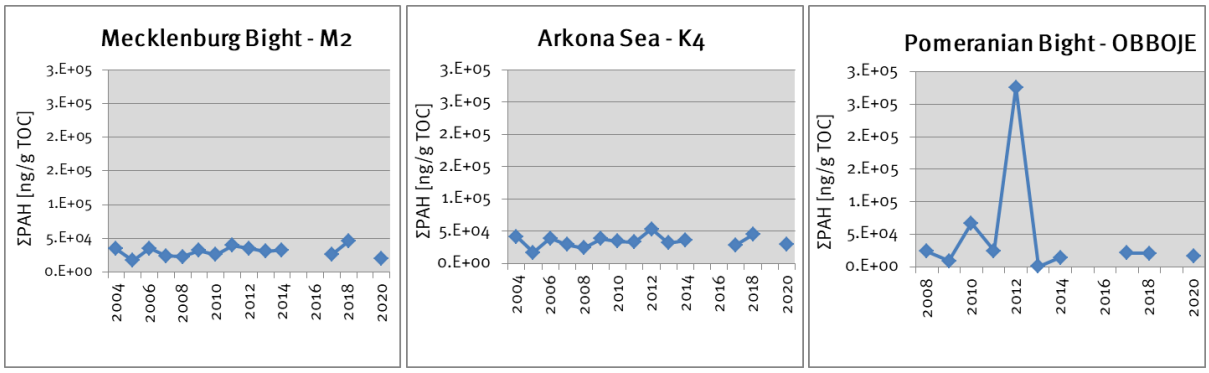

Fig. 50: Times series of PAH contents in surface sediments from 2004 to 2020 for the Mecklenburg Bight as well as the Arkona Basin and from 2008 to 2020 for the Pomeranian Bight. Gaps in the time line indicate no sampling at the respective year.

A detailed analysis of pre-industrial and industrial developments of the Baltic Sea PAH pressure on the basis of surface water and sediment PAH monitoring data as well as sediment deposits can be obtained from KANWISCHER et al. (2020).

4.6.5 Organotin

Organotin compounds are organometallic compounds with one or more tin-carbon bonds. They are mostly of anthropogenic origin and have been used for a variety of applications since the 1940s (HOCH 2001). Since the 1950s triorganotin compounds such as the tributyltin (TBT) have been widely used as biocides, so too, as effective agent in antifouling paints for marine vessels (e.g., ANTIZAR-LADISLAO 2008). Organotin compounds detected in the marine environment mainly originate from this application. Since about the 1980s it is known that the occurrence of imposex in marine organisms is linked to the intensive TBT usage which had severe consequences on the

population level of effected species (ALZIEU 1998). An international ban on the use of TBT as an antifouling agent has been in place since 2003; a general ban since 2008 (International Maritime Organization, 2001). However, due to the intensive use of TBT in the past, high levels of TBT can still be detected, especially in harbor sediments (HOCH 2001); e.g. for Swedish marina sediments up to 1000 ng/g DW (EKLUND et al. 2008).

Among the analyzed organotin compounds mono- and dibutyltin (MBT, DBT) as well as TBT were detected in surface sediments of the Mecklenburg Bight (M2) and the Arkona Basin (K5, K4); at the Fehmarn Belt (N1) MBT and TBT and at the Pomeranian Bight (OBBOJE) only TBT was detected. Obtained data for ΣOC[9] range from 85.7 ng/g TOC (≙ 0.3 ng/g DW) at the Pomeranian Bight (OBBOJE) to 275 ng/g TOC (≙ 12.4 ng/g DW) at the Mecklenburg Bight (Fig. 51, Table Appendix 6).

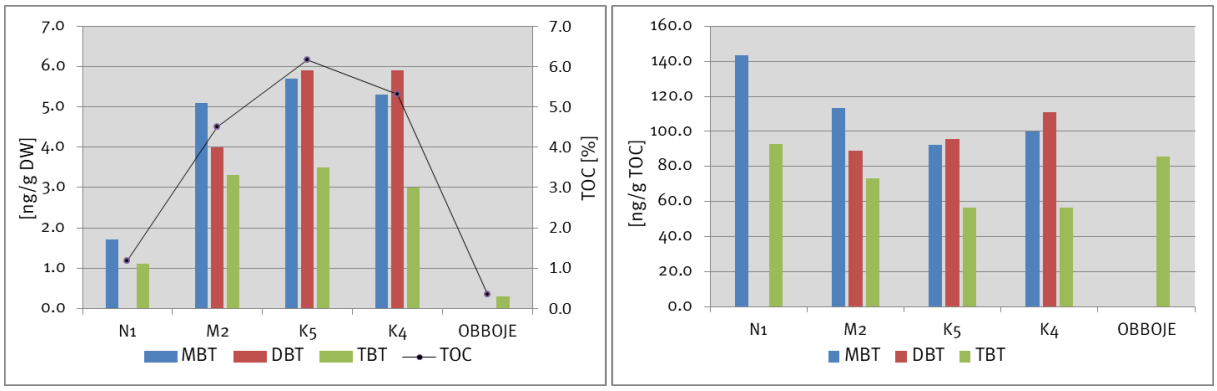

Fig. 51: Contents of organotin compounds in Baltic Sea surface sediments in January/February 2020 in ng/g DW (left) and normalized to the organic carbon content in ng/g TOC (right).

The obtained data are comparable to previous reports (ABRAHAM et al. 2017) and within the time period no decreasing trends for the study area can be observed.

4.6.6 Assessment of the results

Quantitative limits for contaminants in the Baltic Sea have been defined within the framework of European water policy and the HELCOM commitment within the scope of the Baltic Sea Action Plan. Under European legislation monitoring of hazardous substances in the Baltic Sea is directed through the MSFD[10] and the WFD[11]. The Environmental Quality Standards (EQS) for surface waters of the EQS-Directive[12] serve as the basis to evaluate obtained results for Baltic Sea surface water in January/February 2020 (Table 14). Obtained surface sediment data will be evaluated utilizing HELCOM indicators (Table 15).

[9] ΣOT: Sum of MBT, DBT and TBT contents in surface sediment

[10] Directive 2008/56/EC of the European Parliament and of the Council of 17 June 2008 establishing a framework for community action in the field of marine environmental policy

[11] Directive 2000/60/EC of the European Parliament and of the Council of 23 October 2000 establishing a framework for Community action in the field of water policy

[12] Directive 2008/105/EC of the European Parliament and of the Council of 16 December 2008 on environmental quality standards in the field of water policy; amended by directive 2013/39/EU

Table 14: Assessment of obtained Baltic Sea surface water contaminant concentrations in January/February 2020 on the basis of Environmental Quality Standards (EQS) of the EQS-Directive. red values: exceeded EQS, AA-EQS: annual average EQS, MAC-EQS: maximum allowable concentration

Substance	Other Surface waters AA-EQS	Other Surface waters MAC-EQS	Kiel Bight/ Fehmarn-belt (T1)	Mecklenburg Bight (T2)	Arkona Sea (T3)	Pomeranian Bight (T4)	Bornholm Sea (T5)	Central Baltic Sea (T6)	Eastern Gotland Sea (South) (T7)	Eastern Gotland Sea (North) (T8)	Western Gotland Sea (T9)
						[µg/L^{-1}]					
ΣDDT$_{sum}$	0.025	-	0.000006	0.000008	0.000013	0.000013	0.000007	0.000005	0.000002	0.000004	0.000004
p.p'-DDT$_{sum}$	0.01	-	0.000001	0.000002	0.000003	0.000003	0.000001	0.000001	0.000000	0.000001	0.000001
HCB$_{sum}$	-	0.05	0.000005	0.000006	0.000014	0.000009	0.000007	0.000007	0.000003	0.000006	0.000007
ANT$_{sum}$	0.1	0.1	0.00003	0.00003	0.00002	0.00004	0.00002	0.00002	0.00001	0.00003	0.00002
FLU$_{sum}$	0.0063	0.12	0.0005	0.0009	0.0008	0.0014	0.0010	0.0010	0.0002	0.0010	0.0007
BBF$_{sum}$	0.00017	0.017	**0.00019**	0.00007	0.00012	0.00016	0.00012	0.00015	0.00011	**0.00022**	**0.00020**
BKF$_{sum}$	0.00017	0.017	0.00008	0.00003	0.00005	0.00007	0.00004	0.00006	0.00004	0.00007	0.00007
BAP$_{sum}$	0.00017	0.027	0.00008	0.00002	0.00004	0.00008	0.00004	0.00006	0.00005	0.00009	0.00008
BGHIP$_{sum}$	0.00017	0.0082	0.00015	0.00004	0.00010	0.00012	0.00006	0.00007	0.00008	0.00012	0.00010
ICDP$_{sum}$	0.00017	-	0.00015	0.00005	0.00011	0.00013	0.00007	0.00008	0.00010	0.00013	0.00011

None of the obtained contaminant data in the Baltic Sea surface water exceeded defined maximum allowable concentrations (MAC-EQS, Table 14). In addition, determined concentrations for DDT and metabolites as well as HCB do not exceed annual average EQS (AA-EQS) values. Among the analyzed PAH compounds, the AA-EQS was exceeded only for the high molecular weight PAH compound benzo(*b*)fluoranthene (BBF) at the sites Kiel Bight/Fehmarn Belt (T1), Eastern Gotland Sea (North, T8) and the Western Gotland Sea (T9).

Anthracene contents in surface sediment at the site Fehmarn Belt (N1) exceeded the threshold value of the HELCOM indicator *PAH*. Obtained contents for TBT exceeded the threshold value for the HELCOM indicator *TBT and imposex* at all investigated sites.

Table 15: Assessment of obtained surface sediment contaminant data in January/February 2020 on the basis of HELCOM indicators. red values: exceeded threshold value

indicator	substance	threshold value	Kiel B./Fehmarn B. (N1)	Mecklen-burg B. (M2)	Arkona B. (K5)	Arkona B. (K4)	Pomera-nian B. (OBBOJE)
			[µg/kg TS, 5% TOC]				
PAH	**anthracene**	24	88	9	17	13	16
TBT and imposex	**tributyltin**	1.6	4.64	3.66	2.83	2.82	4.29

Acknowledgements

The authors would like to thank the staff from the Leibniz Institute for Baltic Sea Research Warnemünde, who carried out measurements as part of the HELCOM's Baltic Sea monitoring programme and the IOW's long-term measuring programme, and the captain and crew of the research vessel Elisabeth Mann Borgese for their effort and support during monitoring cruises in 2020. The authors are also grateful to a number of other people and organisations for help: Jürgen Holfort of the Sea Ice Service at the Federal Maritime and Hydrographic Agency, Hamburg and Rostock for advice in the description of the ice winter, and especially for supplying the ice cover chart; the Deutscher Wetterdienst for supplying wind data from Arkona and Warnemünde from its online data portal; Hannah Lutterbeck from LLUR for providing the local assessment of oxygen deficiency at the coast of Schleswig-Holstein during late summer, the Swedish Meteorological and Hydrological Institute, Norrköpping, for providing gauge data from its online data portal; Lotta Fyrberg from SMHI's Oceanographic Laboratory in Gothenburg for providing us with hydrographic and hydrochemical observations from Sweden's Ocean Archive (SHARK) relating to selected stations within the Swedish national monitoring programme; Tamara Zalewska and team from the Maritime Office of the Polish Institute of Meteorology and Water Management (IMGW) in Gdynia providing observational data from the Danzig Deep; Barbara Bogdańska, IMGW in Warsaw, provided data on solar radiation at Gdynia.

References

ABRAHAM, M., L. WESTPHAL, I. HAND, A. LERZ, J. JESCHEK, D. BUNKE, T. LEIPE, SCHULZ-BULL, D., 2017: TBT and its metabolites in sediments: Survey at a German coastal site and the central Baltic Sea. Marine Pollution Bulletin 121: 404–410. doi:10.1016/j.marpolbul.2017.06.020.

ALZIEU, C., 1998: Tributyltin: case study of a chronic contaminant in the coastal environment. Ocean & Coastal Management 40: 23–36. doi:10.1016/S0964-5691(98)00036-2.

ANTIZAR-LADISLAO, B., 2008: Environmental levels, toxicity and human exposure to tributyltin (TBT)-contaminated marine environment. A review. Environment International 34: 292–308. doi:10.1016/j.envint.2007.09.005.

ASMALA, E., HARAGUCHI, L., MARKAGER, S., MASSICOTTE, P., RIEMANN, B., STAEHR, P. A., CARSTENSEN, J., 2018: Eutrophication Leads to Accumulation of Recalcitrant Autochthonous Organic Matter in Coastal Environment. Global Biogeochemical Cycles 32(11): 1673-1687.

BIANCHI, T. S., ROLFF, C., LAMBERT, C. D., 1997: Sources and composition of particulate organic carbon in the Baltic Sea: the use of plant pigments and lignin-phenols as biomarkers. Marine Ecology Progress Series 156: 25-31.

BSH, 2009: Flächenbezogene Eisvolumensumme. http://www.bsh.de/de/Meeresdaten/Beobachtungen/Eis/Kuesten.jsp

BSH, 2020: Wasserstandsvorhersage Ostsee. https://www.bsh.de/DE/DATEN/Wasserstand_Ostsee/wasserstand_ostsee_node.html

V.BODUNGEN, B., GRAEVE, M., KUBE, J., LASS, H.U., MEYER-HARMS, B., MUMM, N., NAGEL, K., POLLEHNE, F., POWILLEIT, M., RECKERMANN, M., SATTLER, C., SIEGEL, H., WODARG, D., 1995: Stoff-Flüsse am Grenzfluss – Transport- und Umsatzprozesse im Übergangsgebiet zwischen Oderästuar und Pommerscher Bucht (TRUMP). Geowiss. **13**, 479-485.

DEUTSCH, B., ALLING, V., HUMBORG, C., KORTH, F. MÖRTH, C. M., 2012: Tracing inputs of terrestrial high molecular weight dissolved organic matter within the Baltic Sea ecosystem. Biogeosciences 9(11): 4465-4475.

DIAZ, R.J., ROSENBERG, R., 2008: Spreading dead zones and consequences for marine ecosystems. Science 321 (5891), 926-929.

DUARTE, C.M., CONLEY, D.J., CARSTENSEN, J., SÁNCHEZ-CAMACHO, M., 2009: Return to Neverland: Shifting baselines affect eutrophication restoration targets. Estuaries and Coasts 32 (1), 29-36.

DWD, 2020: Monatlicher Klimastatus, Nr. 1 – 12. Deutscher Wetterdienst. https://www.dwd.de/DE/derdwd/bibliothek/fachpublikationen/selbstverlag/selbstverlag_node.html

DWD, 2021a: Windmessungen der Station Arkona in Stundenmittelwerten des Jahres 2020. ftp://ftp-cdc.dwd.de/pub/CDC/observations_germany/climate/

DWD, 2021b: Langzeitdaten von Windmessungen der Station Arkona in Tagesmittelwerten. ftp://ftp-cdc.dwd.de/pub/CDC/observations_germany/climate/daily/kl/historical/

EKLUND, B., M. ELFSTRÖM, BORG, H., 2008: Tributyltin Originates from Pleasure Boats in Sweden in Spite of Firm Restrictions. Open envrionmental Sciences Journal2 2: 124–132. doi:10.2174/1876325100802010124.

EMERSON, S., HEDGES, J., 2008: Chemical Oceanography and the Marine Carbon Cycle. Cambridge, Cambridge University Press.

FALKOWSKI, P. G., RAVEN, J. A., 2013: Aquatic Photosynthesis, Princeton University Press.

HANSELL, D. A., CARLSON, C. A., REPETA, D. J., SCHLITZER, R., 2009: Dissolved organic matter in the ocean - a controversy stimulates new insights. Oceanography 22(4): 202-211.

FEISTEL, R. SEIFERT, T., FEISTEL, S., NAUSCH, G., BOGDANSKA, B., BROMAN, B., HANSEN, L., HOLFORT, J., MOHRHOLZ, V., SCHMAGER, G., HAGEN, E., PERLET, I., WASMUND, N., 2008: Digital supplement. In: FEISTEL, R., NAUSCH, G. WASMUND, N. (eds.): State and evolution of the Baltic Sea 1952-2005. John Wiley & Sons, Inc., Hoboken, New Jersey, pp. 625-667.

GAUSS, M., NYIRI, A., KLEIN, H., 2020: Contributions of emissions from different countries and sectors to atmospheric nitrogen input to the Baltic Sea and its Sub-basins; Meteorological Synthesizing Centre-West (MSC-W) OF EMEP, NORWEGIAN METEOROLOGICAL INSTITUTE, OSLO, NORWAY, 2020, P 36.

GRASSHOFF, K., ERHARDT, M., KREMLING, K., 1983: Methods of seawater analysis. 2nd ed., Verlag Chemie, Weinheim.

GRÄWE, U., NAUMANN, M., MOHRHOLZ, V., BURCHARD, H., 2015: Anatomizing one of the largest saltwater inflows in the Baltic Sea in December 2014. J. Geophys. Res. 120, 7676-7697.

HAGEN, E., FEISTEL, R., 2008: Baltic climate change. In: FEISTEL, R., NAUSCH, G., WASMUND, N. (eds.), State and evolution of the Baltic Sea 1952 – 2005. John Wiley & Sons, Inc., Hoboken, New Jersey, pp. 93-120.

HELCOM, 2000: Manual of marine monitoring in the COMBINE programme of HELCOM. Baltic Marine Environment Protection Commission, Helsinki, Updated 2002: www.helcom.fi/Monas/CombineManual2/CombineHome.htm

HELCOM, 2010a: Ecosystem health of the Baltic Sea 2003–2007. Balt. Sea Environ. Proc. 122, pp. 13–14.

HELCOM, 2010b: Hazardous substances in the Baltic Sea - An integrated thematic assessment of hazardous substances in the Baltic Sea. Balt. Sea Environ. Proc. 120B.

HELCOM, 2013: Approaches and methods for eutrophication target setting in the Baltic Sea region. Helsinki Commission, Helsinki, Finland.

HELCOM, 2015: Updated Baltic Sea pollution load compilation (PLC 5.5). Balt. Sea Environ. Proc. 145, pp. 1-143. www.helcom.fi/Lists/Publications/BSEP145_lowres.pdf

HELCOM, 2018a: State of the Baltic Sea - Second HELCOM holistic assessment 2011-2016. Balt. Sea Environ. Proc. 155. Helsinki, Finland. http://stateofthebalticsea.helcom.fi

HELCOM, 2018b: Sources and pathways of nutrients to the Baltic Sea - HELCOM PLC-6. Helsinki, Finland. www.helcom.fi/Lists/Publications/BSEP143.pdf

HELCOM, 2018c: Inputs of hazardous substances to the Baltic Sea. Baltic Sea Environment Proceedings 162.

HOCH, M., 2001: Organotin compounds in the environment - an overview. *Applied Geochemistry* 16: 719–743. doi:10.1016/S0883-2927(00)00067-6.

HOLFORT, J., 2020: Der Eiswinter 2019/20. Eisdienst, Bundesamt für Seeschifffahrt und Hydrographie Rostock, 6 S.

IMGW, 2021: Solar radiation in J/m² at the station Gdynia 2020 – unpublished data

JACOBSEN, T.S., 1980: Sea water exchange of the Baltic. Measurements and methods. The Belt Project. The National Agency for Environmental Protection, Denmark: p107

KANWISCHER, M., BUNKE, D., LEIPE, T., MOROS, M., SCHULZ-BULL, D. E., 2020: Polycyclic aromatic hydrocarbons in the Baltic Sea — Pre-industrial and industrial developments as well as current status. Marine Pollution Bulletin 160. Elsevier: 111526. doi:10.1016/j.marpolbul.2020.111526.

KATSOYIANNIS, A., BREIVIK, K., 2014: Model-based evaluation of the use of polycyclic aromatic hydrocarbons molecular diagnostic ratios as a source identification tool. Environmental Pollution, 184, pp. 488-494. doi: 10.1016/j.envpol.2013.09.028.

KEITH, L.H., 2015: The source of U.S. EPA's sixteen PAH priority pollutants, polycyclic aromatic compounds. Taylor & Francis, 35 (2–4), pp. 147–160. doi: 10.1080/10406638.2014.892886.

KHARBUSH, J. J., CLOSE, H. G., VAN MOOY, B. A. S., ARNOSTI, C., RSMITTENBERG, . H., LE MOIGNE, F. A. C., MOLLENHAUER, G., SCHOLZ-BÖTTCHER, B., OBREHT, I., KOCH, B. P., BECKER, K. W., IVERSEN, M. H. MOHR, W., 2020: Particulate Organic Carbon Deconstructed: Molecular and Chemical Composition of Particulate Organic Carbon in the Ocean. Frontiers in Marine Science 7(518).

KOSLOWSKI, G., 1989: Die flächenbezogene Eisvolumensumme, eine neue Maßzahl für die Bewertung des Eiswinters an der Ostseeküste Schleswig-Holsteins und ihr Zusammenhang mit dem Charakter des meteorologischen Winters. Dt. Hydrogr. Z. 42, 61-80.

KRÜGER, S., 2000: Basic shipboard instrumentation and fixed autonomic stations for monitoring in the Baltic Sea. In: EL-HAWARY, F. (ed.): The ocean engineering handbook. CRC Press, Boca Raton, USA, pp. 52-61.

KRÜGER, S., ROEDER, W., WLOST, K.-P., KOCH, M., KÄMMERER, H., KNUTZ, T., 1998: Autonomous instrumentation carrier (APIC) with acoustic transmission for shallow water profiling. Oceanology International 98: The Global Ocean Conf. Proc. 2, 149-158.

KULINSKI, K., PEMPKOWIAK, J. 2012: Carbon Cycling in the Baltic Sea. Berlin Heidelberg, Springer-Verlag.

LASS, H.U., MATTHÄUS, W. 2008: General oceanography of the Baltic Sea. In: FEISTEL, R., NAUSCH, G., WASMUND, N. (eds.): State and evolution of the Baltic Sea 1952 – 2005. John Wiley & Sons, Inc., Hoboken, New Jersey, pp. 5-43.

LASS, H.U., MOHRHOLZ, V., SEIFERT, T., 2001: On the dynamics of the Pomeranian Bight. Cont. Shelf. Res. 21, 1237-1261.

LE MOIGNE, F. A. C., 2019: Pathways of Organic Carbon Downward Transport by the Oceanic Biological Carbon Pump. Frontiers in Marine Science 6(634).

LEIPE, T., TAUBER, F., VALLIUS, H., VIRTASALO, J., UŚCINOWICZ, S., KOWALSKI, N., HILLE, S., LINDGREN, S. MYLLYVIRTA, T., 2011: Particulate organic carbon (POC) in surface sediments of the Baltic Sea. Geo-Marine Letters 31(3): 175-188.

LISITZIN, E., 1974: Sea-level changes. Elsevier Oceanography Series, Vol. 8, Amsterdam: p286

LLUR, 2019: Sauerstoffmangel im bodennahen Wasser der westlichen Ostsee. https://www.schleswig-holstein.de/DE/Fachinhalte/M/meeresschutz/chemMonitoring.html: 7.

LLUR, 2020: "Sauerstoffmangel im bodennahen Wasser der westlichen Ostsee." https://www.schleswig-holstein.de/DE/Fachinhalte/M/meeresschutz/Downloads/Bericht_LLUR_Sauerstoff_2020.pdf: 6.

MATTHÄUS W., FRANCK, H., 1992: Characteristics of major Baltic inflows - a statistical analysis. Cont. Shelf Res., 12, 1375-1400.

MOHRHOLZ, V., 1998: Transport- und Vermischungsprozesse in der Pommerschen Bucht. Meereswiss. Ber. Warnemünde 33, 1-106.

MOHRHOLZ, V., NAUMANN, M., NAUSCH, G., KRÜGER, S. and GRÄWE, U. (2015): Fresh oxygen for the Baltic Sea – an exceptional saline inflow after a decade of stagnation. – Journal Mar. Syst. **148**, 152-166.

MOHRHOLZ, V., 2018: Major Baltic inflow statistics – reviewed. Front. Mar. Sci. 5, 384. doi: 10.3389/fmars.2018.00384

NAUMANN, M., UMLAUF, L., MOHRHOLZ, V., KUSS, J., SIEGEL, H., WANIEK, J.J., SCHULZ-BULL, D.E., 2018: Hydrographic-hydrochemical assessment of the Baltic Sea 2017, Meereswiss. Ber. Warnemünde 107, 97 pp. doi:10.12754/msr-2018-0107

NAUMANN, M., GRÄWE, U., MOHRHOLZ, V., KUSS, J., KANWISCHER, M., FEISTEL, S., HAND, I., WANIEK, J.J., SCHULZ-BULL, D.E., 2020: Hydrographic-hydrochemical assessment of the Baltic Sea 2019. Meereswiss. Ber. Warnemünde 114, 85 pp. doi:10.12754/msr-2020-0110

NAUSCH, G. and NEHRING, D. (1996): Baltic Proper, Hydrochemistry. In: Third Periodic Assessment of the State of the Marine Environment of the Baltic Sea. – Balt. Sea Environ. Proc. **64B**, 80-85.

NAUSCH, G., BACHOR, A., PETENATI, T., VOSS, J., V. WEBER, M., 2011b: Nährstoffe in den deutschen Küstengewässern der Ostsee und angrenzenden Seegebieten. Meeresumwelt Aktuell Nord- und Ostsee 2011/1.

NAUSCH, G., FEISTEL, R., LASS, H.-U., NAGEL, K., SIEGEL, H., 2002: Hydrographisch-chemische Zustandseinschätzung der Ostsee 2001. Meereswiss. Ber. Warnemünde 49, 3-77.

NAUSCH, G., NAUMANN, M., UMLAUF, L., MOHRHOLZ, V., SIEGEL,H., 2014: Hydrographisch-hydrochemische Zustandseinschätzung der Ostsee 2013. Meereswiss. Ber. Warnemünde 93, 1-104.

NAUSCH, G., NEHRING, D., NAGEL, K., 2008: Nutrient concentrations, trends and their relation to eutrophication. In: FEISTEL, R., NAUSCH, G., WASMUND, N. (eds.): State and evolution of the Baltic Sea, 1952-2005. John Wiley & Sons, Inc. Hoboken, New Jersey, 337-366.

NEHRING, D., MATTHÄUS, W., 1991: Current trends in hydrographic and chemical parameters and eutrophication in the Baltic Sea. Int. Revue ges. Hydrobiol. 76, 297-316.

NEHRING, D., MATTHÄUS, W., LASS, H.U., 1993: Die hydrographisch-chemischen Bedingungen in der westlichen und zentralen Ostsee im Jahre 1992. Dt. Hydrogr. Z. 45, 281-331.

NEHRING, D., MATTHÄUS, W., LASS, H.U., NAUSCH, G., NAGEL, K., 1995: Hydrographisch-chemische Zustandseinschätzung der Ostsee 1994. Meereswiss. Ber. Warnemünde 9, 1-71.

OSBURN, C. L., STEDMON, C. A., 2011: Linking the chemical and optical properties of dissolved organic matter in the Baltic–North Sea transition zone to differentiate three allochthonous inputs. Marine Chemistry 126(1): 281-294.

PERLET-MARKUS, I. 2020a: BSH-Bericht, Die Sturmflut vom 05.02.2020. https://www.bsh.de/DE/THEMEN/Wasserstand_und_Gezeiten/Sturmfluten/_Anlagen/Downloads/Ostsee_Sturmflut_20200205.pdf?__blob=publicationFile&v=3

PERLET-MARKUS, I. 2020b: BSH, Hydrologischer Monatsbericht Oktober 2020 für die Schleswig-Holsteinische und Mecklenburg-Vorpommersche Ostseeküste. https://www2.bsh.de/aktdat/wvd/Berichte/Ostsee/A_2020/Monatsbericht_12_Oktober_2020.pdf

REDFIELD, A. C., 1934: On the proportions of organic derivations in sea water and their relation to the composition of plankton. James Johnstone Memorial Volume. R. J. Daniel. Liverpool, University Press**:** 177-192.

REDFIELD, A.C., KETCHUM, B.H., RICHARDS, F.A., 1963: The influence of organisms on the composition of sea water. In: HILL, M.N. (ed.): The sea. J. Wiley & Sons, pp. 26-77.

REYNOLDS, R. W., SMITH, T.M., LIU, C., CHELTON, D.B., CASEY, K.S., SCHLAX, M.G., 2007: Daily high-resolution-blended analyses for sea surface temperature. J. Clim. 20, 5473–5496.

SCHLITZER, R., 2018: OCEAN DATA VIEW 5, ODV5 RELEASE 5.1.7 (WINDOWS 64BIT) OCT. 2018. AWI-BREMERHAVEN, 2018.

SCHMELZER, N., SEINÄ, A., LUNDQUIST, J.-E. and SZTOBRYN, M. (2008): Ice, in: Feistel, R., Nausch, G., and Wasmund, N. (Eds.), State and Evolution of the Baltic Sea 1952 – 2005. – John Wiley & Sons, Inc., Hoboken, New Jersey, p. 199-240.

SCHNEIDER, B., SCHLITZER, R., FISCHER, G., NÖTHIG, E.-M., 2003: Depth-dependent elemental compositions of particulate organic matter (POM) in the ocean. Global Biogeochemical Cycles **17**(2).

SCHULZ-BULL, D., HAND, I., LERZ, A., SCHNEIDER, R., TROST, E., WODARG, D., 2011: Regionale Verteilung chlorierter Kohlenwasserstoffe (CKW) und polycyclischer aromatischer Kohlenwasserstoffe (PAK) im Pelagial und Oberflächensediment in der deutschen ausschließlichen Wirtschaftszone (AWZ) im Jahr 2010. Leibniz-Institut für Ostseeforschung an der Universität Rostock im Auftrag des Bundesamtes für Seeschifffahrt und Hydrographie Hamburg, Rostock Warnemünde.

SZYMCZYCHA, B., WINOGRADOW, A., KULIŃSKI, K., KOZIOROWSKA, K. PEMPKOWIAK, J. 2017: Diurnal and seasonal DOC and POC variability in the land-locked sea. Oceanologia 59(3): 379-388.

SEIDEL, M., MANECKI, M., HERLEMANN, D. P. R., DEUTSCH, B., SCHULZ-BULL, D., JÜRGENS K., DITTMAR, T., 2017: Composition and Transformation of Dissolved Organic Matter in the Baltic Sea. Frontiers in Earth Science 5: 31.

SIEGEL, H., GERTH, M., SCHMIDT, T., 1996: Water exchange in the Pomeranian Bight – investigated by satellite data and shipborne measurements. Cont. Shelf Res 16, 1793-1817.

SMHI, 2021a: Tide gauge data at station Landort Norra in hourly means of the year 2020; geodesic reference level RH2000. http://opendata-download-ocobs.smhi.se/explore/

SMHI, 2021b: Accumulated inflow through the Öresund 2014-2020. http://www.smhi.se/hfa_coord/BOOS/Oresund.html

STRANDBERG, B., VAN BAVEL, B., BERGQVIST, P.-A., BROMAN, D., ISHAQ, R., NÄF, C., PETTERSEN, H., RAPPE, C., 1998: Occurrence, sedimentation, and spatial variations of organochlorine contaminants in settling particulate matter and sediments in the northern part of the Baltic Sea. Environmental Science & Technology. American Chemical Society 32 (12), pp. 1754–1759. doi: 10.1021/es970789m.

TRUMP, 1998: Transport- und Umsatzprozesse in der Pommerschen Bucht (TRUMP) 1994-1996. Abschlussbericht, Warnemünde, 1-32 (unveröffentlicht).

WINOGRADOW, A., MACKIEWICZ, A., PEMPKOWIAK, J., 2019: Seasonal changes in particulate organic matter (POM) concentrations and properties measured from deep areas of the Baltic Sea. Oceanologia 61(4): 505-521.

WITT, G., LEIPE, T., EMEIS, K.-C., 2001: Using Fluffy Layer Material To Study the Fate of Particle-Bound Organic Pollutants in the Southern Baltic Sea. Environmental Science & Technology 35: 1567–1573. doi:10.1021/es000187u.

YUNKER, M. B., MACDONALD, R.W., VINGARZAN, R., MITCHELL, R., GOYETTE, D., SYLVESTRE, S., 2002: PAHs in the Fraser River basin: A critical appraisal of PAH ratios as indicators of PAH source and composition. Organic Geochemistry 33 (4), 489–515. doi: 10.1016/S0146-6380(02)00002-5.

Appendix: Organic hazardous substances

Table Appendix 1: Concentrations of DDT and metabolites in Baltic surface water in winter 2020.

Dissolved	Transect	DDE-*p.p'*	DDD-*p.p'*	DDT-*o.p'* [pg/L]	DDT-*p.p'*	Σ DDT_{diss}
Kiel Bight/ Fehmarnbelt	T1	1.56	0.89	0.13	0.36	2.94
Mecklenburg Bight	T2	2.53	1.07	0.35	1.08	5.03
Arkona Sea	T3	2.90	0.96	0.36	1.13	5.35
Pomeranian Bight	T4	3.51	1.59	0.53	1.46	7.10
Bornholm Sea	T5	2.76	1.36	0.38	1.21	5.70
Central Baltic Sea	T6	1.92	0.95	0.25	0.77	3.90
Eastern Gotland Sea (South)	T7	0.77	0.37	0.08	0.22	1.45
Eastern Gotland Sea (North)	T8	1.79	1.10	0.17	0.61	3.66
Western Gotland Sea	T9	1.49	0.86	0.17	0.57	3.08

Particulate	Transect	DDE-*p.p'*	DDD-*p.p'*	DDT-*o.p'* [pg/L]	DDT-*p.p'*	Σ DDT_{part}
Kiel Bight/ Fehmarnbelt	T1	1.67	0.62	0.10	0.38	2.78
Mecklenburg Bight	T2	1.70	0.35	0.23	0.64	2.93
Arkona Sea	T3	1.40	0.21	0.18	0.62	2.40
Pomeranian Bight	T4	3.61	0.78	0.36	1.21	5.96
Bornholm Sea	T5	0.64	0.15	0.07	0.26	1.13
Central Baltic Sea	T6	0.43	0.13	0.05	0.16	0.76
Eastern Gotland Sea (South)	T7	0.27	0.12	0.04	0.08	0.52
Eastern Gotland Sea (North)	T8	0.30	0.12	0.03	0.11	0.57
Western Gotland Sea	T9	0.26	0.11	0.03	0.10	0.51

Sum (dissolved + particulate)	Transect	DDE-*p.p'*	DDD-*p.p'*	DDT-*o.p'* [pg/L]	DDT-*p.p'*	Σ DDT_{sum}
Kiel Bight/ Fehmarnbelt	T1	3.23	1.52	0.23	0.74	5.72
Mecklenburg Bight	T2	4.23	1.42	0.58	1.72	7.95
Arkona Sea	T3	4.30	1.17	0.54	1.75	7.75
Pomeranian Bight	T4	7.12	2.37	0.89	2.67	13.06
Bornholm Sea	T5	3.40	1.51	0.45	1.46	6.83
Central Baltic Sea	T6	2.35	1.08	0.30	0.93	4.66
Eastern Gotland Sea (South)	T7	1.04	0.50	0.12	0.31	1.96
Eastern Gotland Sea (North)	T8	2.09	1.22	0.20	0.73	4.23
Western Gotland Sea	T9	1.75	0.97	0.21	0.66	3.59

Table Appendix 2: Concentrations of HCB and PCB_{ICES} in surface waters of the Baltic Sea in winter 2020.

Dissolved	Transect	HCB	PCB 28/31	PCB 52	PCB 101	PCB 118	PCB 153	PCB 138	PCB 180	ΣPCB_{diss}
					[pg/L]					
Kiel Bight/ Fehmarnbelt	T1	4.30	0.84	0.46	0.50	0.27	0.46	0.31	0.06	2.90
Mecklenburg Bight	T2	5.52	0.94	0.44	0.44	0.24	0.35	0.24	0.07	2.73
Arkona Sea	T3	6.67	0.75	0.39	0.37	0.20	0.33	0.21	0.01	2.27
Pomeranian Bight	T4	8.48	1.00	0.52	0.42	0.18	0.30	0.17	0.05	2.64
Bornholm Sea	T5	6.48	0.75	0.38	0.29	0.19	0.23	0.15	0.05	2.04
Central Baltic Sea	T6	6.82	0.63	0.30	0.22	0.19	0.19	0.14	0.05	1.72
Eastern Gotland Sea (South)	T7	3.28	0.27	0.12	0.11	0.08	0.11	0.07	0.03	0.78
Eastern Gotland Sea (North)	T8	5.54	0.72	0.26	0.23	0.26	0.22	0.17	0.05	1.93
Western Gotland Sea	T9	6.66	0.64	0.29	0.26	0.23	0.25	0.18	0.06	1.91

Particulate	Transect	HCB	PCB 28/31	PCB 52	PCB 101	PCB 118	PCB 153	PCB 138	PCB 180	ΣPCB_{part}
					[pg/L]					
Kiel Bight/ Fehmarnbelt	T1	0.59	0.27	0.17	0.54	0.62	1.34	0.94	0.41	4.29
Mecklenburg Bight	T2	0.36	0.14	0.06	0.19	0.18	0.47	0.30	0.13	1.47
Arkona Sea	T3	0.26	0.03	0.02	0.07	0.13	0.29	0.21	0.11	0.87
Pomeranian Bight	T4	0.83	0.14	0.07	0.23	0.36	0.85	0.56	0.30	2.51
Bornholm Sea	T5	0.16	n.d.	0.00	0.02	0.10	0.15	0.11	0.06	0.45
Central Baltic Sea	T6	0.13	0.00	0.00	0.01	0.07	0.10	0.07	0.04	0.30
Eastern Gotland Sea (South)	T7	0.15	0.11	0.07	0.04	0.07	0.07	0.05	0.03	0.44
Eastern Gotland Sea (North)	T8	0.10	0.02	0.004	0.01	0.07	0.09	0.07	0.04	0.31
Western Gotland Sea	T9	0.16	n.d.	n.d.	0.01	0.06	0.09	0.06	0.04	0.26

Sum (dissolved+ particulate)	Transect	HCB	PCB 28/31	PCB 52	PCB 101	PCB 118	PCB 153	PCB 138	PCB 180	ΣPCB_{sum}
					[pg/L]					
Kiel Bight/ Fehmarnbelt	T1	4.90	1.11	0.64	1.04	0.89	1.80	1.25	0.47	7.20
Mecklenburg Bight	T2	5.88	1.08	0.50	0.63	0.42	0.82	0.55	0.20	4.20
Arkona Sea	T3	6.94	0.78	0.42	0.44	0.33	0.62	0.42	0.12	3.14
Pomeranian Bight	T4	9.30	1.14	0.59	0.65	0.54	1.15	0.72	0.35	5.15
Bornholm Sea	T5	6.63	0.75	0.39	0.30	0.29	0.38	0.27	0.11	2.49
Central Baltic Sea	T6	6.94	0.63	0.30	0.23	0.26	0.29	0.21	0.09	2.02
Eastern Gotland Sea (South)	T7	3.43	0.37	0.18	0.15	0.15	0.18	0.12	0.07	1.22
Eastern Gotland Sea (North)	T8	5.64	0.74	0.27	0.24	0.34	0.31	0.25	0.09	2.24
Western Gotland Sea	T9	6.82	0.64	0.29	0.26	0.30	0.34	0.24	0.10	2.17

Table Appendix 3: Concentrations of dissolved and particulate PAH in Baltic Sea surface water in winter 2020.

Dissolved	Transect	ACNLE	ACNE	FLE	ANT	PA	FLU	PYR	BAA	CHR	BBF	BKF	BAP	DBAHA	ICDP	BGHIP	ΣPAHdiss
										[pg/L]							
Kiel Bight/ Fehmarnbelt	T1	133	94.8	757	17.4	1914	430	173	6.8	22.8	15.3	7.1	2.3	0.66	2.8	2.6	3580
Mecklenburg Bight	T2	191	117	1002	28.7	1215	810	341	16.2	69.0	19.4	8.4	3.7	0.73	3.0	3.4	3829
Arkona Sea	T3	131	109	889	17.2	644	691	287	17.1	62.1	23.5	8.3	3.8	1.0	3.5	3.1	2891
Oder Bight	T4	143	132	1467	22.9	954	1213	421	22.0	90.7	30.7	12.8	8.6	1.4	4.4	5.5	4528
Bornholm Sea	T5	89.1	103	1043	16.5	837	1013	433	46.3	115	72.8	24.1	18.7	2.4	10.7	11.4	3835
Central Baltic Sea	T6	117.3	87.1	950	16.0	980	925	438	66.6	142	108	37.9	34.5	3.4	18.1	18.7	3943
Eastern Gotland Sea (South)	T7	17.9	17.9	200	7.0	194	192	99	18.4	40.2	21.7	11.5	8.9	1.2	6.4	5.7	842
Eastern Gotland Sea (North)	T8	78.7	70.0	886	24.5	952	912	448	93.5	184	133	40.0	38.3	3.8	21.0	18.1	3904
Western Gotland Sea	T9	52.0	57.1	593	18.4	730	674	339	73.5	134	108	40.4	33.9	4.1	21.5	19.6	2899

Particulate	Transect	ACNLE	ACNE	FLE	ANT	PA	FLU	PYR	BAA	CHR	BBF	BKF	BAP	DBAHA	ICDP	BGHIP	ΣPAH_{part}
										[pg/L]							
Kiel Bight/ Fehmarnbelt	T1	6.5	2.9	11.7	10.4	80.3	116	101	49.2	62.7	179	72.3	75.8	23.0	143	147	1081
Mecklenburg Bight	T2	1.9	1.0	4.1	1.4	16.7	54.4	34.5	10.7	25.5	46.6	21.0	16.7	5.5	47.2	41.4	329
Arkona Sea	T3	3.4	3.9	10.2	2.3	31.0	85.1	60.7	20.9	47.2	95.7	38.2	36.7	12.6	106	94.6	649
Oder Bight	T4	9.3	15.2	34.5	17.7	85.6	167	104	50.0	89.6	134	61.3	73.9	17.3	129	110	1099
Bornholm Sea	T5	1.6	0.60	1.9	1.1	8.5	31.9	21.5	9.8	19.2	47.6	20.4	20.7	5.6	56.6	46.8	294
Central Baltic Sea	T6	2.5	0.52	2.4	1.6	11.9	32.0	24.4	12.5	19.6	46.9	21.8	28.2	6.6	64.5	53.4	329
Eastern Gotland Sea (South)	T7	4.6	0.94	4.8	2.5	25.1	42.4	33.6	18.7	26.1	92.0	30.0	39.3	10.5	95.7	75.3	502
Eastern Gotland Sea (North)	T8	3.5	3.4	4.1	2.7	21.2	41.6	35.9	22.8	32.7	84.0	33.0	47.5	12.9	106.8	97.3	550
Western Gotland Sea	T9	5.6	0.65	3.9	3.1	26.3	56.2	50.8	27.0	32.0	94.6	31.2	49.3	10.0	91.7	77.4	560

App. Table 3 continued

Sum (particulate + dissolved)	Transect	ACNLE	ACNE	FLE	ANT	PA	FLU	PYR	BAA	CHR	BBF	BKF	BAP	DBAHA	ICDP	BGHIP	ΣPAHsum
										[pg/L]							
Kiel Bight/ Fehmarnbelt	T1	140	97.7	769	27.7	1995	545	274	56.0	85.5	194	79.4	78.1	23.6	146	150	4660
Mecklenburg Bight	T2	193	118	1006	30.2	1232	865	376	26.9	94.6	66.0	29.4	20.4	6.2	50.2	44.8	4158
Arkona Sea	T3	134	113	899	19.6	675	776	348	38.0	109	119	46.5	40.5	13.6	110	97.8	3540
Oder Bight	T4	152	147	1501	40.6	1039	1380	525	72.0	180	165	74.1	82.5	18.8	133	115	5626
Bornholm Sea	T5	90.7	103	1045	17.6	846	1045	454	56.1	134	120	44.4	39.4	7.9	67.4	58.3	4129
Central Baltic Sea	T6	120	87.7	953	17.6	992	957	463	79.1	162	155	59.7	62.7	10.0	82.5	72.1	4272
Eastern Gotland Sea (South)	T7	22.5	18.9	205	9.5	219	234	133	37.2	66.3	114	41.6	48.1	11.6	102	81.0	1344
Eastern Gotland Sea (North)	T8	82.2	73.4	890	27.2	973	954	484	116	216	217	73.0	85.8	16.7	128	115	4453
Western Gotland Sea	T9	57.6	57.8	597	21.5	756	731	390	100	166	203	71.7	83.2	14.0	113	97.0	3459

Table Appendix 4: Contents of DDT/metabolites as well as TOC in Baltic Sea surface sediments in winter 2020. Contents are in ng/g DW and normalized to the organic carbon content in ng/g TOC. n.d. not detected

Station	DDE-*p,p'*	DDD-*p,p'*	DDT-*o,p'*	DDT-*p,p'*	Σ DDT_{Sed}	TOC
			[pg/g dw]			[%]
N1 (TF0010)	161	284	n.d.	n.d.	445	1.18
M2 (TF0012)	872	1244	56.6	102	2274	4.50
K5 (TF0113)	2134	3078	117	268	5597	6.17
K4 (TF0109)	1625	2075	114	233	4047	5.31
Oder (OBBOJE)	83.7	108	16.3	22.8	231	0.35
			[ng/g TOC]			
N1 (TF0010)	13.6	24.0	n.d.	n.d.	37.6	
M2 (TF0012)	19.4	27.6	1.3	2.3	50.5	
K5 (TF0113)	34.6	49.9	1.9	4.3	90.7	
K4 (TF0109)	30.6	39.1	2.1	4.4	76.2	
Oder (OBBOJE)	23.9	30.8	4.7	6.5	65.9	

Table Appendix 5: Contents of HCB and PCB_{ICES} in Baltic Sea surface sediments in winter 2020. Contents are in ng/g DW and normalized to the organic carbon content in ng/g TOC. n.d. not detected

Station	HCB	PCB 28/31	PCB 52	PCB 101	PCB 118	PCB 153	PCB 138	PCB 180	$\Sigma PCB_{ICES,Sed}$
					[pg/g DW]				
N1 (TF0010)	56.5	91.3	58.8	115	89.0	241	178	98.1	872
M2 (TF0012)	142	238	135	415	409	971	761	402	3330
K5 (TF0113)	193	463	351	794	751	1595	1121	562	5637
K4 (TF0109)	266	351	243	618	496	1176	740	397	4020
Oder (OBBOJE)	30.8	18.2	11.2	13.3	14.3	34.7	20.0	13.8	126
					[ng/g TOC]				
N1 (TF0010)	4.8	7.7	5.0	9.7	7.5	20.3	15.0	8.3	73.6
M2 (TF0012)	3.1	5.3	3.0	9.2	9.1	21.6	16.9	8.9	73.9
K5 (TF0113)	3.1	7.5	5.7	12.9	12.2	25.8	18.2	9.1	91.3
K4 (TF0109)	5.0	6.6	4.6	11.6	9.3	22.2	13.9	7.4	75.7
Oder (OBBOJE)	8.8	5.2	3.2	3.8	4.1	9.9	5.7	3.9	35.9

Table Appendix 6: Contents of organotin (OT) compounds in surface sediments of the Baltic Sea in winter 2020. OT contents are in ng/g DW and normalized to the organic carbon content in ng/g TOC. TBT: tributyltin, MBT monobutyltin, DBT dibutyltin, TPhT triphenyltin, n.d. not detected

Station	TBT	MBT	DBT	TPhT	ΣOT_{SED}
			[ng/g DW]		
N1 (TF0010)	1.1	1.7	n.d.	n.d.	2.8
M2 (TF0012)	3.3	5.1	4.0	n.d.	12.4
K5 (TF0113)	3.5	5.7	5.9	n.d.	15.1
K4 (TF0109)	3.0	5.3	5.9	n.d.	14.2
Oder (OBBOJE)	0.3	n.d.	n.d.	n.d.	0.3
			[ng/g TOC]		
N1 (TF0010)	92.9	144	n.d.	n.d.	236
M2 (TF0012)	73.3	113	88.8	n.d.	275
K5 (TF0113)	56.7	92.3	95.6	n.d.	245
K4 (TF0109)	56.5	99.8	111	n.d.	267
Oder (OBBOJE)	85.7	n.d.	n.d.	n.d.	85.7

Table Appendix 7: PAH contents in Baltic Sea surface sediments in winter 2020. Contents are presented in ng/g DW and normalized to the organic carbon content in ng/g TOC. n.d. not detected

Station	ACNLE	ACNE	FLE	ANT	PA	FLU	PYR	BAA	CHR	BBF	BKF	BAP	DBAHA	ICDP	BGHIP	$\Sigma PAH_{ICES,Sed}$
									[ng/g DW]							
N1 (TF0010)	1.9	1.2	9.7	20.9	35.2	79.8	59.6	26.7	57.4	41.0	18.8	21.2	7.2	27.7	28.6	437
M2 (TF0012)	9.1	1.6	6.0	8.3	34.2	85.5	74.4	38.7	42.8	151	62.0	59.5	24.4	159	146	902
K5 (TF0113)	13.2	5.3	13.2	20.9	95.5	244	174	83.5	112	376	176	139	61.9	369	384	2267
K4 (TF0109)	10.8	4.2	9.9	14.0	63.2	141	112	50.7	70.4	302	118	93.9	45.7	277	273	1587
Oder (OBBOJE)	0.5	0.9	1.7	1.1	4.7	7.7	5.5	3.3	4.2	6.6	3.5	4.7	1.2	5.3	5.2	56.0
									[ng/g TOC]							
N1 (TF0010)	161	100	817	1769	2970	6738	5033	2250	4846	3460	1588	1787	608	2334	2414	36877
M2 (TF0012)	203	36.0	133	185	759	1898	1652	860	951	3354	1378	1321	543	3518	3234	20024
K5 (TF0113)	214	85.1	214	339	1547	3957	2809	1353	1811	6083	2848	2245	1003	5979	6243	36730
K4 (TF0109)	203	78.4	186	264	1190	2652	2116	955	1326	5691	2226	1769	860	5215	5144	29874
Oder (OBBOJE)	132	248	473	318	1348	2190	1568	949	1194	1891	991	1353	354	1509	1492	16010

Naumann, M., Gräwe, U.,
Mohrholz, V., Kuss, J., Kanwischer, M.,
Osterholz, H., Feistel, S., Hand, I.,
Waniek, J.J., Schulz-Bull, D.E.:
Hydrographic-hydrochemical assessment of the Baltic Sea 2020

CONTENT

Leibniz-Institut für Ostseeforschung Warnemünde
IOW